Eocene volcanism during the incipient stage of Izu Ogasawara Arc: Geology and petrology of the Mukojima Island Group, the Ogasawara Islands.

Eocene volcanism during the incipient stage of Izu-Ogasawara arc: Geology and petrology of the Mukojima Island Group, the Ogasawara Islands

Kyoko Kanayama [a*], Susumu Umino [a] and Osamu Ishizuka [b]

[a] Department of Earth Science, Graduate School of Natural Science and Technology, Kanazawa University, Kakuma-machi, Kanazawa, Ishikawa, 920-1192, Japan

[b] Institute of Geoscience and Geoinformation, Geological Survey of Japan/AIST, Central 7, 1-1-1, Higashi, Tsukuba, Ibaraki, 305-8567, Japan

*Corresponding author: Department of Earth Science, Graduate School of Natural Science and Technology, Kanazawa University, Kakuma-machi, Kanazawa, Ishikawa, 920-1192, Japan. Tel.: +81-076-264-6522; fax: +81-076-264-6545.

E-mail address: ka78ma@stu.kanazawa-u.ac.jp.

Abstract

The Ogasawara Islands mainly comprise Eocene volcanic strata formed when the Izu-Ogasawara-Mariana arc began. We present the first detailed volcanic geology, petrography and geochemistry of the Mukojima Island Group, northernmost of the Ogasawara Islands, and show that the volcanic stratigraphy consists of arc tholeiitic rocks, ultra-depleted boninite-series rocks, and less-depleted boninitic andesites which are correlatable to the Maruberiwan, Asahiyama and Mikazukiyama Formations on the Chichijima Island Group to the south. On Chichijima, a short hiatus is identified between the Maruberiwan (boninite, bronzite andesite and dacite) and Asahiyama Formation (quartz dacite and rhyolite). In contrast, these lithologies are interbedded on the Nakodojima of the Mukojima Island Group. The stratigraphically lower portion of Mukojima is mainly composed of pillow lava, which is overlain by reworked volcaniclastic rocks in the middle, whereas the upper portion is dominated by pyroclastic rocks. This suggests that volcanic activity now preserved on Mukojima Island Group records growth of one or more volcanoes, beginning with quiet extrusion of lava under relatively deep water followed by volcaniclastic deposition, and then changed into moderately explosive eruptions that took place in shallow water or above sea level. This is consistent with the uplift of the entire Ogasawara Ridge during the Eocene. Boninites from the Mukojima Island Group are divided into three types on the basis of geochemistry. Type 1 boninites have high SiO_2 (>57.0 wt%) and Zr/Ti (>0.022) and are the most abundant type in both Mukojima and Chichijima Island Groups. Type 2 boninites have low SiO_2 (<57.1 wt%) and Zr/Ti (<0.010). Type 3 boninites have 57.6-60.7 wt% SiO_2 and are characterized by high CaO/Al_2O_3 (0.9-1.1). Both type 2 and 3 boninites are common on Mukojima but are rare in the Chichijima Island Group.

Key words

Ogasawara (Bonin) Islands; Mukojima Island Group; subduction zone; volcanic geology; geochemistry;

petrography; boninite; arc tholeiite; pillow lava; pyroclastic rock

Introduction

Subduction zones play an essential role in producing continental crust and developing terrestrial environment through material exchange between the Earth's interior and surface (e.g. Kelemen 1995; Rudnick 1995; Tatsumi 2005; Kodaira *et al*. 2007; Tatsumi *et al*. 2008). Oceanic arc originally initiate in an oceanic environment, causing a juvenile arc to form above ~~them~~, which develops into a mature arc-trench system (Stern 2010). However, it is poorly understood how immature arcs develop into mature arcs and how subarc mantle evolves as a new subduction zone is established. The Izu-Ogasawara-Mariana (Izu-Bonin-Mariana, or IBM) arc-trench system is an ideal site for addressing these issues because it provides a complete volcanic record of the arc, which we can interpret to reveal the thermo-chemical evolution of the wedge mantle from the beginning of subduction to the establishment of the stable arc-trench system.

The Ogasawara (Bonin) Archipelago represents an emergent section of the Izu-Ogasawara-Mariana fore-arc basement, which separates the Izu-Ogasawara-Mariana Trench from the Ogasawara Trough and the active volcanic arc (Figs 1). Subduction of the Pacific plate started with voluminous igneous activity, perhaps seafloor spreading, along the entire eastern margin of the overriding Philippine Sea plate (Stern & Bloomer 1992). This is coincident with the change in plate motion in the western Pacific at ca. 50 Ma (Sharp & Clague 2002; Wessel *et al*. 2006). Initial volcanism was MORB-like basalt at 52-[illegible]a (Reagan *et al*. 2010; Ishizuka *et al*. 2011), followed by arc tholeiite which was replaced by boninite magmatism after 49 Ma (Cosca *et al*. 1998; Ishizuka *et al*. 2006). Boninite, a high-Mg andesite with SiO_2 >52 wt%, MgO >8 wt% and TiO_2 <0.5 wt% (Le Bas 2000), is intimately associated with more differentiated variety of rocks ranging in composition from bronzite andesite to quartz-bearing rhyolite (Umino 1985; Umino & Nakano 2007). These boninite and related rocks are hereafter referred to "boninite-series rocks". Two types of boninite series are recognized by distinct trends in major elements

and by trace element abundances. High-Si boninite-series rocks are distinguished from low-Si boninite-series rocks by their higher SiO_2 at a given FeO*/MgO and severely depleted REEs (rare earth elements) and HFSEs (high field strength elements). The initial boninite magmatism at 49-46 Ma is represented by high-Si boninite-series rocks which include the “type” boninite of Chichijima. This boninitic magmatism was followed by eruption of low-Si boninite and bronzite andesite associated with calc-alkalic andesite and dacite, beginning at 45 Ma (Ishizuka *et al.* 2006). These lavas are widespread in the Mikazukiyama Formation of the Chichijima Island Group (Umino & Nakano 2007) (Figs 2a, 3) and on the western scarp of the Ogasawara Ridge (Ishizuka *et al.* 2006). These activities are the transitional stage from incipient to typical arc magmatism, which were followed by eruption of arc tholeiitic and calc-alkaline magmas since 45 Ma (Ishizuka *et al.* 2006; unpubl. data, 2011). The progressive change in magma compositions reflects the thermo-chemical evolution of the wedge mantle during the establishment of the Izu-Ogasawara-Mariana subduction zone during the beginning ~10 myr of plate subduction (e.g. Hussong *et al.* 1982; Ishii 1985; Bloomer & Hawkins 1987; Fryer *et al.* 1990; Arculus *et al.* 1992; Pearce *et al.* 1992a, b; Cosca *et al.* 1998; Ishizuka *et al.* 2006) (Fig. 4).

Boninite-series volcanic rocks are widespread over the Ogasawara Ridge (Fig. 2a, 4). Besides the Chichijima Island Group, including the type locality of boninite (Kikuchi 1890; Petersen 1891), the Mukojima Island Group (Fig. 2b), the northernmost Ogasawara Archipelago, is also known to have boninitic rock suites (Shiraki *et al.* 1979; Yuasa *et al.* 1981), which are similar to those of the Chichijima Island Group (Fig. 3; e.g. Kuroda & Shiraki 1975; Maruyama & Kuramoto 1981; Umino 1985; Taylor *et al.* 1994; Umino & Nakano 2006; 2007). Boninite has also been recovered from the submarine Ogasawara Ridge, inner slope of the Ogasawara Trench (Ishizuka *et al.* 2011) and Hahajima Seamount (Ishiwatari *et al.* 2006). Recently, $^{40}Ar/^{39}Ar$ ages of 48.04±0.17-44.3±0.3 Ma have been reported for the volcanic rocks from the Mukojima Island Group (Ishizuka *et al.* 2011). These ages span the entire period of volcanic

activity on the Chichijima Island Group, which shows a wide spectrum of magma compositions from boninite-series rocks to arc tholeiitic and calc-alkaline rocks. Likewise, the Mukojima Island Group is expected to show a wide variety of magma compositions and variable style of volcanic products. However, detailed volcanic geology, petrology and stratigraphic relationships between these volcanic suites are poorly known.

This study provides the first detailed studies on the geology, petrography and geochemistry of the Mukojima Island Group and discusses the style of volcanic activities, stratigraphic relationships among the Ogasawara Islands and the genetic conditions of boninite magmas.

Analytical techniques

Preparation of bulk rock samples was conducted at Shizuoka University and the Geological Survey of Japan. Normally 50 g of rock chips were ultrasonically cleaned and then soaked in distilled water at 80C° for 4 to 5 days to remove seawater contamination. The rock chips were then pulverized using an agate mortar.

Whole rock major element abundances were determined by a Philips PW1404 XRF spectrometer at the Geological Survey of Japan (GSJ, AIST) using glass beads prepared by fusion of 0.5-g rock with 5-g of lithium tetraborate ($Li_2B_4O_7$). Analytical error is generally <2%.

Whole rock trace element compositions were determined by an inductively coupled plasma mass spectrometry (ICP-MS) at the Geological Survey of Japan. About 100 mg of powder from each sample was dissolved in a HF-HNO_3 mixture (5:1). After evaporation to dryness, the residues were re-dissolved with 2% HNO_3 prior to analysis. REEs, V, Cr, Rb, Sr, Y, Zr, Nb, Cs, Ba, Hf, Ta, Pb, Th and U concentrations were analyzed by ICP-MS on a VG Platform instrument. Reproducibility is better than ±4% (2 σ) for REE and better than ±6% (2 σ) for other elements.

Major elements of glass shards in pumice and scoria samples and constituent minerals (>0.4 mm diameter) were analyzed by a JEOL JXA-8800 electron probe microanalyzer (EPMA) at Kanazawa University. The accelerating voltage was 15 kV and the specimen current was 12 nA. Analyses of glass followed the procedures of Noguchi *et al*. (2004) using broad beam diameters <30 μm. The corrections were made using ZAF method.

Trace element compositions (REEs, V, Cr, Co, Ni, Li, B, Sc, Rb, Sr, Y, Zr, Nb, Cs, Ba, Hf, Ta, Pb, Th and U) of glass were analyzed by laser ablation (193 nm ArF excimer: MicroLas GeoLas Q-plus) inductively coupled plasma mass spectrometry (Agilent 7500S) (LA-ICP-MS) at Kanazawa University (Ishida *et al*. 2004). Each analysis was performed by ablating spots of 100 μm in diameter at 5 Hz with energy density of 8 J/m^2 per pulse. Signal integration times were 40 seconds for a gas background interval and 30 seconds for an ablation interval. The NIST SRM 612 glass was used as the primary calibration standard and was analyzed at the beginning of each batch of <3-5 unknowns, with a linear drift correction applied between each calibration. The element concentration of NIST SRM 612 for the calibration is selected from the preferred values of Pearce *et al*. (1997). Data reduction was facilitated using ^{29}Si as internal standards for glass, based on SiO_2 contents obtained by EPMA analysis, and followed a protocol essentially identical to that outlined by Longerich *et al*. (1996). Details of the analytical method and data quality for the LA-ICP-MS system at Kanazawa University are described in Morishita *et al*. (2005a, b).

Geology of the Mukojima Island Group

Mukojima Island Group comprises three clusters of islands spread about 30 km northwest to southeast: 1) Kitanoshima and Nakanoshima, and the adjacent reefs to the northeast (Ninoiwa and Yon'noiwa; 2) Mukojima, Harinoiwa, Tatamiiwa, Nakodojima; and 3) Yomejima (Fig. 2b). Total thickness of volcanic strata of the Mukojima Island Group is more than 1900 m.

136

137 ***1. Ninoiwa, Kitanoshima and Nakanoshima***

138 Ninoiwa, Kitanoshima and Nakanoshima are composed of altered aphyric tholeiitic andesite to

139 dacite.

140 Ninoiwa (Fig. 5) is the largest rocky reef among the islets in the northern end of the Ogasawara

141 Archipelago. It consists of altered agglutinate composed of densely welded ash- and lapilli-sized clasts of

142 aphyric andesite.

143 Kitanoshima, Nakanoshima and the surrounding reefs and islets form two volcanic edifices of

144 aphyric arc tholeiitic andesite to dacite similar to that of Ninoiwa (Figs 5, 6a). Nakanoshima is composed

145 of pillow lava (Fig. 7a) more than 180 m in thickness and dipping 20° to 54° to northeast. Pillows are

146 locally overlain by volcanic breccia above a SE-dipping erosional surface. Pillow lava sequences exposed

147 on reefs to the southeast of Kitanoshima also dip northeast, whereas pillows on the southeastern end of

148 Kitanoshima and the adjacent islet dip northwest, indicating an anticline plunging to the northeast. The

149 northwestern half of Kitanoshima and the surrounding reefs are composed of more than 660 m of

150 agglutinate consisting of densely to moderately welded lava clasts up to 10 cm in diameter (Fig. 7b, c),

151 which represents a proximal facies deposited very close to the source vent(s). The agglutinate is intruded

152 by dikes and overlain by 140 m of pillow lava on the southeast of Kitanoshima dipping 30°-52° SE, which

153 are underlain by the northwesterly dipping pillows forming the western limb of the anticline. All these

154 lavas on Kitanoshima, Nakanoshima and the surrounding reefs suffered low-temperature alteration and

155 weather reddish brown because of hematite and limonite covering surfaces and infillings of cracks in

156 pillow lobes. Bifurcating pillow lobes indicate flow directions to east on the north of Nakanoshima and

157 northwest on the southern Nakanoshima. The anticlinal structure affecting pillow lava on Nakanoshima and

158 adjacent reefs suggests that they reflect a pillowed ridge elongated northeast-southwest, which were

dissected and covered by the welded fall-out tephras and then by the uppermost pillow flows comprising most of Kitanoshima.

2. Yon'noiwa and Sasayojima

Yon'noiwa (Fig. 5), a small reef 1.5 km north of Nakanoshima, consists of southwesterly dipping bedded tuff breccia with intercalated sheet flows (<1 m thick) of porphyritic olivine-bronzite boninite. Sasayojima (Figs 5, 6b), east off Nakanoshima, consists of pillow lava and tuff breccia of boninite and bronzite andesite dipping 16°-22° west-southwest. The massive part of the tuff breccia includes lenticular volcanic bombs, consisting of poorly vesiculated scoriae and lithic clasts. Well stratified tuff breccia includes lapillistone and agglomerate lenses consisting of clasts several to tens of centimeters in diameter. These tuff breccias are intruded by dikes of bronzite andesite that dip 85°-90° and strike NW. The interiors of pillows and dikes are brecciated. The total thickness exceeds 55 m.

3. Mukojima

Mukojima (Figs 5, 6c), the largest island of the Mukojima Island Group, is mainly composed of gently to moderately (12° to 40°) inclined boninite bedded tuff breccia and pillow lava. The total thickness reaches 750 m. A south-southeasterly plunging anticline and a northerly plunging syncline are in the northwest and east of the island, respectively. Faults with northwest-southeast strikes are dominant. The lowest 297-m thick portion of the island is exposed in the northwest and consists of bedded tuff breccia intercalated with partially brecciated pillows showing rare chilled margins and closely packed pillows with thick chilled margins (Fig. 7d, e). The pillow lava and tuff breccia are type 3 high-Si boninites (to be defined later) with the highest CaO/Al_2O_3 ratio (0.9-1.4) on the island. The middle portion consists of 316-m thick bedded tuff breccia with an intercalated 32-m thick pillow lava of porphyritic boninite which

includes clinoenstatite as long as 5 cm concentrated in the core of pillows. The bedded tuff breccias include fragments of boninite pillows, coarse ash- to lapilli-sized poorly vesiculated scoria. The uppermost portion consists of pillow flows of type 2 high-Si boninite (to be defined later), white tuffaceous siltstone-sandstone-conglomerate (Fig. 8a, b), a boninite lobate sheet flow and massive tuff breccia (Fig. 7f), in ascending order. The uppermost massive tuff breccia is widely distributed in the center and east of the island (Fig. 7g). The ubiquitous presence of volcanic bombs in the massive tuff breccia indicates the products of middle strombolian eruptions, suggesting the eruptive center(s) was in the vicinity of the island.

4. Harinoiwa and Tatamiiwa

Harinoiwa (Figs 5, 6d) is located between Mukojima and Nakodojima and consists of NW-dipping alternating beds of pillow lava, hyaloclastite and bedded tuff breccia of nearly aphyric bronzite andesite. The total thickness attains 340 m. Pillow lobes are brecciated into glassy fragments and laterally changes into hyaloclastite as the degree of fragmentation increases (Fig. 7h). Lenticular lava tongues show subparallel arrangement embedded in hyaloclastite. The bedded tuff breccia comprises pillow fragments and volcanic bombs which show graded bedding in the matrix of poorly vesiculated lithic clasts and angular glassy fragments. Some dikes with undulating margins bud pillow lobes on the upper end, while another dikes are short and closed at both ends within hyaloclastite and pillow lava (Fig. 7h).

Tatamiiwa (Fig. 5) is a small reef composed of bronzite andesite lapilli tuff located in north off Nakodojima.

5. Nakodojima

Nakodojima (Figs 5, 6e) is divided into the eastern, central and western blocks by faults running

NNE-SSW in the center of the island and N-S on the east of Tsurugiyama. The western block reaches 230 m in thickness and comprises boninite and bronzite andesite pillow lava overlain by quartz rhyolite hyaloclastite. The central block moderately inclines toward south and has a thickness of 280 m and consists of pillow lava of boninite and bronzite andesite in the lower part and hyaloclastite and lobate sheet flows of nearly aphyric bronzite andesite with minor dacite and quartz rhyolite hyaloclastite in the upper part. Boninite pillows are distributed in the lowermost part along the northern coast. Bronzite andesite forms lobate sheet flows on the ridge behind the central embayment. The eastern block is composed of quartz rhyolite hyaloclastite interbedded with bronzite andesite hyaloclastite. Brecciated pillow lava of bronzite andesite and boninite occurs in the lowermost level below andesite hyaloclastite and in the upper level beneath white pumice tuff (Fig. 8g) and quartz rhyolite hyaloclastite on the top of Byobuyama. The lowermost brecciated pillow lava in the southeast of the island forms a composite flow of bronzite andesite and boninite. Most boninite and andesite pillow lavas and quartz rhyolite lava are brecciated to glassy and lithic fragments which grade into massive hyaloclastite (Fig. 7i). En echelon NW-trending alteration zones are aligned in the central block, where lavas are hydrothermally bleached (Fig. 7j). A secondary copper-bearing mineral deposit (Chrysocolla) is present in a narrow cove along the fault bounding the central and the western block (Ishizuka *et al.* 2012). Nakodojima is considered to be a discrete volcanic center, because the island is the only volcano that has felsic lava flows and fall deposits and intense hydrothermal alteration and mineralization occurred associated with the rhyolite dikes.

6. Yomejima

Yomejima (Figs 5, 6f) is the southernmost of the Mukojima Island Group. Most of Yomejima comprises bedded tuff breccia with intercalated pillow lava, up to 480 m thick. An E-W trending anticline runs through the center of Yomejima and the adjacent Ushirojima, where stratigraphically lowest

composite pillow lavas of bronzite andesite and boninite are exposed beneath the bedded tuff breccia. The northern limb of the anticline dips 9°-30° N- to NW-, where the uppermost bedded volcanic breccia of olivine-augite-bronzite andesite is distributed in the northwest of Yomejima. The southern limb of the anticline is composed of composite pillow lava of boninite and bronzite andesite which is unconformably overlain by tuff breccia, pillow lava, a surge deposit and welded fall-out scoria and volcanic bombs. The surge deposit mainly consists of dense, glassy scoria, coarse ash and volcanic bombs of boninite. Poorly vesiculated angular pyroclastic materials show finely stratified cross stratification, which is disturbed by bomb sags. Weakly welded boninite agglomerate including driblets and distorted spindle-shaped volcanic bombs intercalated with boninite pillow flows, which grade laterally into pyroclastic N-S dikes, 50-328 cm thick on the western coast of central Yomejima. A synform on the southern end of the island is formed by northeasterly dipping pillow lava which abuts bedded tuff breccia dipping to the south. Polymict breccia consisting of boninite and two-pyroxene andesite rest unconformably on the bedded tuff breccia on top of the northwestern cliff of Yomejima.

Maejima southwest off Yomejima is composed of bedded volcanic and tuff breccia which are weakly to moderately welded (Fig. 7k). Welded breccia surrounding an embayment of Maejima comprises lenticular deposits of poorly vesiculated blocks and lapilli, which are considered to be a vent-filling talus deposit. Intense Fe-Cu sulfide mineralization and quartz veining are pervasive throughout Maejima (Ishizuka *et al*. 2012).

A number of dikes of boninite and altered bronzite andesite intruded into the tuff breccia in the center of Yomejima and Maejima (Fig. 7l). The dikes show variable strikes, dipping 36°-90° with an average of 72°W. The thickness of measured 28 dikes vary from 11 cm to 800 cm, averaging 115 cm with a median of 88 cm.

Petrography

1. Boninite-series rocks

Boninite was first described by Kikuchi (1890) and introduced by Petersen (1891) for rock samples from Chichijima. The term “boninite” is defined as a feldspar-free andesite carrying bronzite as a phenocryst and/or microphenocryst. Boninite is a compact, black gray rock and has abundant glass more than 20% even in the core of a pillow and a dike, showing a vitreous fracture. Boninite-series rocks of Chichijima are comprised of boninite, bronzite andesite, dacite and quartz-bearing dacite and rhyolite, these form an almost continuous geochemical trend (Umino, 1985), although quartz-bearing dacite is absent from the Mukojima Island Group lavas. Boninite-series can be readily distinguished from other associated volcanic rock suites such as calc-alkalic and tholeiitic rocks as shown in the following chapters.

1-1. Boninite

Boninite occurs in Yon’noiwa, Sasayojima, Mukojima, Nakodojima and Yomejima as pillow lava, clasts in bedded tuff breccia, scoriae and bombs in massive tuff breccia, and dikes. Generally, boninite shows a bimodal or trimodal distribution in crystal size. Besides bronzite, olivine and clinoenstatite are present as phenocrysts and/or microphenocrysts (Fig. 9a, b). Pyroxene phenocrysts form one millimeter to a few centimeter thick prisms. Pyroxene microphenocrysts are several hundred μm to 2 mm-long prisms and skeletal forms indicates relatively rapid growth. Small amounts of minute chrome spinel grains are found as inclusions in phenocrysts and microphenocrysts of olivine, clinoenstatite and bronzite, and as discrete equant crystals in the matrix glass. Groundmass consists of Ca-rich clinopyroxene microlites embedded in glass (Fig. 9a, b).

In addition to the above general features, Mukojima boninites have some special features. Some type 1 boninites (described later) have augite phenocrysts and microphenocrysts. Augite and hypersthene phenocrysts are common in type 3 boninites (Fig. 9c), some of which have numerous inclusions of glass,

clinopyroxene, orthopyroxene and magnetite in a resorbed core surrounded by reversely zoned, euhedral rim. Others show irregular, resorbed outlines. Rounded clots of plagioclase are rarely included. Clots of subhedral augite without inclusions are present in some samples. Type 2 and 3 boninites commonly have augite microphenocrysts (Fig. 9d).

Boninite from the upper central block of Nakodojima is nearly aphyric and have rare hypersthene and augite phenocrysts which have resorbed, irregular shaped cores surrounded by more magnesian bronzite rim.

1-2. Bronzite andesite

Bronzite andesite occurs in Sasayojima, Nakodojima, Harinoiwa, Tatamiiwa and Yomejima as massive tuff breccia (hyaloclastite), clasts in bedded tuff breccia, pillow lava and dikes. In addition to bronzite, plagioclase, olivine, augite, hypersthene, magnetite and rare clinoenstatite occur as phenocrysts, but some bronzite andesites lack some or most of these phenocrysts. Bronzite andesites from Harinoiwa, Tatamiiwa and the upper central block of Nakodojima are exclusively aphyric. Bronzite and augite are common as microphenocrysts, and sometimes plagioclase and hypersthene are present. The groundmass is generally glassy, and consists of microlites of plagioclase and clinopyroxene (Fig. 9e).

1-3. Dacite

Distribution of dacite is limited in Nakodojima and Yomejima as tuff breccia. Plagioclase, augite, hypersthene and magnetite are present as phenocrysts and/or microphenocrysts (Fig. 9f). Glassy groundmass consists of microlites of plagioclase and magnetite, and clinopyroxene may be present in some samples.

1-4. Quartz rhyolite

Quartz rhyolite occurs in Nakodojima as tuff breccia and dikes, and rarely in Yomejima as dikes. Quartz, plagioclase, hypersthene, augite and magnetite are present as phenocrysts and/or microphenocrysts

297 (Fig. 9g). The groundmass is almost holohyaline with rare plagioclase microlites, magnetite and
298 clinopyroxene, and shows aphanitic texture in some samples.
299
300 ***2. Arc tholeiitic rocks***
301 Arc tholeiitic andesite to dacite occurs as welded tuff breccia in Ninoiwa, welded tuff breccia and
302 pillow lava in Kitanoshima and pillow lava in Nakanoshima. These rocks are generally aphyric, and small
303 amount of plagioclase and clinopyroxene are present as phenocrysts and microphenocrysts. Andesites have
304 rare olivine phenocrysts. Groundmass consists of plagioclase, magnetite and pyroxene. Some clasts in
305 welded tuff breccia of Ninoiwa have altered glassy groundmass. Most of these rocks suffered from
306 greenschist-facies metamorphism. The primary mineral assemblage is partially or completely replaced by
307 secondary minerals. Plagioclase is replaced by albite, epidote and quartz. Clinopyroxene is converted into
308 actinolite, chlorite, epidote, sphene, quartz and magnetite. Quartz, zeolites, epidote, chlorite, calcite,
309 apatite and magnetite occur as vesicle fillings and veins (Fig. 9h).
310
311 **Tephras from Mukojima and Nakodojima**
312 Because the Mukojima Island Group consists of several clusters of islands spread over 30 km
313 north-south, stratigraphic correlations among the islands are poorly constrained. Waterlain tephra deposits
314 from the upper Mukojima and Nakodojima correlate between the discrete two islands.
315 ***1. Description of tephras***
316 Pumice and scoria tuff and lapillistone (M3-07) interbedded with boninite pillow lavas in a
317 stratigraphically high level are exposed on the eastern and southeastern coasts of Mukojima (Figs 6c, 8a, b).
318 They are 18 m in maximum thickness and are divided into three units; 1) a lower unit of pale green
319 sandstone 2 m thick. This unit is overlain by 6-m thick middle unit of turbiditic deposits consisting of 5- to

15-cm thick alternating beds of medium- to fine-grained tuff with 1 mm thick laminae (Fig. 8b). The upper unit is 10 m thick and consists of 5-10 cm thick alternating beds of coarse tuff and lapillistone. Lapilli generally show imbrication which indicates a paleo-current toward S50-88°E (Fig. 8b). Both the middle and upper units are intruded by a boninite sheet lava which thins to the north.

The lapillistone in the upper unit and is relatively fresh and preserves original textures, although most glass shards are completely palagonitized except some pumice and scoriae. Constituents of the lapillistone (M3-07G, H; Fig. 8b) are white and gray woody pumice (~80 vol%) (Fig. 8c), black dense scoria (~5 vol%) (Fig. 8d, e), fragments of orthopyroxene and quartz and trivia clinopyroxene and plagioclase. Maximum grain size of pumice and scoria is 20 and 5 mm, respectively. Most pumice has minor quartz, plagioclase and hypersthene phenocrysts set in a glassy matrix with a few microlites. Scoria is of two types; one is crystal-free boninite scoria consisting of glass only (Fig. 8d), and the other is porphyritic boninite scoria with 10-20 vol% orthopyroxene phenocrysts and microphenocrysts with rare clinopyroxene phenocrysts in a glassy matrix with some clinopyroxene microlites (Fig. 8e). A few lithic clasts have ~80 vol% groundmass minerals and phenocrysts. Coarse tuff is intervened by lenticular beds of fine tuff in the upper part of the unit. The upper coarse tuff (M3-07I; Fig. 8b) is mainly composed of woody pumice and fragments of orthopyroxene, quartz, clinopyroxene, and minor plagioclase. An agate layer intercalates between the coarse tuff and the overlaying pillow lava.

On the northeastern coast of Mukojima, a ~~forty centimeter-thick~~ tuff (M2-06D) (Figs 6c, 8f) is intercalated between overlaying massive boninite tuff breccia and underlying boninite pillow lava. The lower half of the tuff is mainly composed of coarse ash-sized pumice, mineral fragments and minor scoria. The upper half is alternating beds of lapillistone and coarse tuff. The lapillistone consists of white pumice <15 mm in diameter and a small amount of scoria <3 mm in diameter and crystal fragments of orthopyroxene, plagioclase, quartz and clinopyroxene. Glassy matrices of pumice and scoria are partially

and completely altered to clay minerals, respectively.

A pumice tuff layer (N2-09) (Figs 6e, 8g) is exposed in the eastern cliff of Nakodojima. The pumice tuff about 2 m in maximum thickness is overlain by rhyolite tuff breccia and underlain by bronzite andesite tuff breccia. Samples of the tuff were recovered from the top of a ridge south of Mt. Byobuyama (Fig. 6e), where the pumice tuff becomes thinner to the north about 30 cm in thickness. Most of the constituents are gray and white woody pumice <5 cm in diameter and minor amounts of orthopyroxene and quartz fragments. Because pumice is nearly aphyric, mineral fragments are most likely derived from phenocrysts from quartz rhyolite and boninite lavas. The majority of the pumice tuff is altered to clay minerals.

2. Glass and mineral compositions of tephras

Glass and mineral compositions are shown in Fig. 10, Table S1 and S2. The most magnesian glass compositions from samples M3-07G and M3-07H were obtained for crystal-free boninite scoriae, which contain 56.9 to 61.1 wt% SiO_2, 6.7 to 8.3 wt% MgO, 8.3 to 11.4 wt% CaO and 0.43 to 0.45 ppm Yb with Zr/Ti ratio of 0.016. In contrast, the matrix glass of crystal-rich boninite scoriae has 58.2-63.6 wt% SiO_2, 5.4-5.9 wt% MgO, 8.2-10.5 wt% CaO, and 0.66-0.80 ppm Yb, with 0.021-0.023 Zr/Ti ratio (Fig. 10a, b). Orthopyroxene phenocrysts and microphenocrysts in crystal-rich scoriae mostly range in Mg# (Mg/(Mg+Fe)) from 0.85 to 0.90 and rarely from 0.66 to 0.78. Few clinopyroxene in the scoriae has Mg# 0.72 (Fig. 10c). Glass matrices of pumice have 68-82 wt% SiO_2, 0.1-2.1 wt% MgO and 0.62-1.48 ppm Yb (Fig. 10a, b). The sample M3-07I includes pumice with a glass composition of 75.6-77.9 wt% SiO_2 and 1.0-1.7 wt% MgO (Fig. 10a).

Glass of scoriae in sample M2-06D was not analyzed due to severe alteration. Pumice contains 70.0-80.0 wt% SiO_2 and 0.1-2.3 wt% MgO (Fig. 10a).

Fragmental orthopyroxenes included in samples M3-07G, H, I and M2-06D have a similar

compositional range, which forms two clusters. Most orthopyroxene crystals have 0.77-0.91 Mg#, while the rest has Mg# = 0.64-0.75. Samples M3-07G, H and M2-06D contain minor fragmental augite, while M3-07I carries more common clinopyroxenes ranging from augite to sub-calcic augite and a lesser amount of pigeonite. Sub-calcic augite has higher in Al_2O_3 content than augite (Fig. 10c). M2-06D commonly has fragmental plagioclase, most of which ranges in An_{83-90}, whereas M3-07G, H and I rarely have plagioclase.

Glass compositions of pumice in N2-09 have narrow ranges from 77.1 to 78.7 wt% SiO_2, 0.3 to 0.5 wt% MgO and 0.91 to 1.1 ppm Yb (Fig. 10a, b). Fragmental orthopyroxenes have Mg#0.79-0.87 (Fig. 10c).

Trace element compositions of the pumice glass from Nakodojima and Mukojima cannot be reconciled with those of the bulk quartz rhyolite by the addition and subtraction of plagioclase and pyroxenes phenocrysts. Therefore, the pumice must have been derived from a different magma from that of quartz rhyolite in Nakodojima.

Whole rock geochemistry of Ogasawara Islands

1. Major elements

Mukojima Island Group is composed of boninite and arc tholeiitic-rock series. Boninite-series rocks are divided into high- and low-Si boninite series that form two distinct compositional trends. . High-Si boninite-series rocks form the entire Yon'noiwa, Sasayojima, Mukojima, and main portions of Nakodojima and Yomejima, while low-Si boninite-series rocks occur in Harinoiwa, Tatamiiwa, the uppermost Yomejima and also as andesite hyaloclastite in Nakodojima. Arc tholeiite-series rocks compose Ninoiwa, Kitanoshima and Nakanoshima (Fig. 11; Table S3).

High-Si boninite-series rocks of the Mukojima Island Group consist of boninite, bronzite andesite, dacite and quartz rhyolite, which range in SiO_2 from 54.6 to 77.1 wt%. In general, high-Si boninite-series shows sharp bends around 60 wt% SiO_2 on MgO, Al_2O_3, CaO and FeO*/MgO vs. SiO_2 diagrams (Fig. 11;

Table S3). For example, with increasing SiO_2, MgO decreases and Al_2O_3 increases until 60 wt% SiO_2, and both gradually decrease in higher (>60 wt%) SiO_2. These compositional range and characteristics are the same as those of the Maruberiwan and Asahiyama Formations in the Chichijima Island Group (Umino 1985; 1986; Taylor *et al*. 1994; Umino & Nakano 2007), which is distinctive from arc tholeiitic and calc-alkalic rocks from the Ogasawara Islands (Taylor & Nesbitt 1995; Yajima *et al*. 2001; Umino & Nakano 2007; Haraguchi *et al*. 2008; Kanayama *et al*. 2010), Quaternary volcanic front (Taylor & Nesbitt 1998; Ishizuka *et al*. 2007) and the Ogasawara forearc (Ishizuka *et al*. 2011). However, high-Si boninite-series rocks that fall between 65 and 73 wt% SiO_2 (dacite) in the Mukojima island Group are very few, whereas boninite series of the Maruberiwan Formation varies continuously from 54 to 78 wt% SiO_2. Some high-Si boninite-series rocks with 60-64 wt% SiO_2 from the upper central block of Nakodojima form a distinct trend which plots off the compositional trend of the main high-Si boninite-series rocks of the Ogasawara Islands (Fig. 11). They plot on a tie line connecting a boninite with 60 wt% SiO_2 and a dacite with 64 wt% SiO_2, suggesting magma mixing of these two end components. This is supported by the presence of disequilibrium textures such as resorbed hypersthene and augite enclosed by magnesian bronzite.

Low-Si boninite series-rocks of the Mukojima Island Group consist of bronzite andesite with 57.9-60.9 wt% SiO_2. They have 0.26-0.41 wt% TiO_2, 5.5-4.1wt% MgO and 1.6-2.6 FeO*/MgO, which generally plot within the compositional range of low-Si boninite series of the Mikazukiyama Formation (Yajima & Fujimaki 2001; Umino & Nakano 2007) unconformably overlying the Maruberiwan and Asahiyama Formations in the Chichijima Island Group (Umino & Nakano 2007) (Fig. 11; Table S3). Compositional variations of these low-Si boninite-series rocks of the Ogasawara Islands partially overlap with those of bronzite andesite from DSDP Site 458 (Meijer *et al*. 1981; Wood *et al*. 1981; Reagan *et al*. 2010). Such low-Si boninite-series rocks show intermediate compositional ranges between high-Si boninite-series rocks in the Mukojima and Chichijima Island Groups and arc lavas of the Hahajima Island

Group.

Arc tholeiitic rocks of the Mukojima Island Group range from andesite to dacite with 58.3-71.0 wt% SiO_2, 0.43-0.76 wt% TiO_2, 6.0-9.2 wt% FeO*, 1.72-6.3 wt% MgO and 1.4-3.8 FeO*/MgO ratio (Fig. 11; Table S3). These rocks plot within a field of calc-alkaline rocks on the FeO*/MgO vs. SiO_2 diagram (Fig. 11). However, these samples are severely altered under greenschist-facies metamorphism and SiO_2 is significantly raised as indicated by pervasive quartz veins and vesicle fillings. Positive correlations of immobile Ti and Zr indicating Ti enrichment with differentiation, as well as slight LREE-depleted REE patterns are concordant with the view that they are primarily tholeiitic. They plot within the range of the John Beach Volcanics in Chichijima (Umino & Nakano 2007; Ishizuka *et al*. 2012), except for extremely low CaO (1.5-3.7 wt%) and high Na_2O (4.1-6.3 wt%) which can also be ascribed to greenschist-facies alteration. Arc tholeiitic rocks of the Mukojima Island Group and the John Beach Volcanics characteristically show lower P_2O_5 contents than the Hahajima Island Group lavas (Taylor & Nesbitt 1995; Yajima *et al*. 2001; Kanayama *et al*. 2010) (Fig. 11).

2. Trace elements

High-Si boninite-series rocks from the Mukojima Island Group have 3.3-36.5 ppm Rb, 0.75-4.47 ppm Pb, 6.0-72.9 ppm Zr, 0.34-2.62 La ppm and 0.35-3.01 ppm Yb, which is similar to those of the Maruberiwan and Asahiyama Formations in the Chichijima Island Group (Taylor *et al*. 1994) (Fig. 12a, b, Table S3). The high-Si boninite-series rocks have characteristic highly depleted, U-shaped chondrite-normalized REE patterns, positive anomaly of Zr and Hf (Zr/Ti=0.01-0.09) in spider diagrams and higher LILE (large ion-lithophile element)/Nb (Ba/Nb=29-161, Th/Nb=0.21-0.87, Pb/Nb=1.53-10.6) ratios compared with tholeiitic and calc-alkaline lavas of the Eocene and Quaternary volcanic front (Taylor & Nesbitt 1995; 1998; Ishizuka *et al*. 2007; Yajima *et al*. 2001, Kanayama *et al*. 2010), which suggests

larger degrees of source depletion and the contribution of slab input (Fig. 12a, b, 13).

Low-Si boninite-series rocks from the Mukojima Island Group indicate flat REE and slightly LREE-depleted patterns with 9.7-13.3 ppm Rb, 28.5-43.3 ppm Zr and 0.83-1.35 ppm Yb (Fig. 12c, d, Table S3). LILE/Nb ratios (Ba/Nb=38-57, Th/Nb=0.24-0.40, Pb/Nb=2.24-2.81) are similar to or lower than the high-Si boninite-series rocks and higher than the Hahajima arc tholeiitic and calc-alkaline rocks. These rocks are similar to low-Si boninite-series rocks of the Mikazukiyama Formation in HREE, HFSE and LILE abundances (Fig. 12c, d, 13). However, LREE-depleted REE patterns of the low-Si boninite-series rocks of the Mukojima Island Group are similar to bronzite andesite from site 458 (Hickey & Frey 1981; Reagan *et al*. 2010) rather than the U-shaped REE patterns of low-Si boninitic rocks of the Mikazukiyama Formation (Fig. 12c, d).

Arc tholeiitic andesite and dacite of the Mukojima Island Group have compositions (1.78-9.11 ppm Rb, 23.0-66.9 ppm Zr, 01.06-2.68 ppm Yb and La/Yb = 0.67-1.14) that are similar to or more depleted than the John Beach Volcanics (Chichijima) (Fig. 12 e, f, Table S3). Highly scattered LILEs abundances such as Cs, Rb and Ba for tholeiitic rocks from the Mukojima Island Group is most likely due to pervasive low temperature alteration (Fig. 12e). Lower Nb/Yb (0.23-0.34) and higher LILE/Nb (Ba/Nb=47-396, Th/Nb=0.25-0.41, Pb/Nb=1.26-2.17) ratios distinguish them from the Hahajima arc tholeiitic and calc-alkaline rocks (Nb/Yb=0.28-1.49, Pb/Nb=0.21-1.38) (Fig. 13). LREE/HREE ratios of these tholeiites from the Mukojima Island Group and the John Beach Volcanics are higher than those of MORB-like basalt from the Ogasawara Trench (La/Yb=0.27-0.72; Ishizuka *et al*. 2011) (Fig. 12f).

3. Classification of high-Si boninite

High-Si boninite occurs in Yon'noiwa, Sasayojima, Mukojima, Nakodojima and Yomejima. Boninite of Mukojima Island Group is divided into three types on the basis of major and trace element

458 characteristics (Fig. 14). Although REE abundances of type 1, 2 and 3 boninites are similar (e.g.,
459 Yb=0.36-0.61 ppm; Fig. 14c), significant differences are apparent especially for SiO_2, CaO, Al_2O_3, total
460 alkali (Na_2O+K_2O) contents, CaO/Al_2O_3, Zr/Ti and LILE/HREE ratios. Chemical characteristics of each
461 type are described as follows:

462 *Type 1 high-Si boninite* This comprises dikes, pillow lavas, massive and bedded tuff breccia in the
463 stratigraphically middle part of Mukojima as well as most boninite successions in the rest of the Mukojima
464 Island Group. They have high SiO_2 (>57.0 wt%), total alkali (>1.7 wt%), Zr/Ti (>0.022) and LILE/HREE
465 (Ba/Yb>51), medium to high Al_2O_3 (9.4-11.6 wt%), and low CaO (<8.0 wt%) and CaO/Al_2O_3 (<0.8). They
466 plot within the range of “low-Ca boninite” of Crawford *et al*. (1989) that includes most boninites from the
467 Izu-Ogasawara-Mariana forearc. Type 1 high-Si boninites are similar to boninites from the Maruberiwan
468 Formation on Chichijima (“Type I, II and III boninites” of Umino (1986) and most boninites described by
469 Taylor *et al*. (1994)), Mariana Trench such as D28, D50 and site 1403 (e.g. Bloomer & Hawkins 1987),
470 Cape Vogel (e.g. Walker & Cameron 1983) and New Caledonia (Shiraki *et al*. 1984), however, they are
471 discriminated from boninites having lower SiO_2 (<56.7 wt%) contents from ODP Site 786 (Arculus *et al*.
472 1992; Pearce *et al*. 1992b), DSDP Site 458 (e.g. Hickey-Vargas 1989) and the Guam Facpi Formation (e.g.
473 Reagan & Meijer 1984).

474 *Type 2 high-Si boninite* forms pillow lava and pyroclastic rocks in the upper part of Mukojima.
475 This has lower SiO_2 (<57.1 wt%), total alkali (<1.4 wt%), Zr/Ti (<0.010) and LILE/HREE (Ba/Yb<47)
476 ratios, medium CaO (8.8-9.1 wt%) content and CaO/Al_2O_3 (0.8) ratio, and high Al_2O_3 (>10.7 wt%). “Type
477 IV boninite” of Umino (1986) from the Maruberiwan Formation in Chichijima is geochemically and
478 petrographically identical to type 2 boninite. SiO_2, FeO*, Zr/Ti and LILE/HREE ratios of this type are
479 similar to low-Si boninites of the Mikazukiyama Formation. However, CaO, Al_2O_3, total alkali and trace
480 element concentrations are clearly lower, and MgO and CaO/Al_2O_3 are higher than in the low-Si boninites.

Although CaO/Al_2O_3 and total alkali contents of type 2 boninite are similar to “high-Ca boninite” of Crawford *et al*. (1989) of which reference site is the Troodos ophiolite (e.g. Cameron 1985), type 2 boninite is readily distinguished from Crawford’s high-Ca boninite in terms of higher SiO_2 and FeO* contents, and lower Al_2O_3 and CaO contents. REE contents of Mukojima type 2 boninite is more depleted than the Troodos boninite (e.g. Cameron 1985).

Type 3 high-Si boninite forms pillow lavas and bedded and massive tuff breccia of Mukojima. They have remarkably high CaO/Al_2O_3 (0.9-1.1), medium to high CaO (7.8-9.8 wt%) and SiO_2 (57.6-60.7 wt%), medium Zr/Ti (0.018-0.027) and LILE/HREE (Ba/Yb=36-76), and low to medium total alkali (1.2-1.9 wt%) and Al_2O_3 (7.9-10.4 wt%) contents. Type 3 boninite has intermediate chemical compositions between type 1 and 2 except that type 3 has the highest CaO/Al_2O_3 and CaO and the lowest Al_2O_3.

Discussion

1. Volcanic activity of the Mukojima Island Group

Common occurrence of pillow lava in the lower portion of Mukojima suggests quiet to moderate eruptions at water depths more than several hundred meters. This agrees with the estimated water depth up to 5000 m (as discussed below) for the lower Maruberiwan Formation on Chichijima, where pillow lava dominates over a few pyroclastic interbeds. Increasingly pyroclastic deposits are found stratigraphically higher on Mukojima suggests that the water depth of the source vent(s) shallowed as the volcanic edifice grew. However, the common presence of poorly vesiculated scoria (<10 vol %) and water-chilled volcanic bombs still indicates submarine eruptions.

Nakodojima andesite lavas have similar SiO_2 contents to the lower boninite lavas in Mukojima, which form intact, close-packed pillows. However, hyaloclastic fragmentation of lava into glassy to aphanitic clasts prevails on Nakodojima. Unlike boninite, hyaloclastic andesite lavas have abundant

plagioclase microlites in the groundmass. Fragmentation of lava into aa clinker may be caused by plagioclase crystallization prior to extrusion, because the presence of plagioclase significantly increases relaxation time of stress induced by cooling and shearing of erupting lava (Polacci *et al.* 1999). This suggests that fragmentation of the Nakodojima lavas was caused by higher viscosities due to crystallization of plagioclase enhanced by degassing under shallower water as well as accompanying fractionation of mafic minerals. The pumice tuff on Nakodojima is composed of "woody pumice" with numerous tubular, subparallel vesicles, suggesting a low vapor pressure during eruption such as under submarine environment (Fisher & Schmincke 1984; Kato 1987). The presence of surge deposits on Yomejima also suggests that the eruption took place about sea level because surges are turbulent low-density currents generally formed above the water level.

Therefore, volcanic activities of the Mukojima Island Group began with quiet extrusion of pillow lava under deep water at a depth of hundreds of meters. As the volcanic edifice grew, the activity changed gradually into moderately explosive and produced pyroclastic rocks under shallow water or above sea level and formed the upper succession of Mukojima, Nakodojima and the uppermost part of Yomejima. The shallowing water depth of the Mukojima Island Group is consistent with the uplift of the entire Ogasawara Ridge during the Eocene period (Fig. 4; Umino & Nakano 2007; Umino *et al.* 2009).

2. Correlation and emplacement of tephras

Lower-MgO (<1 wt%) and higher-SiO_2 (>75 wt%) contents of pumice in M3-07G, H and M2-06D from Mukojima and N2-09 from Nakodojima have similar glass composition, suggesting that these tephras were derived from the same source, maybe the same eruption. Likewise, coincidence of major element compositions of pumice glass with higher MgO (>1 wt%) and lower SiO_2 (<75 wt%) contents of M3-07G,

H, I and M2-06D indicates a similar origin (Fig. 8). Although pumice with higher MgO (>1 wt%) has not been recovered from N2-09 in Nakodojima, limited sampling of Nakodojima tephra does not exclude this as a possible source because it is the only island among Mukojima Island Group that yields felsic magmas. Furthermore, the maximum size of pumice is several cm on Nakodojima, much larger than that on Mukojima. It is very likely that Mukojima tephra was derived from volcano near Nakodojima. On the other hand, scoriae included in M3-07G and H are low-Zr/Ti type 2 boninite. Presumably these were reworked from pyroclastic deposits on Mukojima, which are the main constituent of the upper Mukojima sequence.

Mukojima pumice and scoriae were transported by turbidity currents toward S50-88°E as indicated by imbrication of pyroclastic clasts. It is likely that pumices were erupted near the present site of Nakodojima and were originally transported by currents northwards and deposited on the seafloor. Then, it was transported by turbidity currents which reworked unconsolidated boninite scoriaceous deposits and redeposited these as a mixture of pumice, scoriae, crystal and lithic clasts in the southeast of Mukojima.

3. Correlation of Mukojima and Chichijima Island Group volcanic strata

Volcanic rocks from the Mukojima Island Group are the same rock types that occur in the Chichijima Island Group (Umino 1985; Umino & Nakano 2007). Major and trace element bulk compositions and the differentiation trends of most high-Si boninite-series rocks of the Mukojima Island Group are identical to those of the Maruberiwan and Asahiyama Formations of the Chichijima Island Group (Figs 11, 12, 13). Radiometric dating Mukojima and Chichijima Island Groups boninitic rocks indicate that high-Si boninitic magmatism were simultaneously active at both sites (Fig. 5; Ishizuka *et al.* 2006, 2011; Umino *et al.* 2009). We can make some estimates about the water depth at which these lavas were erupted. The lowermost Maruberiwan Formation on Chichijima is dominated by pillow lava (Fig. 3; Umino 1985; Umino & Nakano 2007). Although H_2O solubility in Maruberiwan boninite melt is

experimentally determined only for pressures >900 MPa (Umino & Kushiro 1989), these data plot on the extrapolated solubility curve for a boninitic melt estimated by the method of Moore *et al.* (1998). Given a primary water content of 2.2 wt% retained in the boninite lava upon extrusion (Dobson *et al.* 1995), the water depth is estimated as 5000 m based on the calculated solubility of H_2O in the boninitic melt. However, the middle to uppermost Maruberiwan Formation and the Asahiyama Formation have a larger amount of pyroclastic deposits including scoriae, volcanic bombs and fragmentary lava clasts. These pyroclastic rocks are overlain by the Mikazukiyama Formation including a subaqueous pyroclastic flow deposit composed of well-vesiculated pumice (Fig. 3; Umino 1985; Umino & Nakano 2007). The coincidental shallowing of eruption depths is ascribed to uplift of the entire Ogasawara Ridge during 48-44 Ma (Umino & Nakano 2007; Umino *et al.* 2009).

The above evidence suggests that most high-Si boninite-series volcanic strata on Mukojima Island Group are likely to have been formed simultaneous with eruptions to form the Maruberiwan and Asahiyama Formations on Chichijima Island Group (Fig. 5).

In Chichijima Island Group, erosional surfaces indicating obvious quiescent period are identified between high-Si boninite, bronzite andesite and dacite of the Maruberiwan Formation and quartz dacite and rhyolite of the Asahiyama Formation, and between the Asahiyama Formations and low-Si boninite series and calc-alkaline rocks of the Mikazukiyama Formations (Umino 1985; Umino & Nakano 2007). However, in Mukojima Island Group, high-Si boninite, bronzite andesite, dacite and quartz rhyolite lavas and breccias alternate on Nakodojima, and radiometric ages for Nakodojima quartz rhyolite (48 Ma) is older than that of Mukojima boninite (46.6 Ma), indicating that these magma types erupted about the same time (Fig. 4, 5).

Whole rock compositions of low-Si boninite-series rocks of the Mukojima Island Group are similar to 45-Ma low-Si boninite-series rocks of the Mikazukiyama Formation (Yajima & Fujimaki 2001;

Ishizuka *et al.* 2006; Umino & Nakano 2007) which occur between 48-46-Ma high-Si boninite and 45-40 Ma arc tholeiitic and calc-alkaline rocks in Hahajima (Ishizuka *et al.* 2006) (Figs 11, 12, 13). The low-Si boninitic andesite breccia from the uppermost Yomejima is correlatable with the Mikazukiyama Formation because of its radiometric age (44 Ma; Ishizuka *et al.* 2011) and isotopic ratios (Ishizuka, unpublished data, 2011) in addition to bulk major and trace element compositions (Fig. 5). In Nakodojima, low-Si boninite-series andesite lava is presumably interbedded with high-Si boninite-series lavas, suggesting that such transitional low-Si boninite magma and high-Si boninite magma are simultaneously active (Figs 4, 5). Although radiometric ages and stratigraphic relationships of the low-Si boninitic andesite of Harinoiwa and Tatamiiwa with the other rock types are unknown, these low-Si boninitic andesites are probably correlatable to the Maruberiwan or Mikazukiyama Formations.

Although radiometric dating has not been successful for John Beach Volcanics tholeiitic andesite and dacite from Chichijima and Mukojima Island Groups, similar geochemical characteristics of these two tholeiitic suites strongly suggest similar sources during pre-boninite volcanism (Fig. 3; Umino 1985; Umino & Nakano 2007). Moreover, tholeiitic lavas and pyroclastics on Ninoiwa, Kitanoshima and Nakanoshima suffered amphibolite-facies metamorphism, whereas Mukojima Island Group boninite-series rocks are relatively fresh. The higher metamorphic grade of the tholeiitic rocks of the former islands is consistent with the view that they are stratigraphic lower than and were once buried beneath boninite-series rocks. Arc tholeiitic rocks of Mukojima Island Group and the John Beach Volcanics may be transitional type between MORB-like and boninitic rocks, like tholeiitic lava of Site 458 and 459 (Figs 12, 13) (Hickey & Frey 1981; Reagan *et al.* 2010).

Consequently, the Maruberiwan, Asahiyama and Mikazukiyama Formations in Chichijima Island Group (Umino 1985; Umino & Nakano 2007) can be correlated with Mukojima Island Group volcanic successions (Figs 4, 5).

596

597

598 ***4. Petrogenesis of boninites from the Mukojima Island Group***

599 As shown in Fig. 14, vectors controlled by phenocrystic phases cannot reproduce chemical trends
600 of type 1 boninite by fractionation of type 2 boninite, and vice versa. Therefore, type 1 and 2 boninites are
601 derived from discrete parental magmas. Type 3 boninite has both normally zoned high-Mg# and reversely
602 zoned low-Mg# pyroxenes, and resorbed plagioclase in a single specimen. Therefore, it is likely that type 3
603 boninite is a mixing product of evolved magmas with augite, hypersthene and plagioclase and type 1 or 2
604 boninite magmas. However, no boninite-series and tholeiitic- and calc-alkaline rock-series lavas plot on
605 the extensions of postulated mixing lines connecting type 1 or 2 and 3 boninites. On the contrary, type 3
606 boninites can be reproduced by adding augite, hypersthene and plagioclase to type 1 boninite (Fig. 14).
607 Compositional variations among type 3 boninites can form by mixing type 1 boninite and the variable
608 proportions of augite, hypersthene and plagioclase. The presence of rare resorbed plagioclase clots in type
609 3 boninite suggest plagioclase dissolution in type 1 boninite magmas which are undersaturated with
610 plagioclase. The absence of evolved end member magma can be reconciled if captured crystals derived
611 from a mushy magma reservoir which were heated and partially remobilized by the supply of hot boninite
612 magma (e.g. Umino & Horio 1998; Costa *et al*. 2010; Huber *et al*. 2012).

613 Boninite-series rocks are geochemically characterized by their U-shaped REE patterns, depletion
614 in HFSEs (high-field-strength elements) and Nd isotope ratios, and enrichment in LILEs (e.g. Hickey &
615 Frey, 1982; Pearce *et al*. 1992a, b). Pearce *et al*. (1992a, b) and Taylor *et al*. (1994) concluded that trace
616 element and isotopic ratios of boninite from ODP Site 786 and those of the Chichijima Maruberiwan
617 Formation are explained by mixing three components: depleted mantle peridotite, hydrous melt resulted
618 from slab melting in the presence of residual amphibole, and typical slab dehydration fluids.

Type 1 boninite from Mukojima has the same range in trace element concentrations and ratios, such as Zr/Ti and Sm/Zr, with most Maruberiwan Formation boninite (Type I, II and III boninites of Umino (1986)) and low-Ca boninite of ODP Site 786 (Pearce *et al*. 1992a, b). In contrast, type 2 boninite has markedly low Zr/Ti and high Sm/Zr ratios. Type 2 boninite is geochemically and petrographically identical to Type IV boninite of Umino (1986) from the Chichijima Maruberiwan Formation, however, the petrogenesis of type 2 has not been discussed by the previous studies.

Boninites are severely depleted in incompatible elements such as HFSEs and REEs, which are inherited from a depleted source mantle. Production of MORB-like basalt may have depleted this source. We will discuss the Zr/Ti versus Yb variations of type 1 and 2 boninites (Fig. 15) based on the model calculation of melting of boninite source which is a mixture of 15%-batch melts of depleted peridotite (0 to 20% partial melts subtracted Depleted MORB Mantle (DMM: Workman & Hart 2005) before 15% melting) and amphibolitic slab melt. The model calculations suggest that the degree of depletion of the source mantle for type 1 and 2 boninites does not vary. This result indicates that boninite sources were considerably more refractory than the sources for MORB and arc basalt such as those of Hahajima and the Quaternary Izu-Ogasawara arc. The modeling also indicates that Zr enrichment of boninites can be explained by contributions of partial melt of hydrated basaltic slab with amphibolite residue. Because Ti is more compatible than Zr in amphibolite (Hilyard *et al*. 2000), melt in equilibrium with amphibolitic residue has a high Zr/Ti. With the consensus that magmas of the Quaternary volcanic front of the Izu-Ogasawara arc are produced by fluxing the mantle by fluids and melts derived from subducted sediments and oceanic crust (Taylor & Nesbitt 1998; Ishizuka *et al*. 2007), the slab melting under amphibolite facies indicates a much hotter shallow wedge mantle at ~48 Ma than in Quaternary time. This is consistent with the suggestion of asthenospheric upwelling at the initiation of the Izu-Ogasawara subduction zone (Stern & Bloomer 1992; Ishizuka *et al*. 2006, 2011; Reagan *et al*. 2010). The modeling also suggests that the

642 difference in Zr/Ti ratio between type 1 and 2 Mukojima boninites can be explained by different
643 proportions of amphibolitic slab melt added to a similar mantle source: Type 1 boninite with higher Zr/Ti
644 reflects more slab melt (7-15%), whereas type 2 boninite with lower Zr/Ti has less (4-5%). Maruberiwan
645 Formation boninite magma is considered to have been produced by partial melting of hydrous and highly
646 depleted mantle at shallow depths (0.8-1.2 GPa and 5% H_2O; Umino & Kushiro 1989; 0.3 GPa and 3% H_2O;
647 van der Laan *et al.* 1989). However, differences in major and trace element compositions between type 1
648 and 2 boninites require different melting conditions, such as temperature, pressure, water content, source
649 depletion, and degrees of melting. Petrogenetic models should explain both major and trace element
650 characteristics and differences of type 1 and 2 boninite magmas, which we will address in the future.
651
652 **Summary**
653 Mukojima Island Group consists of three clusters of islands from NNW to SSE: 1) Ninoiwa,
654 Yon'noiwa, Kitanoshima, Nakanoshima and Sasayojima in the north; 2) Mukojima, Harinoiwa, Tatamiiwa
655 and Nakodojima in the middle; and 3) Yomejima in the south. Kitanoshima, Nakanoshima and Ninoiwa in
656 the northern cluster consist of tholeiitic andesite and dacite, which form agglutinate and pillow and sheet
657 lava suffered from greenschist-facies alteration; these rocks are undated but are thought to be the oldest
658 strata on the Mukojima Island Group. The other two clusters of islands are composed of boninite-series
659 rocks that range in age from 48 to 44.3 Ma. Boninite and bronzite andesite mainly occur as pillow lava and
660 pyroclastic rocks, however, bronzite andesite lava exists as brecciated pillows and hyaloclastite.
661 Nakodojima dacite and quartz dacite occur as hyaloclastite and tephra. Hydrothermal alteration associated
662 with copper-bearing mineral deposits is present on Nakodojima and Maejima. Pumice-bearing tephra occurs
663 at stratigraphically upper levels in Nakodojima and Mukojima, which are correlated based on mineral and
664 glass compositions. Thicknesses of moderately undulating volcanic strata attains more than 830 m on

Kitanoshima and Nakanoshima, 750 m on Mukojima, 240 m on Nakodojima, and 480 m on Yomejima. NW-SE and NNE-SSW trending faults dominate on Mukojima and Nakodojima, respectively. Ninoiwa, Kitanoshima and Nakanoshima tholeiites are correlated with the John Beach Volcanics of Chichijima, which is the lowermost unit Maruberiwan Formation. Other islands in the Mukojima Islands Group comprising boninite-series rocks are correlated with the main part of the 48 to 46-Ma Maruberiwan and Asahiyama Formations, and perhaps correlated with the 45-44 Ma Mikazukiyama Formation of Chichijima. The uppermost Yomejima are correlated to the Mikazukiyama Formation. All boninite-series rocks from boninite to dacite are interbedded on Nakodojima, indicating concurrent activity of these magma types.

Volcanic activity now preserved on the Mukojima Island Group began with quiet submarine extrusion of pillow lava at a depth of hundreds of meters. As the volcanic edifice grew, the activity changed gradually into moderately explosive eruptions that produced pyroclastic fall and flow deposits under shallow water or above sea level; these sequences are preserved in the upper Mukojima and Nakodojima and uppermost Yomejima strata. The shallowing water depth of volcanic sequences exposed in the Mukojima Island Group is consistent with the uplift of the entire Ogasawara Ridge during the Late Eocene period.

Most boninite-series rocks of the Mukojima Island Group belong to high-Si boninite series which show the same major and trace element compositional ranges and differentiation trends as those of the Maruberiwan and Asahiyama Formations of Chichijima. They have remarkably low TiO_2, depleted U-shaped REE patterns, higher LILE/Nb and Zr/Ti ratios. Major and trace element compositions of low-Si boninitic andesites from Harinoiwa, Tatamiiwa, Nakodojima and Yomejima plot within the ranges of low-Si boninite series rocks from the Mikazukiyama Formation of the Chichijima Island Group, which are intermediate between the high-Si boninite series and tholeiitic and calc-alkaline rocks from Hahajima Islands. Tholeiitic rocks of the Mukojima Island Group resemble the John Beach Volcanics in terms of

major and trace elements. They are lower in P_2O_5 and Nb/Yb, and higher in LILE/Nb than the Hahajima andesite and dacite.

Type 1 and 2 boninites have discrete parental magmas. Trace element modeling shows that type 1 and 2 boninites can be produced by partial melting of DMM which experienced 12 to 18 %-melt subtraction before melting. This pre-melting source depletion is most plausibly the consequence of formation of the MORB-like basalt that predates boninite magmatism in this region. The modeling also suggests that difference in Zr/Ti between type 1 and 2 boninites can be explained by varying degrees of amphibolitic slab-melt contribution, which is higher (7-15%) for type 1 boninite with higher Zr/Ti ratios and lower (4-5%) for type 2 boninite with lower Zr/Ti ratios. Type 3 boninite does not represent a liquid composition but is a contaminated type 1 boninite with xenocrysts of augite, hypersthene and plagioclase.

Acknowledgements

This study was carried out as a part of geological mapping project of the Ogasawara Islands by the Geological Survey of Japan (GSJ) and was partly supported by the Monkasho Grant-in-Aid for Scientific Research #20109002. We would like to thank S. Nakano for providing financial support and usage of the GSJ laboratory and N. Honda for her assisting the analytical work. We appreciate H. Wada and S. Arai for their constructive advice and discussion. Mr. and Ms. Ohno, Captains Y. Takase, Stanly and George Minami kindly supported us during field work in Ogasawara.

Reference

ARCULUS R. J., PEARCE J. A., MURTON, B. J. & VAN DER LAAN S. R. 1992. Igneous stratigraphy and major-element geochemistry of Holes 786A and 786B. *In* Fryer P., Pearce J.A., Stokking L. *et al.* (eds.) *Proceeding of the Ocean Drilling Program, Scientific Results* **125**, pp. 623-59, Ocean Drilling

711 Program, College Station, TX.

712 BLOOMER S. H. & HAWKINS J. W. 1987. Petrology and geochemistry of boninite series volcanics rocks

713 from the Mariana trench. *Contribution to Mineralogy and Petrology* **97**, 361-77.

714 CAMERON W. E. 1985. Petrology and origin of primitive lavas from the Troodos ophiolite, Cyprus.

715 *Contributions to Mineralogy and Petrology* **89**, 239-55.

716 COSCA M. A., ARCULUS R. J., PEARCE J. A. & MITCHELL J. G. 1998. $^{40}Ar/^{39}Ar$ and K–Ar

717 geochronological age constraints for the inception and early evolution of the Izu–Bonin–Mariana arc

718 system. *The Island Arc* **7**, 579-95.

719 COSTA F., COOGAN L. A. & CHAKRABORTY S. 2010. The time scales of magma mixing and mingling

720 involving primitive melts and melt–mush interaction at mid-ocean ridges. *Contribution to*

721 *Mineralogy and Petrology* **159**, 371-87.

722 CRAWFORD A. J., FALLOON T. J. & GREEN D. H. 1989. Classification, petrogenesis and tectonic

723 setting of boninites. *In* Crawford, A. J. (ed.) *Boninites and Related Rocks*. pp. 339-56, Unwin Hyman,

724 London.

725 DALLWITZ W. B., GREEN D. H. & THOMPSON J. E. 1966. Clinoenstatite in a volcanic rock from the

726 Cape Vogel area, Papua. *Journal of Petrology* **7**, 375-403.

727 DOBSON P. F. 1986. The petrogenesis of boninite: a field, petrologic, and geochemical study of the

728 volcanic rocks of Chichi-jima, Bonin Islands, Japan. Ph.D Dissertation, Stanford University, CA, 163

729 pp.

730 DOBSON P. F., SKOGBY H. & ROSSMAN G. R. 1995. Water in boninite glass and coexisting

731 orthopyroxene: concentration and partitioning. *Contributions to Mineralogy and Petrology* **118**,

732 414-19.

733 FISHER R. V. & SCHMINCKE H. U. 1984. *Pyroclastic rocks*. 472 pp., Springer-Verlag, Berlin Heidelberg.

734 FLOWER M. F. J. & LEVINE H. M. 1987. Petrogenesis of a tholeiite-boninite sequence from Ayios Mamas,
735 Troodos ophiolite: evidence for splitting of a volcanic arc ?. *Contribution to Mineralogy and*
736 *Petrology* **97**, 509-24.
737 FRYER P., PEARCE J. A., STOKKING L. B. *et al*. 1990. *Proceedings of the Ocean Drilling Program,*
738 *Initial Reports* **125**, 1092 pp, Ocean Drilling Program, College Station, Texas.
739 HARAGUCHI S., ISHII T. & KIMURA J. 2008. Early tholeiitic and calc-alkaline arc magmatism of middle
740 to Late Eocene Age in the southern Ogasawara (Bonin) forearc. *Contribution to Mineralogy and*
741 *Petrology* **155**, 593-618.
742 HICKEY-VARGAS R. 1989. Boninites and tholeiites from DSDP Site 458, Mariana forearc. *In* Crawford A.
743 J. (ed.) *Boninites and Related Rocks*. pp. 339-56, Unwin Hyman, London.
744 HICKEY R. L. & FREY F. A. 1981. Rare-earth element geochemistry of Mariana fore-arc volcanics: Deep
745 Sea Drilling Project Site 458 and Hole 459B. *In* Hussong D. M. and Uyeda S. et al. (eds.) *Initial*
746 *Reports of the Deep Sea Drilling Project* **60**, pp. 709-30, U.S. Govt. Printing Office, Washington.
747 HICKEY R. L. & FREY F. A. 1982. Geochemical characteristics of boninite series volcanics: implications
748 for their source. *Geochimica et Cosmochimica Acta* **46**, 2099-115.
749 HILYARD M., NIELSEN R. L., BEARD J. S. PATIND-DOUCE A. & BLENCOE J. 2000. Experimental
750 determination of the partitioning behavior of rare earth and high field strength elements between
751 pargasitic amphibole and natural silicate melts. *Geochimica et Cosmochimica Acta* **64**, 1103-20.
752 HUBER C., BACHMANN O. & DUFEK J. 2012. Crystal-poor versus crystal-rich ignimbrites: A
753 competition between stirring and reactivation. *Geology* **40**, 115-8.
754 HUSSONG D. M., UYEDA S., KNAPP R., ELLIS H., KLING S. & NATLAND J. 1981. *Initial Reports of*
755 *the Deep Sea Drilling Project* **60**, 929 pp, US Government Printing Office, Washington D.C.
756 ISHIDA H., MORISHITA T., ARAI S. & SHIRASAKA M. 2004. Simultaneous in-situ multi-element

analysis of minerals on thin section using LA-ICP-MS. *The Science Reports of Kanazawa University* **48**, 31–42.

ISHII T. 1985. Dredged samples from the Ogasawara fore-arc seamount or “Ogasawara Paleoland”-“Fore-arc ophiolite”. *In* Nasu N., Kobayashi K., Uyeda S. Kushiro I. & Kagami H. (eds.) *Formation of active ocean margins*, pp. 307-42, Terra Scientific Publishing Company, Tokyo.

ISHIWATARI A., YANAGIDA Y. & LI Y. B. et al. 2006. Dredge petrology of the boninite- and adakite-bearing Hahajima Seamount of the Ogasawara (Bonin) forearc: An ophiolite or a serpentinite seamount? *The Island Arc* **15**, 102-18.

ISHIZUKA O., KIMURA J., LI Y. B. *et al*. 2006. Early stages in the evolution of Izu-Bonin arc volcanism: New age, chemical, and isotopic constraints. *Earth and Planetary Science Letters* **250**, 385-401.

ISHIZUKA O., TAYLOR R. N., YUASA M. *et al*. 2007. Process controlling along-arc isotopic variation of the southern Izu-Bonin arc. *Geochemistry Geophysics Geosystems* **8**, Q06008, doi: 10.119/2006GC001475.

ISHIZUKA O., TANI K., REAGAN M. K. *et al*. 2011. The timescales of subduction initiation and subsequent evolution of an oceanic island arc. *Earth and Planetary Science Letters* **306**, 229-40.

ISHIZUKA O., UMINO S., TAYLOR R. N., KANAYAMA K. 2012. Evidence for hydrothermal activity in the earliest stages of intraoceanic arc formation: implication to ophiolite-hosted hydrothermal activity. *Economic Geology* (in print).

KANAYAMA K., UMINO S. & ISHIZUKA O. 2010. Petrogenesis of primitive basalts formed at an early stage of subduction zone evolution: Geochemical characteristics and the origin of high-Mg basalts from the Hahajima Island Group, the Ogasawara (Bonin) Islands. *Fall Meeting, American Geophysical Union*, V33B-2382.

KATO Y. 1987. Woody pumice generated with submarine eruption. *Journal of the Geological Society of*

Japan **93**, 11-20.

KELEMEN P. B. 1995. Genesis of high Mg-andesites and the continental crust. *Contribution to Mineralogy and Petrology* **120**, 1– 19.

KELEMEN P. B., YOGODZINSKI G. M. & SCHOLL D. W. 2003. Along-strike variation in lavas of the Aleutian Island arc: implications for the genesis of high Mg# andesite and the continental crust. *In* Eiler, J. (ed.) *Inside the Subduction Factory*, Geophysical Monograph **138**, 223-76, American Geophysical Union, Washington, DC.

KELLEY K. A., PLANK T., LUDDEN J. & STAUDIGEL H. 2003. Composition of altered oceanic crust at ODP sites 801 and 1149. *Geochemistry Geophysics Geosystems* **4**, doi:10.1029/2002GC000435.

KIKUCHI Y. 1890. On pyroxenic compositions in certain volcanic rocks from Bonin Island. *Journal of the College of Science. Imperial University of Tokyo, Japan* **3**, 67-89.

KODAIRA S., SATO T., TAKAHASHI N. *et al*. 2007. Seismological evidence for variable growth of crust along the Izu intra-oceanic arc. *Journal of Geophysical Research* **112**, B05104, doi:10.1029/2006JB004593.

KURODA K. & SHIRAKI H. 1975. Boninite and related rocks of Chichi-jima, Bonin Islands, Japan. *Reports of Faculty of Science, Shizuoka University* **10**, 145-55.

LE BAS M. J. 2000. IUGS reclassification of the High-Mg and picritic volcanic rocks. *Journal of Petrology* **41**, 1467-70.

LONGERICH H. P., JACKSON S. E. & GUNTHER D. 1996. Laser ablation inductively coupled plasma mass spectrometric transient signal data acquisition and analyte concentration calculation. *Journal of Analytical Atomic Spectrometry* **11**, 899–904.

MARUYAMA S. & KURAMOTO T. 1981. Geology of Ototojima, Anijima and Chichijima (summary) (in Japanese with English abstract). *Journal of the Volcanological Society of Japan* **26**, 145-46.

MEIJER A., ANTHONY E. & REAGAN M. 1981. Petrology of Volcanic rocks from the fore-arc sites. *In* Hussong D. M. and Uyeda S. et al. (eds.) *Initial Reports of the Deep Sea Drilling Project* **60**, pp. 709-30, U.S. Govt. Printing Office, Washington.

MIYASHIRO A. 1974. Volcanic rock series in island arcs and active continental margins. *American Journal of Science* **274**, 321-55.

MOORE G., VENNEMANN T. & CARMICHAEL I. S. E. 1998. An empirical model for the solubility of H_2O in magmas to 3 kilobars. *American Mineralogist* **83**, 36-42.

MORISHITA T., ISHIDA Y. & ARAI S. 2005a. Simultaneous determination of multiple trace element compositions in thin (<30 μm) layers of BCR-2G by 193 nm ArF excimer laser ablation-ICP-MS: implications for matrix effect and elemental fractionation on quantitative analysis. *Geochemical Journal* **39**, 327-40.

MORISHITA T., ISHIDA Y., ARAI S. & SHIRASAKA M. 2005b. Determination of multiple trace element compositions in thin (30 μm) layers of NIST SRM 614 and 616 using laser ablation-inductively coupled plasma-mass spectrometry (LA-ICP-MS). *Geostandrand and Geoanalytical Research* **29**, 107-122.

NOGUCHI S., MORISHITA T. & TORAMARU A. 2004. Corrections for Na-loss on micro-analysis of glasses by electron probe X-ray micro analyzer (in Japanese with English abstract). *Japanese Magazine of Mineralogical and Petrological Sciences* **33**, 85-95.

PEACE J. A., THIRLWALL M. F., INGRAM G. *et al.* 1992a. Isotopic evidence for the origin of boninites and related rocks drilled in the Izu-Bonin (Ogasawara) forearc, leg 125. *In* Fryer P., Pearce J. A., Stokking L. *et al.* (eds.) *Proceeding of the Ocean Drilling Program, Scientific Results* **125**, pp. 237-61, Ocean Drilling Program, College Station, TX.

PEACE J. A., VAN DER LAAN S. R., ARCULUS R. J *et al.* 1992b. Boninite and harzburgite from Leg 125

(Bonin-Mariana forearc): a case study of magma genesis during the initial stages of subduction. *In* Fryer P., Pearce J. A., Stokking L. *et al.* (eds.) *Proceeding of the Ocean Drilling Program, Scientific Results* **125**, pp. 623-59, Ocean Drilling Program, College Station, TX.

PEARCE N. J. G., PERKINS W. T., WESTGATE J. A. et al. 1997. A compilation of new and published major and trace element data for NIST SRM 610 and NIST SRM 612 glass reference materials. *Geostandards Newsletter* **21**, 115–44.

PEACOCK M. A. 1931. Classification of igneous rock series. *Journal of Geology* **39**, 54-67.

PETERSEN J. 1891. Beitrage zur petrography von Sulphur Island, Peel Island, Hachijo und Mijakeshima. *Jahrbuch der Hamburgischen Wissenschaftl. Astalten* **8**, 1-59.

POLACCI M., CASHMAN K. V. & KAUAHIKAUA J. P. 1999. Textural characterization of the pãoehoe-'a'ã transition in Hawaiian basalt. *Bulletin of Volcanology* **60**, 595-609.

REAGAN M. K. & MEIJER A. 1984. Geology and geochemistry of early arc-volcanic rocks from Guam. *Geological Society of American Bulletin* **95**, 701-13.

REAGAN M. K., ISHIZUKA O., STERN R. J. et al. 2010. Fore-arc basalts and subduction initiation in the Izu-Bonin-Mariana system. *Geochemistry Geophysics Geosystems* **11**, doi:10.1029/2009GC002871.

RUDNICK R. L. 1995. Making continental crust. *Nature* **378**, 571–78.

SHARP W. D. & CLAGUE D. A. 2002. An older slower Hawaii–Emperor bend. *EOS* **83**, Abstract T61C-04.

SHIRAKI K., KURODA N. & URANO H. 1979. Clinoenstatite-bearing boninite of Muko-jima, Bonin Islands (in Japanese). *Journal of Geological Society of Japan* **85**, 591-94.

SMITH P. M. & ASIMOW, P. D. 2005. Adiabat_1ph: A new public front-end to the MELTS, pMELTS, and pHMELTS models. *Geochemistry Geophysics Geosystems* **6**, doi:10.1029/2004GC000816.

STERN R. J. 2010. The Anatomy and Ontogeny of Modern Intra-Oceanic Arc Systems. Kusky T. M., Zhai

M.-G. & Xiao W. (eds.) *The Evolving Continents: Understanding Processes of Continental Growth.* Geological Society, Special Publications, Vol. 338, pp. 7–34 London,.

STERN R. J. & BLOOMER S. H. 1992. Subduction zone infancy: Examples from the Eocene Izu-Bonin-Mariana and Jurassic California arcs. *Geological Society of America Bulletin* **104**, 1621-36.

SUN S-S. & MCDONOUGH W. F. 1989. Chemical characteristics of oceanic basalts: implications for mantle composition and processes. *In* Saunders A. D. & Norry M. J. (eds.) *Magmatism in the Ocean Basalts*. Geological Society, London, Special Publication **42**, 313-45.

TATSUMI Y. 2005. The subduction factory: How it operates in the evolving Earth. *GSA Today* **15**, 4 –10.

TATSUMI Y., SHUKUNO H., TANI K., TAKAHASHI N., KODAIRA S. & KOGISO T. 2008. Structure and growth of the Izu-Bonin-Mariana arc crust: 2. Role of crust-mantle transformation and the transparent Moho in arc crust evolution. *Journal of Geophysical Research* **113**, B02203, doi:10.1029/2007JB005121.

TAYLOR R. N., NESBITT R. W., VIDAL P., HARMON R. S., AUVRAY B. & CROUDACE I. W. 1994. Mineralogy, chemistry, and genesis of the boninite series volcanics, Chichijima, Bonin Islands, Japan. *Journal of Petrology* **35**, 577-617.

TAYLOR R. N. & NESBITT R. W. 1995. Arc volcanism in an extensional regime at the initiation of subduction: a geochemical study of Hahajima, Bonin Islands, Japan. *In* Smellie J. L. (ed.) *Volcanism Associated with Extension at Consuming Plate Margins*. Geological Society, London, Special Publication **81**, 115-34.

TAYLOR R. N. & NESBITT R. W. 1998. Isotopic characteristics of subduction fluids in an intra-oceanic setting, Izu-Bonin Arc, Japan. *Earth and Planetary Science Letters* **164**, 79-98.

UMINO S. 1985. Volcanic geology of Chichi-jima, the Bonin Islands (Ogasawara islands). *Journal of the*

Geological Society of Japan **91**, 505-23.

UMIMO S. 1986. Magma mixing in boninite sequence of Chichijima, Bonin Islands. *Journal of Volcanology and Geothermal Research* **29**, 125-57.

UMINO S. & HORIO A. 1998. Multistage magma mixing revealed in phenocryst zoning of the Yunokuchi pumice, Akagi volcano, Japan. *Journal of Petrology* **39**, 101-24.

UMINO S. & KUSHIRO I. 1989. Experimental studies on boninite petrogenesis. *In* Crawford A. J. (ed.) *Boninites and Related Rocks*. pp. 89-111, Unwin Hyman, London.

UMINO S. & NAKANO S. 2006. *Geological Map of Japan 1:50,000, Chichijima Rettō*. Geological Survey of Japan, AIST, Tsukuba.

UMINO S. & NAKANO S. 2007. Geology of the Chichijima Rettō District (in Japanese with English abstract 3p.). *Quadrangle Series, 1:50,000,* Geological Survey of Japan, AIST, Tsukuba, 71 p.

UMINO S., NAKANO S., ISHIZUKA O. & KOMAZAWA M., 2009. *Geological Map of Japan 1: 200,000, Ogasawara Shotō (in Japanese)*. Geological Survey of Japan, AIST.

VAN DER LAAN S. R., FLOWER M. F. J. & KOSTER VAN GROOS A. F. 1989. Experimental evidence for the origin of boninites: near-liquidus phase relations to 7.5 kbar. *In* Crawford A. J. (ed.) *Boninites and Related Rocks*. pp. 112-47, Unwin Hyman, London.

WALKER D. A. & CAMERON W. E. 1983. Boninite primary magmas: evidence from the Cape Vogel Peninsula, PNG. *Contributions to Mineralogy and Petrology* **83**, 150-8.

WESSEL P., HARADA Y. & KROENKEET L. W. 2006. Toward a self-consistent, high-resolution absolute plate motion model for the Pacific. *Geochemistry Geophysics Geosystems* 7, dio:10.1029/2005GC001000.

WORKMAN R. K. & HART S. T. 2005. Major and trace element composition of the depleted MORB mantle (DMM). *Earth and Planetary Science Letters* **231**, 53-72.

WOOD D. A., MARSH N. G., TARNEY J. JORON J. -L., FRYER P. & TREUIL M. 1981. Geochemistry of igneous rocks recovered from a transect across the Mariana trough, arc, fore-arc, and trench, Site 453 through 461, Deep Sea Drilling Project Leg 60. *In* Hussong D. M. and Uyeda S. et al. (eds.) *Initial Reports of the Deep Sea Drilling Project* **60**, pp. 709-30, U.S. Govt. Printing Office, Washington.

YAJIMA K. & FUJIMAKI H. 2001. High-Ca and low-Ca boninites from Chichijima, Bonin (Ogasawara) archipelago (in Japanese with English abstract). *Japanese Magazine of Mineralogical and Petrological Sciences* **30**, 217-36.

YAJIMA K., FUJIMAKI H. & KURODA N. 2001. Primitive tholeiites and calc-alkaline rocks from Hahajima, Bonin (Ogasawara) archipelago (in Japanese with English abstract). *Japanese Magazine of Mineralogical and Petrological Sciences* **30**, 164-79.

YUASA M., TAMAKI K., NISHIMURA A., & HONZA E. 1981. X. Geological survey on Minami-Iwojima, Yomejima and Nakodojima islands of Ogasawara Islands group, NW Pacific. *In* Honza E., Inoue E. & Ishihara T. (eds.) *Geological Investigation of Ogasawara (Bonin) and Northern Mariana Arcs*. Cruise Report **14**, 116-22, Geological Survey of Japan, Tsukuba.

910 Figure 1 Map of the Philippine Sea Plate showing the location of the Ogasawara Ridge and some tectonic
911 features. Stars: borehole sites of Ocean Drilling Program.
912
913 Figure 2 (a) Enlarged rectangle in Fig. 1 showing the Ogasawara Island Groups. (b) Bathymetric map
914 (rectangle in Fig. 2a) showing the distribution of islands and reefs of the Mukojima Island Group.
915
916 Figure 3 Generalized volcanic stratigraphy of the Chichijima Island Group modified after Umino (1985)
917 and Umino & Nakano (2006, 2007). Data sources of radiometric ages are; a, Dobson (1986); b, Ishizuka *et*
918 *al*. (2006); c, Ishizuka *et al*. (2011).
919
920 Figure 4 Summary of age, stratigraphic variations and environment of the Eocene-Oligocene volcanism on
921 the Ogasawara Ridge. Stratigraphic data: Western scarp of the Ogasawara Ridge (Ishizuka *et al*. 2006),
922 Hahajima Island Group (Umino *et al*. 2009), Chichijima Island Group (Umino & Nakano 2007) and
923 Ogasawara Trench slope (Ishizuka *et al*. 2011). Radiometric ages are from Ishizuka *et al*. (2006; 2011).
924
925 Figure 5 Geological columns showing the stratigraphic relationships of the Mukojima Island Group.
926 Symbols are the same as those in Fig. 6. $^{40}Ar/^{39}Ar$ ages from Ishizuka *et al*. (2011) are shown on the side of
927 the columns. Tholeiitic strata of Ninoiwa, Kitanoshima and Nakanoshima are presumably correlatable to
928 the John Beach Volcanics in the lowermost Maruberiwan Formation of Chichijima. High-Si boninite-series
929 rocks of Yon'noiwa, Sasayojima, Mukojima, Nakodojima and most of Yomejima are correlatable to the
930 Maruberiwan and Asahiyama Formations of Chichijima. Low-Si boninitic andesite of the uppermost part of
931 Yomejima is correlated to the Mikazukiyama Formation because of the younger $^{40}Ar/^{39}Ar$ ages for andesite
932 clast. Harinoiwa and Tatamiiwa low-Si boninitic andesites may be correlated with the Maruberiwan and

933 Mikazukiyama Formations.

934

935 Figure 6 Geological maps and sampling localities of the Mukojima Island Group. (a) Kitanoshima and

936 Nakanoshima, (b) Sasayojima, (c) Mukojima, (d) Harinoiwa, (e) Nakodojima, (f) Yomejima.

937

938 Figure 7 Representative outcrops of the Mukojima Island Group. (a) Pillow lava of Nakanoshima. (b)

939 Northwestern cliff of Kitanoshima showing steeply inclined agglutinate layers to east. (c) Close-up view of

940 the agglutinate in b consisting of densely to moderately welded lava clasts up to 10 cm in diameter. Scale is

941 20 cm. (d) Pillow lava exposed on the southwestern cliff of Mukojima. (e) Western cliff of Torishima,

942 southwest of Mukojima. Bedded tuff breccia is underlain by pillowed boninite. (f) Volcanic bombs and

943 scoriae in massive tuff breccia of the uppermost Mukojima. (g) The uppermost massive tuff breccia is

944 widely exposed on central Mukojima. (h) Northeastern cliff of Harinoiwa. Andesite pillow lobes are

945 brecciated into glassy fragments and laterally change into hyaloclastite. Some dikes terminate within the

946 hyaloclastite and pillow lava. (i) South reef of Nakodojima. Bronzite andesite pillow lava on the right is

947 in-situ brecciated to glassy and lithic fragments which grade into massive hyaloclastite to the left. (j)

948 Western and central areas of Nakodojima. White alteration zones in front right and back left run northwest

949 in echelon in the central block. (k) Maejima, an islet southwest off Yomejima, is composed of bedded

950 volcanic and tuff breccia which are weakly to moderately welded. (l) Dike swarm of boninite and altered

951 bronzite andesite intruded into the tuff breccia in the center of Yomejima.

952

953 Figure 8 Tephras in Mukojima (M3-07 and M2-06D) and Nakodojima (N2-09). Sample localities are shown

954 in Fig. 3. (a) Pumice and scoria tuff and lapillistone (M3-07) are exposed on the east cliff of Mukojima. (b)

955 Columnar section at M3-07. (c)-(e) Microphotographs of (c) woody pumice, (d) crystal-free scoria and (e)

crystal-rich scoria in M3-07G and H. (f) Pumice and scoria tuff (M2-06) exposed on the east coast cliff of Mukojima. (g) Pumice tuff (N2-09) lies between overlying quartz rhyolite and underlying bronzite andesite tuff breccia on the eastern cliff of Nakodojima. N2-09 sample was recovered on the ridge to the left of the photograph, where the pumice tuff becomes thinner to the north about 30 cm in thickness.

Figure 9 Microphotographs of volcanic rocks from the Mukojima Island Group. bz: bronzite, cpx: clinopyroxene, cen: clinoenstatite, aug: augite, hyp: hypersthene, pl: plagioclase, qtz: quartz. (a) Typical type 1 boninite. All boninite contain bronzite as a phenocryst and a microphenocryst, and clinopyroxene as a groundmass mineral (plane-polarized light). (b) Clinoenstatite phenocryst in type 1 boninite (plane-polarized light). (c) Type 2 boninite commonly has both augite and bronzite microphenocrysts (crossed polars). (d) Irregular-shaped augite and reversely zoned hypersthene with glass inclusions in the core in type 3 boninite (plane-polarized light). (e) Bronzite andesite resembles boninite in terms of mineral assemblages but is distinguished by the presence of plagioclase laths in the vesicular groundmass (plane-polarized light). (f) Dacite has small phenocrysts of plagioclase, augite, hypersthene and magnetite embedded in a glassy groundmass with a small amount of microlites (plane-polarized light). (g) Quartz rhyolite is similar to dacite but carries quartz as a phenocryst. The groundmass is holohyaline with abundant microspherulites (plane-polarized light). (h) Tholeiitic andesite tuff breccia in Ninoiwa. Groundmass crystal size differs from clast to clast. Plagioclase and pyroxene are mainly altered to albite, epidote, chlorite, sphene and magnetite (plane-polarized light).

Figure 10 Glass and mineral compositions of tephra samples from Mukojima and Nakodojima. (a) SiO_2 vs. MgO (wt%) of matrix glass of scoria and pumice in tephra. (b) Chondrite (Sun & McDonough 1989)-normalized REE patterns of matrix glass of scoria and pumice. (c) Pyroxene compositions of

phenocrysts and microphenocrysts in tephra.

Figure 11 Bulk major element compositions of Mukojima Island Group volcanic rocks. The line on the FeO*/MgO vs. SiO_2 diagram shows the boundary of tholeiitic and calc-alkaline series for the Quaternary volcanic rocks from Izu-Hakone region after Miyashiro (1974). Data sources: boninite series rocks of the Maruberiwan and Asahiyama Formations of the Chichijima Island Group (Umino, 1986; Taylor *et al.* 1994; Umino & Nakano 2007; original data), the John Beach Volcanics (Umino & Nakano 2007; Ishizuka *et al.* 2012), low-Si boninite series of the Mikazukiyama Formation (Yajima & Fujimaki 2001; Umino & Nakano 2007; original data), tholeiite and calc-alkaline rock series from the Hahajima Island Group (Taylor & Nesbitt 1995; Yajima *et al.* 2001; Kanayama *et al.* 2010), MORB-like basalt from the Ogasawara (Ishizuka *et al.*, 2011) and Mariana Trench (Reagan *et al.* 2010), bronzite andesite from Site 458 and tholeiitic rocks from Site 458 and 459 (Meijer *et al.* 1981; Wood *et al.* 1981; Reagan *et al.* 2010).

Figure 12 Representative trace element compositions for volcanic rocks from the Mukojima Island Group. Boninites, bronzite andesite, dacite and quartz rhyolite (a, b), bronzite andesite of low-Si boninite series (c, d), arc tholeiitic rocks (e, f). (a, c, e) N-MORB-normalized trace element patterns. (b, d, f) Chondrite-normalized REE patterns. Normalizing factors are after Sun & McDonough (1989). Data sources for the gray hatched patterns are the same as in Fig. 11.

Fig 13 Bulk (a) Ba/Yb, (b) Th/Yb and (c) Pb/Yb vs. Nb/Yb diagrams of the Mukojima Island Group volcanic rocks. Symbols and data sources are the same as those in Fig. 11.

Figure 14 Variation diagrams of bulk chemical compositions of type 1, 2 and 3 boninites. (a) Total alkali

1002 (Na_2O+K_2O) vs. SiO_2, (b) Al_2O_3 vs. CaO. Broken lines show CaO/Al_2O_3 = 0.6, 0.8, 1.0 and 1.2, (c) Zr/Ti
1003 ratio vs. Yb concentration, (d) Zr/Ti vs. Ba/Yb ratios. Gray thick arrows are compositional trends of 20
1004 wt% fractionation of olivine (OL, Fo_{91}), orthopyroxene (OPX, Mg#=0.91) and clinopyroxene (CPX,
1005 Mg#=0.90) from type 2 boninite. Fine arrows show vectors of 20 wt% addition of xenocrysts of OPX
1006 (Mg#=0.69) and CPX (Mg#=0.75) and An_{75} plagioclase (PL) to type 1 boninite. Stars show the average
1007 compositions of CPX (Mg#=0.62-75) xenocrysts. Compositional fields enclosed by solid and broken lines
1008 show arc tholeiitic rocks and high-Si boninite series rocks (bronzite andesite, dacite, quartz rhyolite) from
1009 the Mukojima Island Group, respectively. Black and gray lines with ticks show postulated mixing lines of
1010 type 1 boninite and 0-100 wt% arc tholeiitic dacite and 0-100 wt% of quartz rhyolite, respectively. Data
1011 sources: Mariana Trench (D28,D50 and site 1403) (Hickey & Frey 1982; Bloomer & Hawkins 1987), Guam
1012 Facpi Formation (Reagan & Meijer 1984), Cape Vogel (Dallwitz *et al.* 1966; Walker & Cameron 1983),
1013 Chichijima Maruberiwan Formation (Umino 1986; Taylor *et al.* 1994), Leg 125 Hole 786A, B (Pearce *et al.*
1014 1992b), Troodos ophiolite (Cameron 1985; Flower & Levine 1987), Low-Si boninite of the Mikazukiyama
1015 Formation (Yajima & Fujimaki 2001; original data).
1016
1017 Figure 15 Zr/Ti vs. Yb for type 1 and 2 boninites. Also shown are mixing lines (black lines) between 15%
1018 batch melt of depleted MORB source mantle (DMM: Walkman & Hart 2005) and slab melt. Relative
1019 depletion of source mantle is shown by mixing lines (for example, “DMM-5%” means mixing line of slab
1020 melt and 15 wt% batch partial melt of residual DMM after 5 wt%-melt subtraction). Dashed lines are
1021 contours of iso-mixing-ratios of DMM and slab melts. Slab melt is calculated as 5% fractional melt of
1022 altered oceanic slab (average of Site 1149; Kelley *et al.* 2003) under amphibolite facies (clinopyroxene:
1023 amphibole: plagioclase=7:88:5). Partition coefficient for clinopyroxene-melt: Kelemen *et al.* (2003),
1024 amphibole-melt: Hilyard *et al.* (2000), plagioclase-melt: Smith & Asimow (2005). Hahajima basalts are

from Taylor & Nesbitt (1995), Yajima *et al*. 2001, and Kanayama *et al*. (2010). Data source for low-Si boninite of the Mikazukiyama Formation is the same as in Fig. 14.

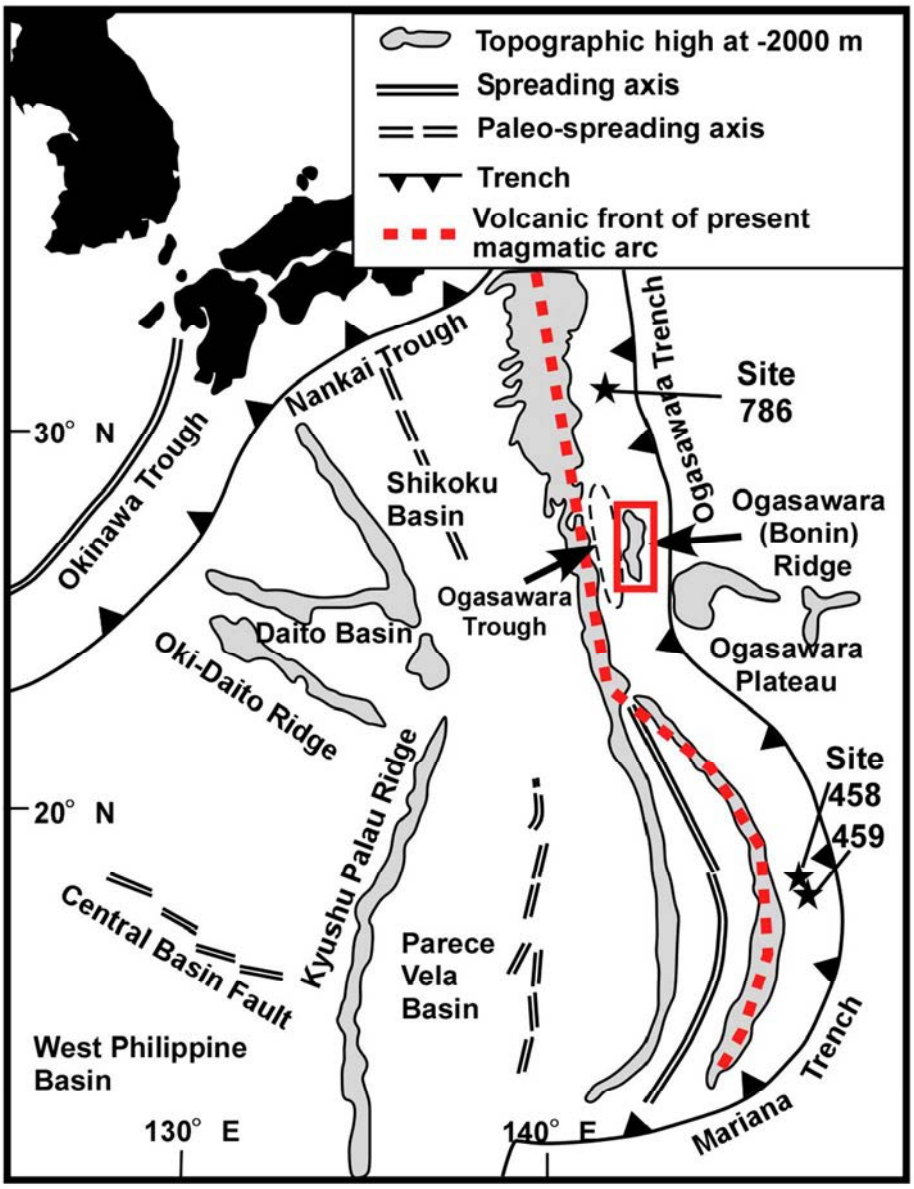

Figure 1 Map of the Philippine Sea Plate showing the location of the Ogasawara Ridge and some tectonic features. Stars: borehole sites of Ocean Drilling Program.
90x118mm (300 x 300 DPI)

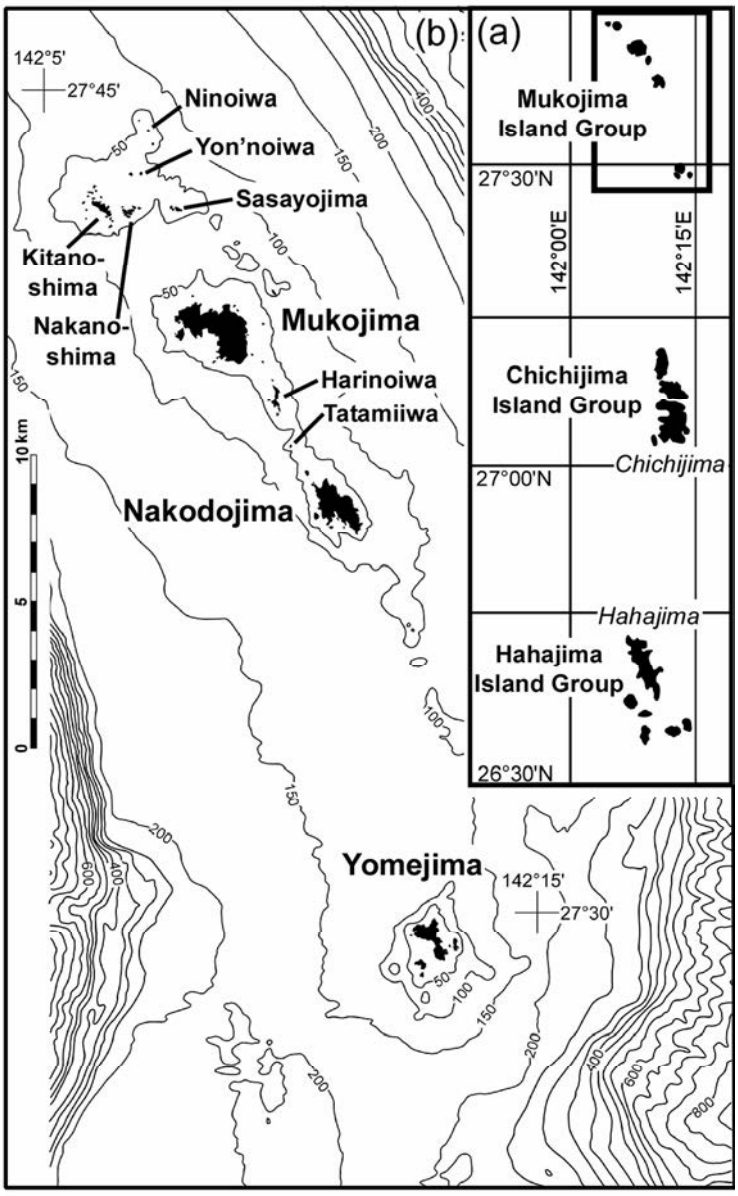

Figure 2 (a) Enlarged rectangle in Fig. 1 showing the Ogasawara Island Groups. (b) Bathymetric map (rectangle in Fig. 2a) showing the distribution of islands and reefs of the Mukojima Island Group.
86x139mm (300 x 300 DPI)

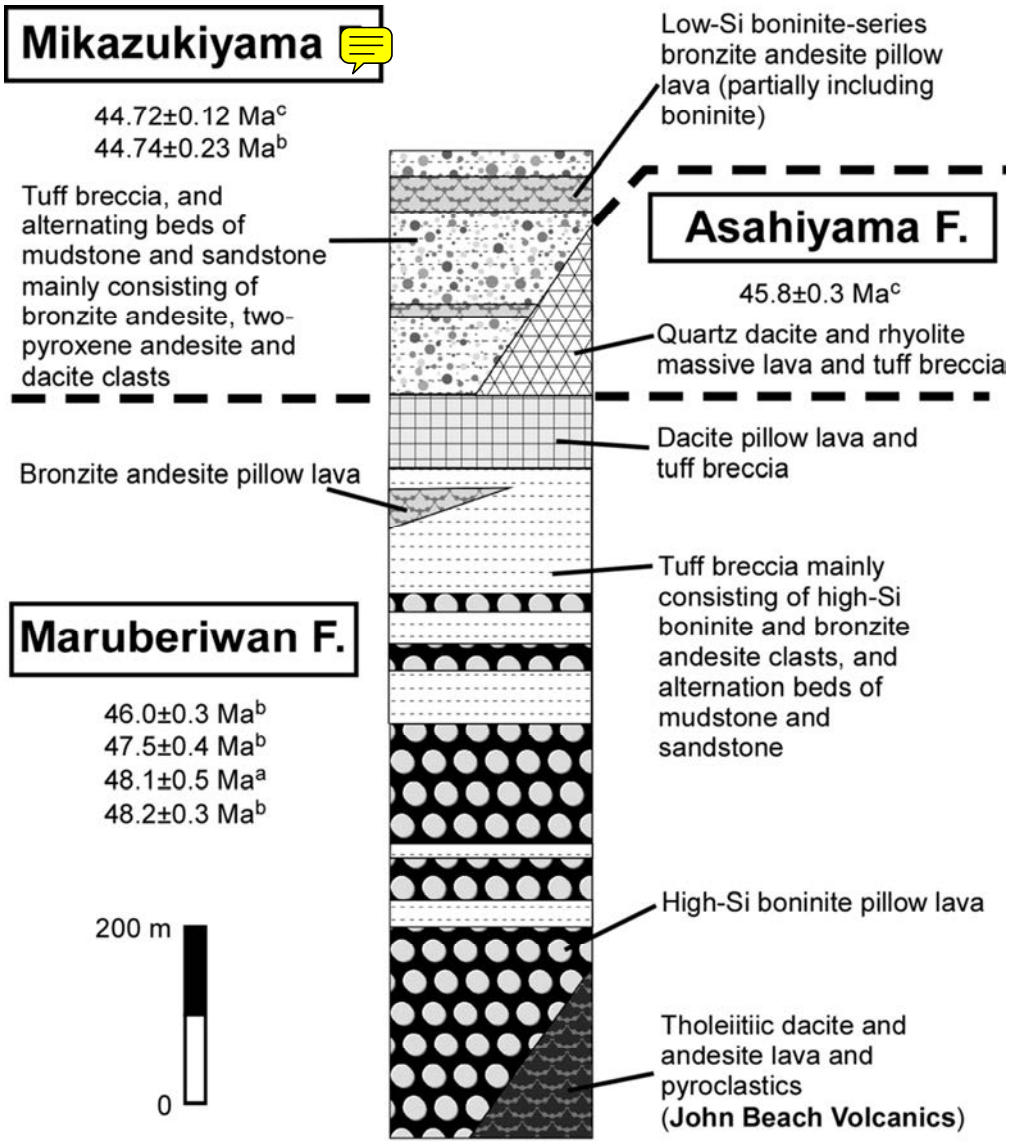

Figure 3 Generalized volcanic stratigraphy of the Chichijima Island Group modified after Umino (1985) and Umino & Nakano (2006, 2007). Data sources of radiometric ages are; a, Dobson (1986); b, Ishizuka *et al*. (2006); c, Ishizuka *et al*. (2011).
89x102mm (300 x 300 DPI)

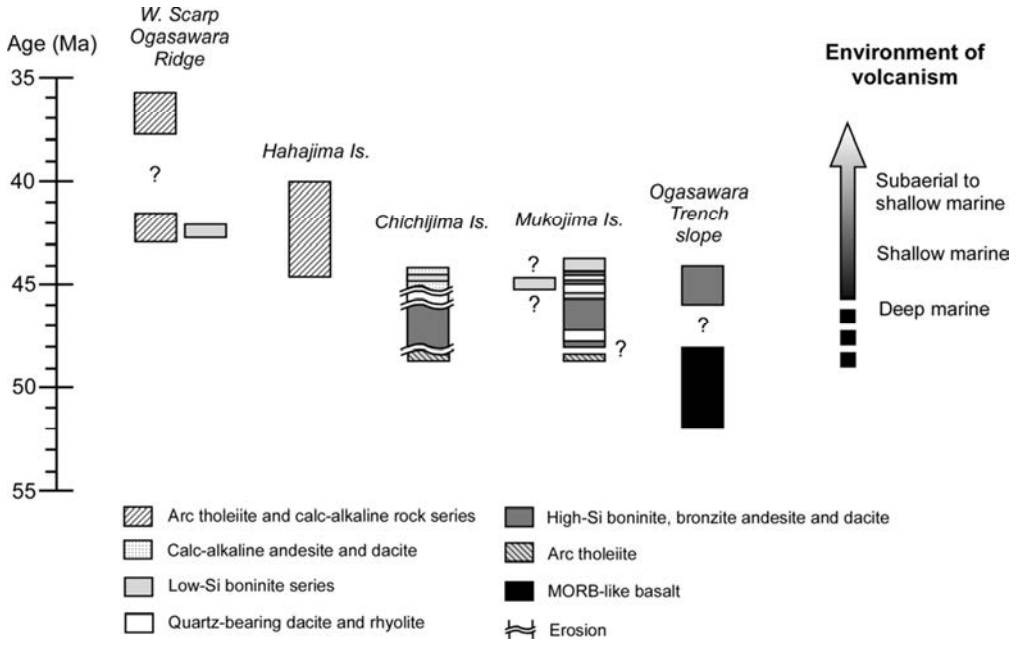

Figure 4 Summary of age, stratigraphic variations and environment of the Eocene-Oligocene volcanism on the Ogasawara Ridge. Stratigraphic data: Western scarp of the Ogasawara Ridge (Ishizuka *et al*. 2006), Hahajima Island Group (Umino *et al*. 2009), Chichijima Island Group (Umino & Nakano 2007) and Ogasawara Trench slope (Ishizuka *et al*. 2011). Radiometric ages are from Ishizuka *et al*. (2006; 2011).
91x57mm (300 x 300 DPI)

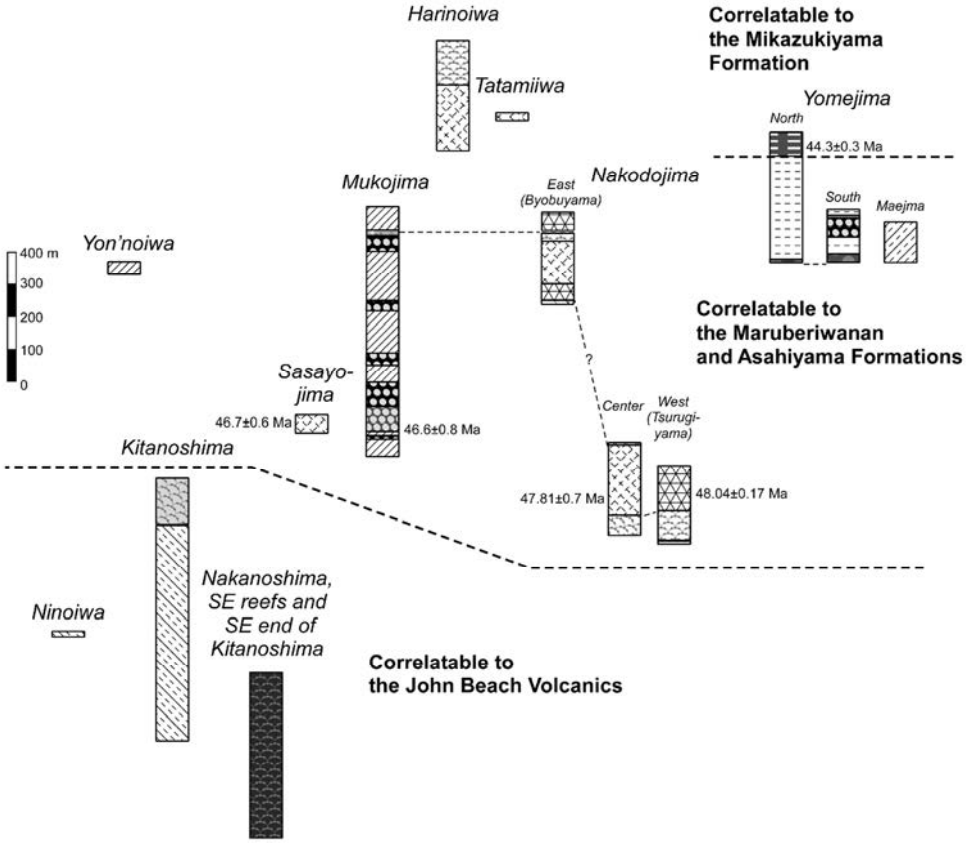

Figure 5 Geological columns showing the stratigraphic relationships of the Mukojima Island Group. Symbols are the same as those in Fig. 6. $^{40}Ar/^{39}Ar$ ages from Ishizuka *et al*. (2011) are shown on the side of the columns. Tholeiitic strata of Ninoiwa, Kitanoshima and Nakanoshima are presumably correlatable to the John Beach Volcanics in the lowermost Maruberiwan Formation of Chichijima. High-Si boninite-series rocks of Yon'noiwa, Sasayojima, Mukojima, Nakodojima and most of Yomejima are correlatable to the Maruberiwan and Asahiyama Formations of Chichijima. Low-Si boninitic andesite of the uppermost part of Yomejima is correlated to the Mikazukiyama Formation because of the younger $^{40}Ar/^{39}Ar$ ages for andesite clast. Harinoiwa and Tatamiiwa low-Si boninitic andesites may be correlated with the Maruberiwan and Mikazukiyama Formations.
132x116mm (300 x 300 DPI)

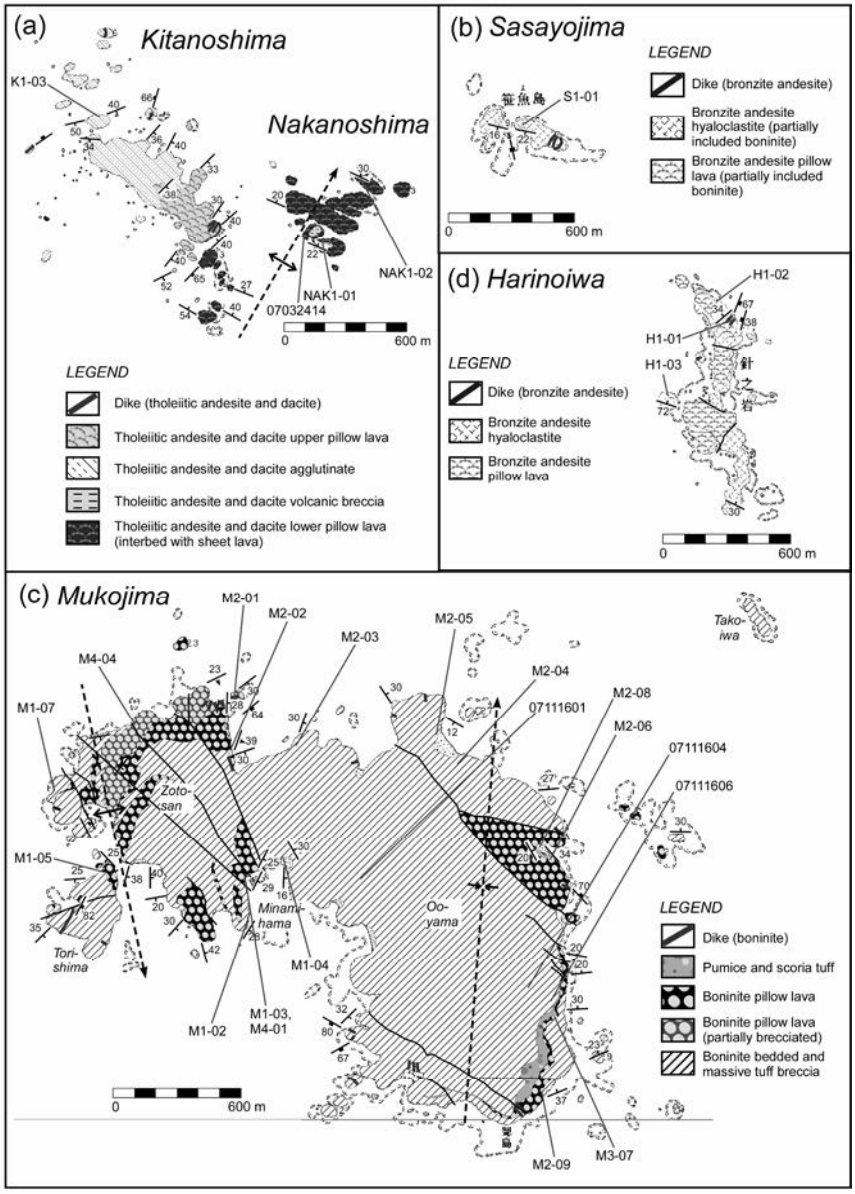

Figure 6 Geological maps and sampling localities of the Mukojima Island Group. (a) Kitanoshima and Nakanoshima, (b) Sasayojima, (c) Mukojima, (d) Harinoiwa, (e) Nakodojima, (f) Yomejima.
223x313mm (300 x 300 DPI)

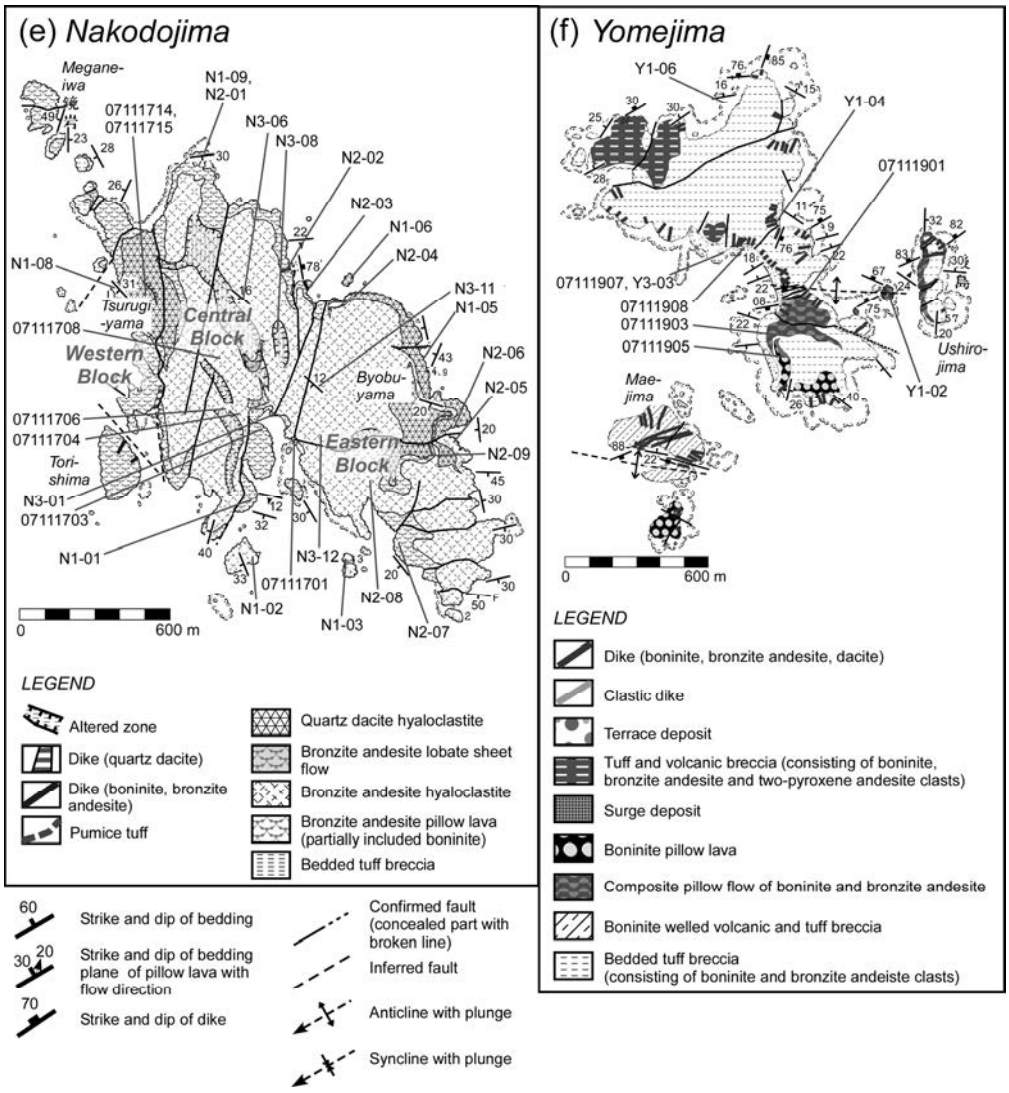

(continued)
171x184mm (300 x 300 DPI)

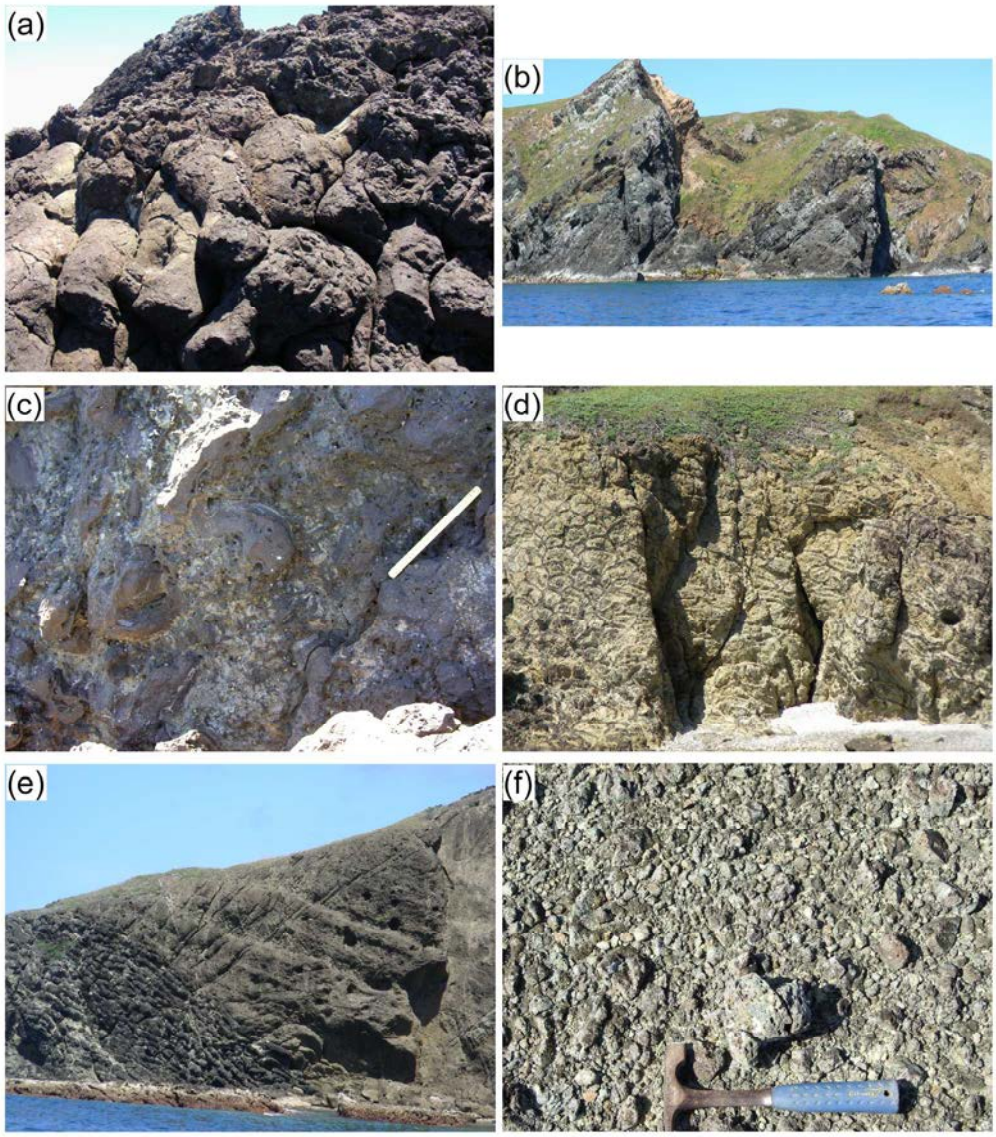

Figure 7 Representative outcrops of the Mukojima Island Group. (a) Pillow lava of Nakanoshima. (b) Northwestern cliff of Kitanoshima showing steeply inclined agglutinate layers to east. (c) Close-up view of the agglutinate in b consisting of densely to moderately welded lava clasts up to 10 cm in diameter. Scale is 20 cm. (d) Pillow lava exposed on the southwestern cliff of Mukojima. (e) Western cliff of Torishima, southwest of Mukojima. Bedded tuff breccia is underlain by pillowed boninite. (f) Volcanic bombs and scoriae in massive tuff breccia of the uppermost Mukojima. (g) The uppermost massive tuff breccia is widely exposed on central Mukojima. (h) Northeastern cliff of Harinoiwa. Andesite pillow lobes are brecciated into glassy fragments and laterally change into hyaloclastite. Some dikes terminate within the hyaloclastite and pillow lava. (i) South reef of Nakodojima. Bronzite andesite pillow lava on the right is in-situ brecciated to glassy and lithic fragments which grade into massive hyaloclastite to the left. (j) Western and central areas of Nakodojima. White alteration zones in front right and back left run northwest in echelon in the central block. (k) Maejima, an islet southwest off Yomejima, is composed of bedded volcanic and tuff breccia which are weakly to moderately welded. (l) Dike swarm of boninite and altered bronzite andesite intruded into the tuff breccia in the center of Yomejima.
182x209mm (300 x 300 DPI)

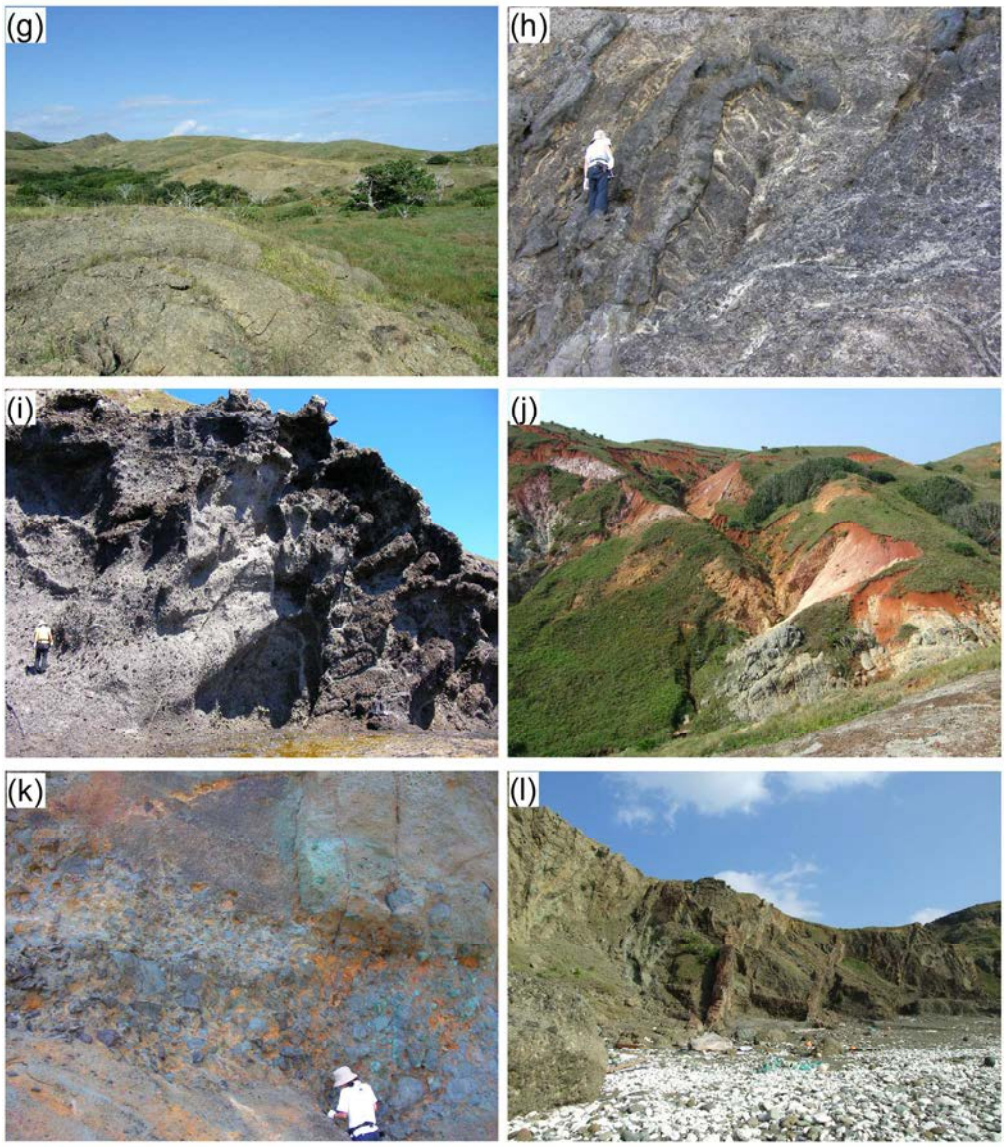

(continued)
182x211mm (300 x 300 DPI)

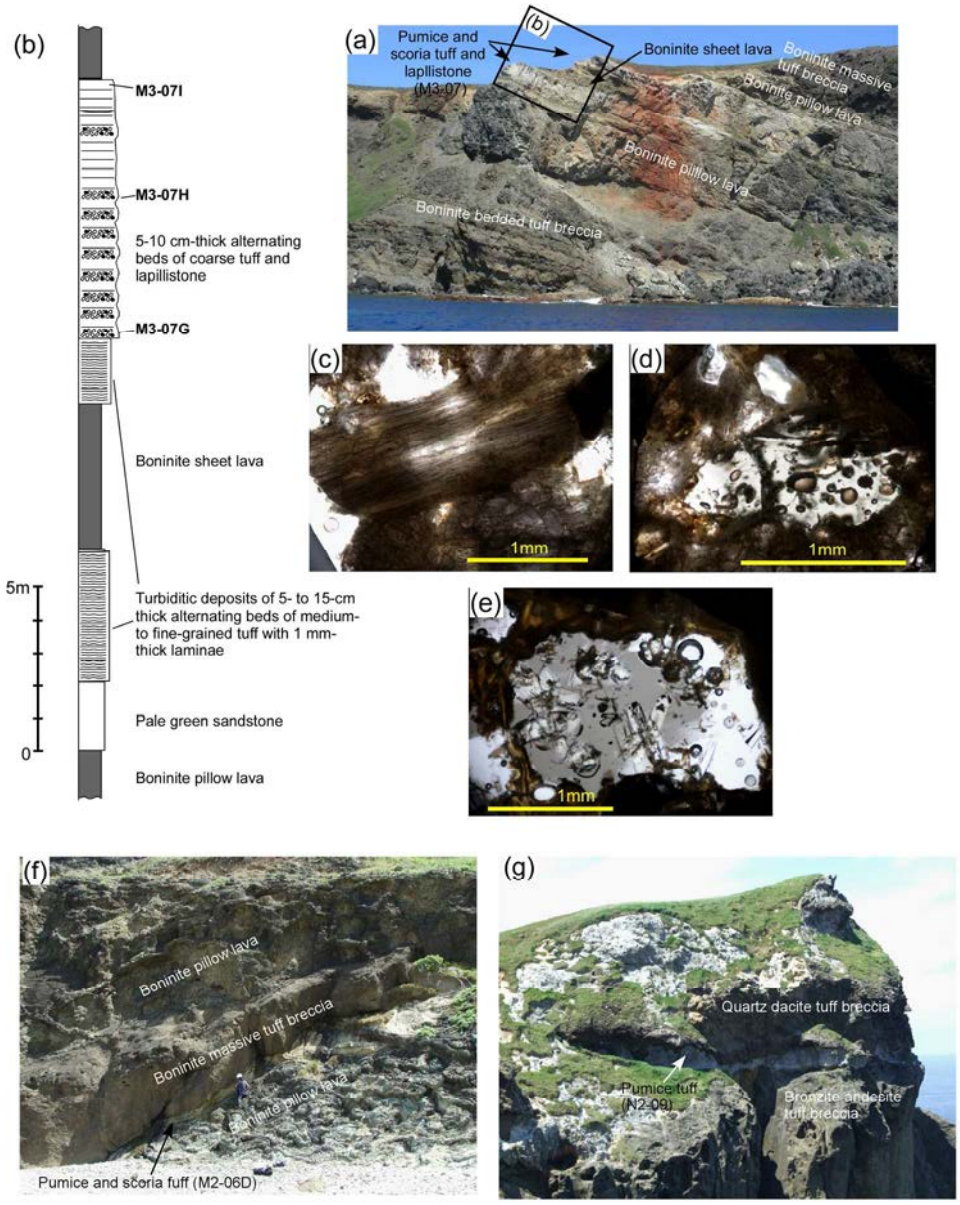

Figure 8 Tephras in Mukojima (M3-07 and M2-06D) and Nakodojima (N2-09). Sample localities are shown in Fig. 3. (a) Pumice and scoria tuff and lapillistone (M3-07) are exposed on the east cliff of Mukojima. (b) Columnar section at M3-07. (c)-(e) Microphotographs of (c) woody pumice, (d) crystal-free scoria and (e) crystal-rich scoria in M3-07G and H. (f) Pumice and scoria tuff (M2-06) exposed on the east coast cliff of Mukojima. (g) Pumice tuff (N2-09) lies between overlying quartz rhyolite and underlying bronzite andesite tuff breccia on the eastern cliff of Nakodojima. N2-09 sample was recovered on the ridge to the left of the photograph, where the pumice tuff becomes thinner to the north about 30 cm in thickness.
196x245mm (300 x 300 DPI)

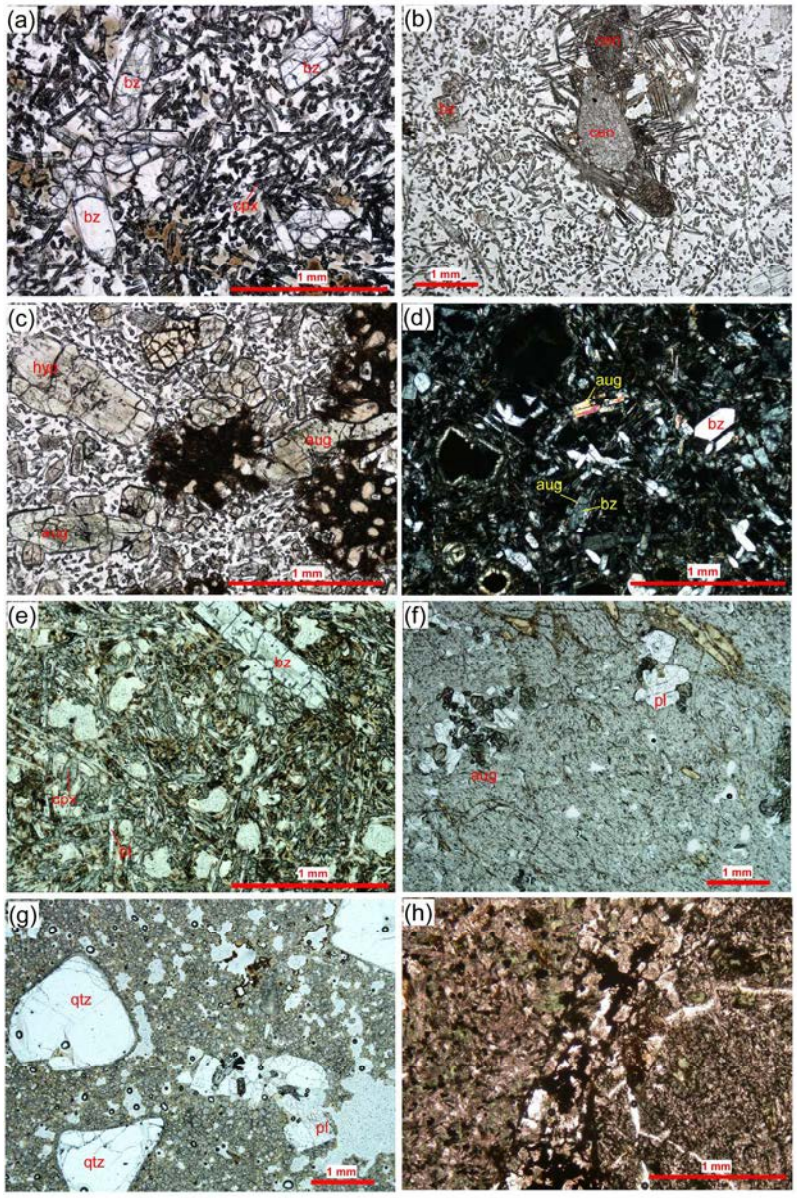

Figure 9 Microphotographs of volcanic rocks from the Mukojima Island Group. bz: bronzite, cpx: clinopyroxene, cen: clinoenstatite, aug: augite, hyp: hypersthene, pl: plagioclase, qtz: quartz. (a) Typical type 1 boninite. All boninite contain bronzite as a phenocryst and a microphenocryst, and clinopyroxene as a groundmass mineral (plane-polarized light). (b) Clinoenstatite phenocryst in type 1 boninite (plane-polarized light). (c) Type 2 boninite commonly has both augite and bronzite microphenocrysts (crossed polars). (d) Irregular-shaped augite and reversely zoned hypersthene with glass inclusions in the core in type 3 boninite (plane-polarized light). (e) Bronzite andesite resembles boninite in terms of mineral assemblages but is distinguished by the presence of plagioclase laths in the vesicular groundmass (plane-polarized light). (f) Dacite has small phenocrysts of plagioclase, augite, hypersthene and magnetite embedded in a glassy groundmass with a small amount of microlites (plane-polarized light). (g) Quartz rhyolite is similar to dacite but carries quartz as a phenocryst. The groundmass is holohyaline with abundant microspherulites (plane-polarized light). (h) Tholeiitic andesite tuff breccia in Ninoiwa. Groundmass crystal size differs from clast to clast. Plagioclase and pyroxene are mainly altered to albite, epidote, chlorite, sphene and magnetite (plane-

polarized light).
215x324mm (300 x 300 DPI)

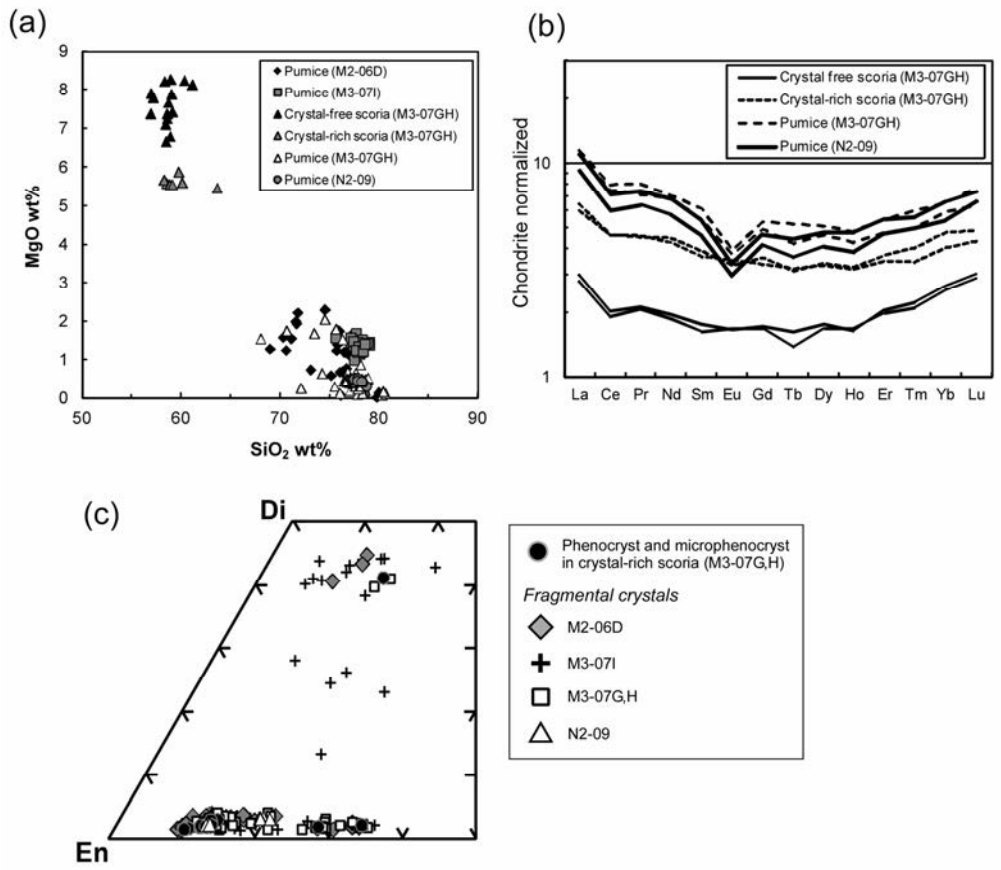

Figure 10 Glass and mineral compositions of tephra samples from Mukojima and Nakodojima. (a) SiO_2 vs. MgO (wt%) of matrix glass of scoria and pumice in tephra. (b) Chondrite (Sun & McDonough 1989)-normalized REE patterns of matrix glass of scoria and pumice. (c) Pyroxene compositions of phenocrysts and microphenocrysts in tephra.
138x121mm (300 x 300 DPI)

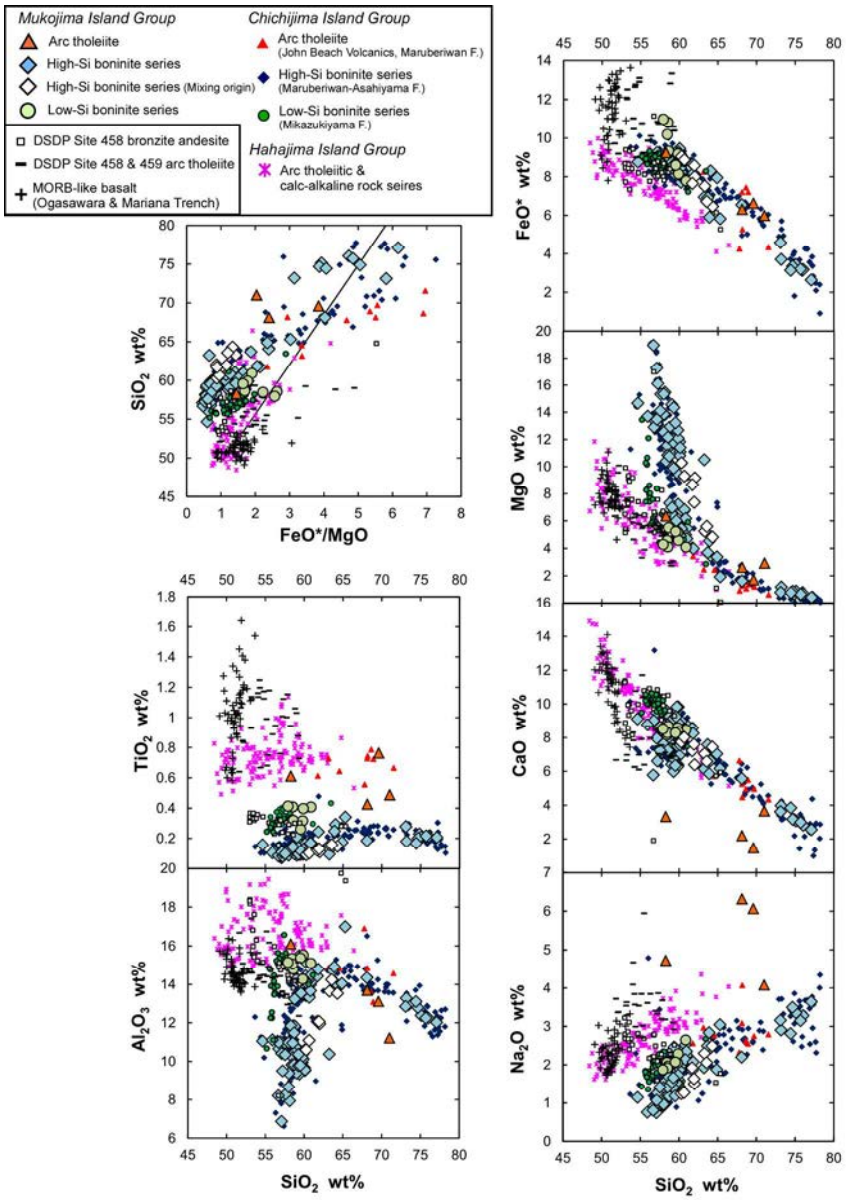

Figure 11 Bulk major element compositions of Mukojima Island Group volcanic rocks. The line on the FeO*/MgO vs. SiO_2 diagram shows the boundary of tholeiitic and calc-alkaline series for the Quaternary volcanic rocks from Izu-Hakone region after Miyashiro (1974). Data sources: boninite series rocks of the Maruberiwan and Asahiyama Formations of the Chichijima Island Group (Umino, 1986; Taylor *et al*. 1994; Umino & Nakano 2007; original data), the John Beach Volcanics (Umino & Nakano 2007; Ishizuka *et al*. 2012), low-Si boninite series of the Mikazukiyama Formation (Yajima & Fujimaki 2001; Umino & Nakano 2007; original data), tholeiite and calc-alkaline rock series from the Hahajima Island Group (Taylor & Nesbitt 1995; Yajima *et al*. 2001; Kanayama *et al*. 2010), MORB-like basalt from the Ogasawara (Ishizuka *et al*., 2011) and Mariana Trench (Reagan *et al*. 2010), bronzite andesite from Site 458 and tholeiitic rocks from Site 458 and 459 (Meijer et al. 1981; Wood *et al*. 1981; Reagan *et al*. 2010).
221x316mm (300 x 300 DPI)

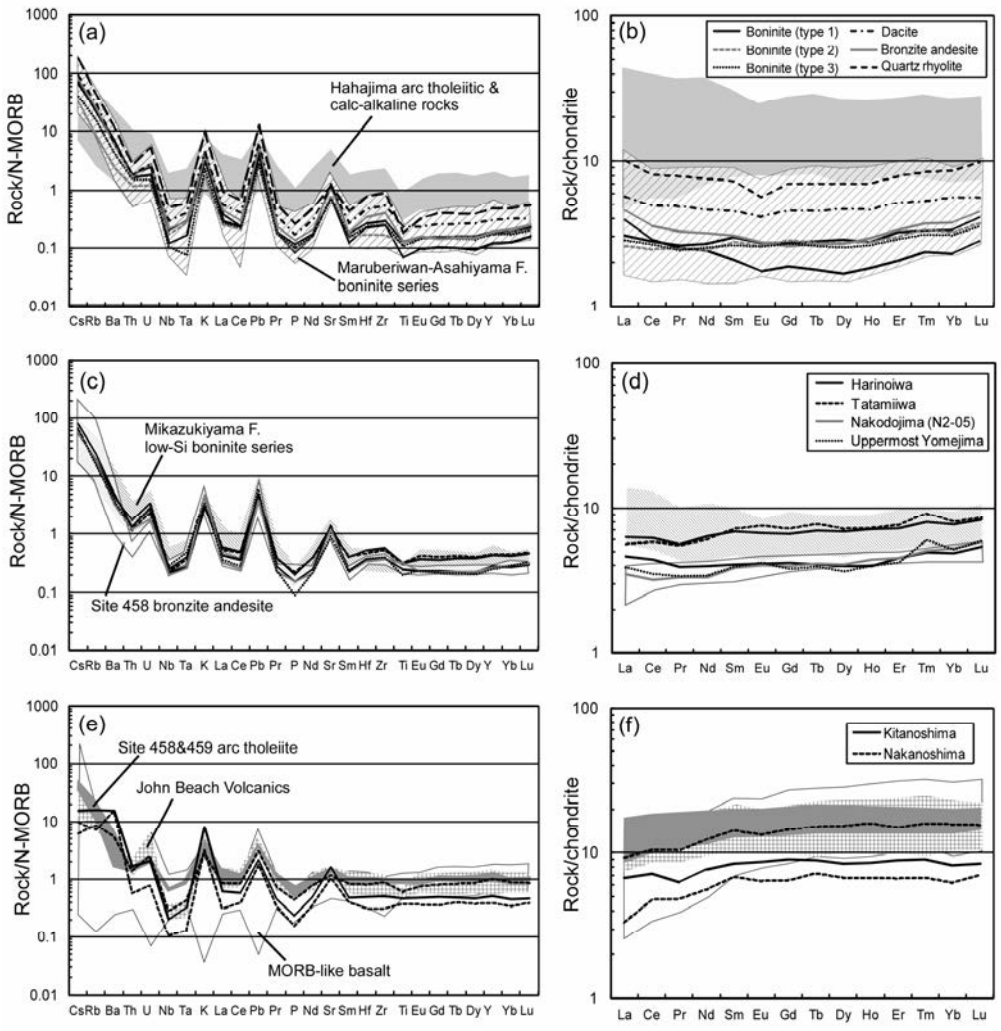

Figure 12 Representative trace element compositions for volcanic rocks from the Mukojima Island Group. Boninites, bronzite andesite, dacite and quartz rhyolite (a, b), bronzite andesite of low-Si boninite series (c, d), arc tholeiitic rocks (e, f). (a, c, e) N-MORB-normalized trace element patterns. (b, d, f) Chondrite-normalized REE patterns. Normalizing factors are after Sun & McDonough (1989). Data sources for the gray hatched patterns are the same as in Fig. 11.
163x169mm (300 x 300 DPI)

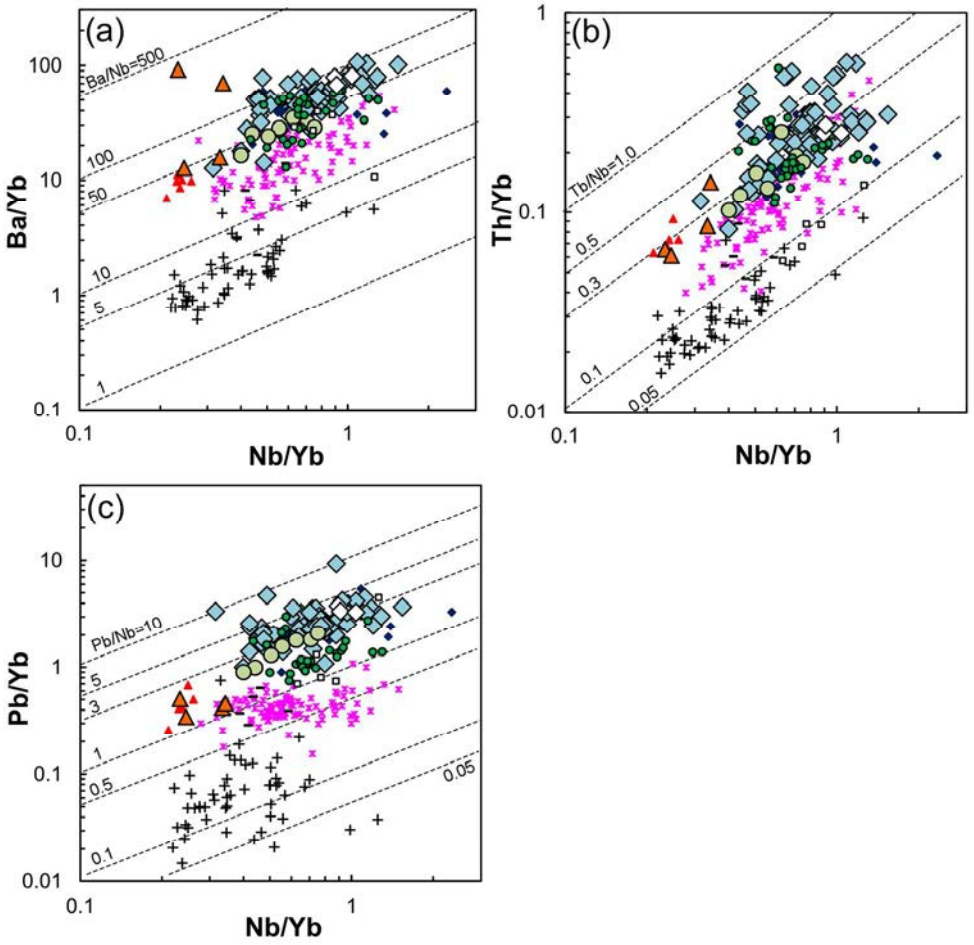

Fig 13 Bulk (a) Ba/Yb, (b) Th/Yb and (c) Pb/Yb vs. Nb/Yb diagrams of the Mukojima Island Group volcanic rocks. Symbols and data sources are the same as those in Fig. 11.
144x138mm (300 x 300 DPI)

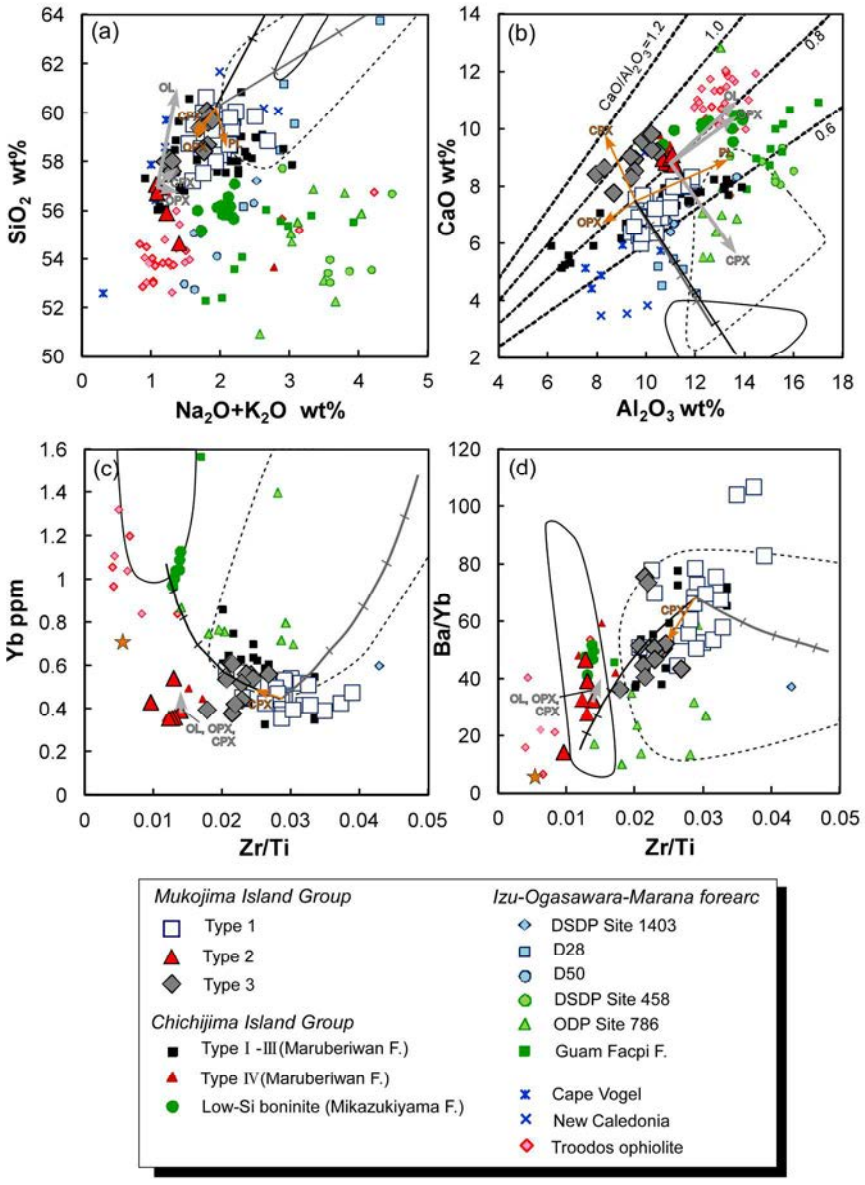

Figure 14 Variation diagrams of bulk chemical compositions of type 1, 2 and 3 boninites. (a) Total alkali (Na_2O+K_2O) vs. SiO_2, (b) Al_2O_3 vs. CaO. Broken lines show CaO/Al_2O_3 = 0.6, 0.8, 1.0 and 1.2, (c) Zr/Ti ratio vs. Yb concentration, (d) Zr/Ti vs. Ba/Yb ratios. Gray thick arrows are compositional trends of 20 wt% fractionation of olivine (OL, Fo_{91}), orthopyroxene (OPX, Mg#=0.91) and clinopyroxene (CPX, Mg#=0.90) from type 2 boninite. Fine arrows show vectors of 20 wt% addition of xenocrysts of OPX (Mg#=0.69) and CPX (Mg#=0.75) and An_{75} plagioclase (PL) to type 1 boninite. Stars show the average compositions of CPX (Mg#=0.62-75) xenocrysts. Compositional fields enclosed by solid and broken lines show arc tholeiitic rocks and high-Si boninite series rocks (bronzite andesite, dacite, quartz rhyolite) from the Mukojima Island Group, respectively. Black and gray lines with ticks show postulated mixing lines of type 1 boninite and 0-100 wt% arc tholeiitic dacite and 0-100 wt% of quartz rhyolite, respectively. Data sources: Mariana Trench (D28,D50 and site 1403) (Hickey & Frey 1982; Bloomer & Hawkins 1987), Guam Facpi Formation (Reagan & Meijer 1984), Cape Vogel (Dallwitz *et al*. 1966; Walker & Cameron 1983), Chichijima Maruberiwan Formation (Umino 1986; Taylor *et al*. 1994), Leg 125 Hole 786A, B (Pearce *et al*. 1992b), Troodos ophiolite

(Cameron 1985; Flower & Levine 1987), Low-Si boninite of the Mikazukiyama Formation (Yajima & Fujimaki 2001; original data).
220x303mm (300 x 300 DPI)

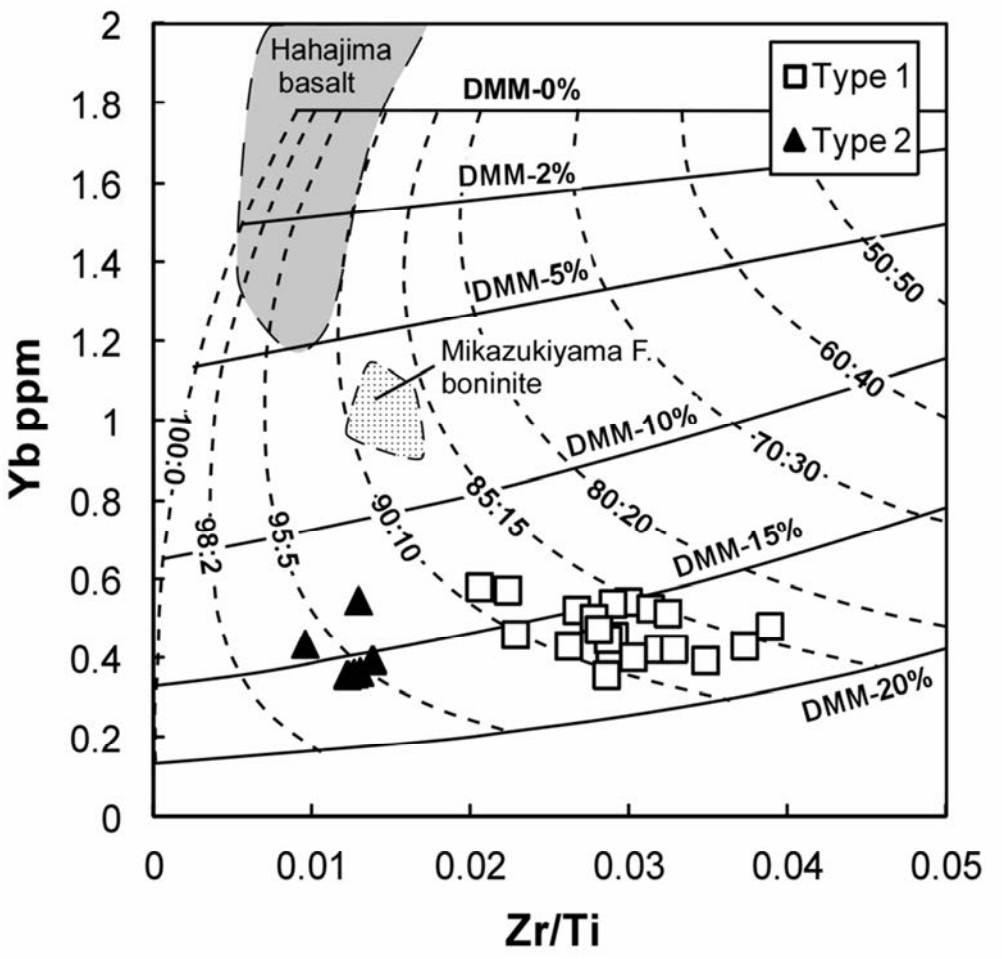

Figure 15 Zr/Ti vs. Yb for type 1 and 2 boninites. Also shown are mixing lines (black lines) between 15% batch melt of depleted MORB source mantle (DMM: Walkman & Hart 2005) and slab melt. Relative depletion of source mantle is shown by mixing lines (for example, "DMM-5%" means mixing line of slab melt and 15 wt% batch partial melt of residual DMM after 5 wt%-melt subtraction). Dashed lines are contours of iso-mixing-ratios of DMM and slab melts. Slab melt is calculated as 5% fractional melt of altered oceanic slab (average of Site 1149; Kelley *et al*. 2003) under amphibolite facies (clinopyroxene: amphibole: plagioclase=7:88:5). Partition coefficient for clinopyroxene-melt: Kelemen *et al*. (2003), amphibole-melt: Hilyard *et al*. (2000), plagioclase-melt: Smith & Asimow (2005). Hahajima basalts are from Taylor & Nesbitt (1995), Yajima *et al*. 2001, and Kanayama *et al*. (2010). Data source for low-Si boninite of the Mikazukiyama Formation is the same as in Fig. 14.
82x79mm (300 x 300 DPI)

Table S1 Representative glass compositions of scoria and pumice in tephra samples from Mukojima and Nakodojima

Sample ID	M3-07G	M3-07G	M3-07H	M3-07H	M3-07H	M3-07G	M3-07H	M3-07H	M3-07H	M3-07H	M3-07H	M3-07G	M3-07G	M3-07G	M3-07G	M3-07G	M3-07G	M3-07H	M3-07H
Type	Crystal-free scoria	Crystal-free scoria	Crystal-free scoria	Crystal-free scoria	Crystal-free scoria	Crystal-rich scoria	Crystal-rich scoria	Crystal-rich scoria	Crystal-rich scoria	Crystal-rich scoria	Crystal-rich scoria	Pumice	Pumice	Pumice	Pumice	Pumice	Pumice	Pumice	Pumice
(wt% oxides on an anhydrous basis)																			
SiO_2	57.17	56.96	58.59	58.32	58.71	63.64	58.54	58.24	58.85	59.09	59.74	80.30	78.02	74.23	77.76	77.88	77.61	77.09	76.74
TiO_2	0.15	0.14	0.19	0.04	0.10	0.10	0.20	0.17	0.17	0.18	0.08	0.02	0.13	0.15	0.12	0.12	0.15	0.12	0.13
Al_2O_3	13.30	13.33	14.04	12.81	13.39	13.24	13.87	13.95	13.60	13.32	13.72	11.99	12.26	11.64	12.02	11.87	11.80	12.37	11.95
FeO*	8.05	8.10	7.77	8.71	8.09	6.54	8.66	8.62	8.60	8.63	8.40	0.35	2.25	5.90	2.87	2.70	2.73	2.89	2.73
MnO	0.16	0.16	0.14	0.20	0.10	0.08	0.19	0.18	0.16	0.14	0.16	0.07	0.07	0.00	0.04	0.06	0.07	0.06	0.07
MgO	7.80	7.91	7.25	8.23	7.67	5.46	5.59	5.68	5.57	5.55	5.88	0.08	0.21	0.65	0.37	0.31	0.31	0.54	0.43
CaO	11.36	11.38	9.81	9.62	9.83	8.27	10.33	10.47	10.45	10.50	10.02	4.61	2.76	3.41	3.13	2.91	2.85	3.24	3.16
Na_2O	1.61	1.61	1.84	1.71	1.64	2.08	2.15	2.16	2.11	2.12	1.61	2.53	3.13	3.02	2.27	2.26	2.41	2.45	3.54
K_2O	0.28	0.27	0.37	0.28	0.43	0.56	0.40	0.45	0.44	0.42	0.36	0.06	1.18	0.99	1.40	1.87	2.06	1.21	1.22
FeO*/MgO	1.03	1.02	1.07	1.06	1.06	1.20	1.55	1.52	1.55	1.55	1.43	4.50	10.91	9.09	7.89	8.72	8.90	5.62	6.42
(ppm)																			
Li	7.2	7.3				9.9	6.8	6.7	6.8	6.9		0.2	1.6	1.5	37.1	0.9	0.6	16.0	1.2
B	10.2	12.0				25.2	10.5	10.9	10.5	10.1		38.7	35.3	31.1	21.6	21.7	21.2	30.5	31.7
Sc	47.0	47.1				36.3	41.8	41.5	41.4	41.9		14.1	12.9	13.6	24.5	11.6	12.3	17.1	13.1
Ti	627	626				937	1077	1087	1083	1079		810	713	744	1321	853	862	960	845
V	240	241				182	239	244	245	243		17	15	17	37	14	15	41	18
Cr	286	292				112	32	30	33	36		2	4	6	10	1	1	11	1
Co	40.6	41.3				27.0	34.8	35.0	35.5	35.2		3.9	3.3	4.1	14.9	3.4	3.6	6.9	4.1
Ni	73.4	74.8				66.0	24.3	24.2	24.7	24.6		1.0	1.0	3.6	53.4	0.7	0.6	10.4	1.0
Rb	8.7	9.1				15.1	10.4	10.3	10.4	10.2		29.1	30.1	27.4	30.4	45.7	34.0	29.2	31.5
Sr	66	67				76	117	117	118	117		88	79	82	99	96	89	98	94
Y	2.9	3.0				5.4	5.3	5.3	5.3	5.3		8.0	7.2	7.3	9.2	7.7	8.2	7.9	8.2
Zr	10	10				22	23	23	23	23		42	37	39	68	42	43	49	44
Nb	0.45	0.46				1.19	1.74	1.77	1.74	1.78		2.47	2.17	2.17	2.96	2.30	2.32	2.35	2.35
Cs	0.47	0.50				0.78	0.39	0.37	0.38	0.37		1.42	1.25	1.20	1.31	1.57	1.45	1.31	1.50
Ba	39	40				75	57	58	59	58		140	123	126	120	128	141	135	147
La	0.66	0.71				1.52	1.41	1.40	1.42	1.42		2.87	2.57	2.63	2.89	2.50	2.69	2.53	2.76
Ce	1.17	1.24				2.82	2.83	2.81	2.89	2.84		5.15	4.57	4.66	4.21	4.45	4.83	4.48	4.91
Pr	0.20	0.20				0.43	0.43	0.43	0.43	0.44		0.75	0.68	0.69	0.85	0.70	0.74	0.70	0.76
Nd	0.87	0.91				2.08	1.97	1.94	1.97	1.98		3.49	3.19	3.24	3.80	2.99	3.30	3.12	3.40
Sm	0.25	0.27				0.59	0.57	0.57	0.57	0.56		0.91	0.83	0.84	1.06	0.77	0.87	0.90	0.90
Eu	0.10	0.10				0.19	0.20	0.20	0.20	0.20		0.24	0.22	0.22	0.30	0.21	0.22	0.21	0.23
Gd	0.34	0.35				0.74	0.72	0.70	0.72	0.70		1.11	1.00	1.03	1.29	1.02	1.09	1.03	1.13
Tb	0.05	0.06				0.12	0.13	0.12	0.12	0.12		0.17	0.16	0.16	0.24	0.17	0.18	0.18	0.17
Dy	0.43	0.45				0.87	0.83	0.82	0.83	0.85		1.27	1.17	1.18	1.61	1.13	1.22	1.16	1.22
Ho	0.09	0.09				0.18	0.18	0.19	0.18	0.18		0.27	0.24	0.24	0.31	0.24	0.26	0.25	0.28
Er	0.33	0.34				0.62	0.58	0.57	0.59	0.58		0.86	0.78	0.79	1.06	0.82	0.86	0.84	0.89
Tm	0.05	0.06				0.10	0.09	0.09	0.09	0.09		0.14	0.13	0.12	0.19	0.12	0.14	0.14	0.14
Yb	0.43	0.45				0.80	0.67	0.66	0.67	0.68		1.10	1.00	1.02	1.48	0.90	1.01	0.99	1.06
Lu	0.07	0.08				0.12	0.11	0.11	0.11	0.11		0.18	0.16	0.16	0.26	0.16	0.18	0.18	0.19
Hf	0.29	0.28				0.64	0.62	0.60	0.62	0.61		1.26	1.10	1.13	2.05	1.15	1.26	1.43	1.34
Ta	0.03	0.04				0.09	0.11	0.10	0.11	0.10		0.18	0.16	0.16	0.24	0.14	0.17	0.19	0.18
Pb	1.93	2.11				3.66	1.49	1.45	1.49	1.48		7.74	7.11	6.08	11.89	8.75	7.09	7.61	7.29
Th	0.09	0.10				0.23	0.19	0.20	0.19	0.20		0.46	0.41	0.42	0.58	0.40	0.44	0.44	0.48
U	0.13	0.13				0.25	0.15	0.15	0.16	0.16		0.49	0.42	0.41	0.50	0.45	0.48	0.47	0.52
Zr/Ti	0.016	0.016				0.023	0.021	0.021	0.021	0.021		0.052	0.052	0.052	0.052	0.049	0.050	0.051	0.052

*Total Fe as FeO.

†BCR-2G reported value: Pearce et al. (1997)

M3-07H	M3-07H	M3-07H	M3-07H	M2-06D	M2-06D	M2-06D	M2-06D	M2-06D	M3-07I	M3-07I	M3-07I	M3-07I	M3-07I	N2-09	N2-09	N2-09	N2-09	N2-09	N2-09
Pumice	Pumice	Pumice	Pumice	Pumice	Pumice	Pumice	Pumice	Pumice	Pumice	Pumice	Pumice	Pumice	Pumice	Pumice	Pumice	Pumice	Pumice	Pumice	Pumice
76.75	77.56	77.67	76.68	79.96	75.63	71.79	74.53	71.58	77.75	77.33	77.51	77.72	75.63	77.21	77.14	77.38	77.85	77.30	77.46
0.13	0.12	0.14	0.12	0.06	0.02	0.08	0.09	0.03	0.06	0.00	0.07	0.06	0.03	0.16	0.16	0.17	0.15	0.15	0.21
12.08	12.17	11.97	12.05	13.39	15.15	15.67	14.92	14.15	14.57	14.78	13.96	14.54	15.24	12.25	12.06	12.27	11.92	12.03	12.30
2.73	2.84	2.79	2.87	0.08	0.96	2.77	1.96	3.96	0.07	0.04	0.12	0.17	0.83	2.32	2.22	2.15	2.10	2.05	2.13
0.05	0.09	0.04	0.07	0.06	0.13	0.18	0.10	0.06	0.04	0.05	0.01	0.01	0.04	0.04	0.05	0.04	0.04	0.05	0.10
0.43	0.44	0.66	0.45	0.14	1.56	2.22	2.30	2.00	1.50	1.40	1.00	1.67	1.57	0.50	0.51	0.47	0.45	0.42	0.51
3.06	3.21	2.96	3.17	2.53	2.76	3.13	2.95	3.89	1.62	1.59	1.48	1.95	2.36	2.79	2.71	2.79	2.66	2.60	2.79
3.69	2.42	2.29	3.47	3.41	2.79	2.81	1.85	3.45	2.68	3.12	4.46	2.66	2.87	3.53	3.92	3.54	3.62	4.20	3.29
1.04	1.12	1.45	1.13	0.32	1.01	1.34	1.28	0.86	1.69	1.68	1.34	1.21	1.43	1.17	1.19	1.16	1.18	1.19	1.20
6.42	6.55	5.23	6.45	0.53	0.61	1.25	0.85	1.98	0.05	0.03	0.13	0.10	0.53	4.65	4.46	4.62	4.64	4.87	4.17
17.5	39.2	16.5	3.0											4.4	3.7	3.5	2.9	8.7	3.2
31.3	34.1	31.9	30.0											18.5	22.2	24.5	24.1	26.5	36.8
18.2	26.1	17.6	12.7											11.7	13.7	13.3	9.9	18.9	14.0
1013	1278	1018	798											1007	1219	1179	1017	1451	811
46	67	37	18											45	43	45	36	52	42
19	30	8	2											22	24	15	3	58	17
8.0	14.4	7.7	3.8											4.7	4.3	4.4	3.6	5.5	4.7
12.7	28.4	10.9	0.7											6.4	6.3	4.6	1.1	13.3	7.5
31.2	31.0	33.2	27.4											29.4	34.6	35.8	33.5	35.8	27.9
101	107	103	90											70	81	79	73	83	61
8.2	7.8	8.3	7.8											7.1	8.4	8.5	7.9	8.8	6.5
51	62	51	42											61	77	76	62	102	52
2.45	2.88	2.57	2.12											1.41	1.79	1.73	1.45	2.22	1.30
1.40	1.36	1.47	1.28											1.42	1.61	1.73	1.65	1.72	1.32
142	126	150	133											92	110	107	106	109	81
2.63	2.42	2.69	2.53											2.17	2.59	2.62	2.38	2.72	2.02
4.67	4.27	4.85	4.49											3.69	4.39	4.38	4.12	4.38	3.60
0.72	0.66	0.76	0.69											0.61	0.71	0.72	0.68	0.72	0.55
3.25	2.96	3.29	3.04											2.69	3.22	3.24	3.01	3.23	2.47
0.99	0.85	0.94	0.80											0.70	0.83	0.82	0.76	0.81	0.67
0.22	0.21	0.23	0.22											0.17	0.20	0.20	0.19	0.20	0.16
1.06	1.00	1.09	0.98											0.85	0.96	1.05	0.95	1.07	0.75
0.19	0.17	0.19	0.17											0.14	0.17	0.17	0.16	0.16	0.13
1.22	1.18	1.28	1.16											1.03	1.22	1.25	1.15	1.23	1.00
0.27	0.25	0.27	0.25											0.22	0.27	0.26	0.26	0.28	0.23
0.87	0.87	0.90	0.82											0.78	0.91	0.95	0.89	0.96	0.73
0.15	0.14	0.15	0.13											0.13	0.14	0.15	0.14	0.15	0.12
1.04	1.07	1.11	0.96											0.92	1.13	1.12	1.06	1.10	0.98
0.19	0.19	0.20	0.17											0.17	0.19	0.19	0.19	0.20	0.15
1.44	1.74	1.58	1.21											1.66	2.02	2.12	1.73	2.77	1.43
0.19	0.23	0.20	0.15											0.11	0.14	0.14	0.12	0.18	0.11
8.24	11.50	9.10	6.26											4.40	5.28	5.54	4.58	5.20	3.83
0.47	0.49	0.49	0.41											0.36	0.42	0.43	0.39	0.50	0.32
0.52	0.54	0.55	0.44											0.34	0.40	0.39	0.35	0.42	0.27
0.050	0.048	0.050	0.052											0.061	0.063	0.064	0.061	0.070	0.064

N2-09 Pumice	BCR-2G average[†]	σ
	n=9	
77.94	55.28	0.32
0.14	2.32	0.08
12.15	13.63	0.11
1.93	12.42	0.32
0.01	0.17	0.09
0.42	3.61	0.08
2.57	7.39	0.12
3.54	3.33	0.08
1.27	1.85	0.05
4.63		
	n=14	
2.9	9.1	0.2
40.3	12.2	2.8
11.1	34.9	0.7
847	13872	306
36	415	4
22	16.2	0.4
3.8	36.5	0.6
4.9	14.9	0.7
29.9	46.3	1.0
62	326	6
6.6	32.7	1.0
53	172	7
1.38	12.62	0.24
1.42	1.09	0.03
85	660	16
2.13	24.77	0.61
3.83	50.78	1.35
0.57	6.38	0.14
2.59	28.36	0.94
0.64	6.42	0.20
0.17	1.91	0.05
0.83	6.41	0.24
0.13	0.95	0.03
0.98	6.25	0.23
0.21	1.23	0.04
0.73	3.48	0.12
0.12	0.49	0.02
0.91	3.43	0.11
0.16	0.49	0.02
1.45	4.50	0.15
0.11	0.80	0.02
4.15	11.21	0.57
0.35	5.88	0.18
0.31	1.59	0.03
0.063		

Table S2 Representative microprobe analyses of minerals in tephra samples from Mukojima and Nakodojima

	Crystal-rich scoria								
	Orthopyroxene								
Sample ID	M3-07G	M3-07G	M3-07G	M3-07G	M3-07G	M3-07H	M3-07H	M3-07H	M3-07H
(wt%)									
SiO_2	58.03	58.23	56.52	57.38	57.47	53.98	54.12	57.21	56.53
TiO_2	0.06	0.01	0.07	0.07	0.00	0.01	0.09	0.00	0.00
Al_2O_3	0.48	0.61	1.11	1.04	0.74	0.92	0.80	0.76	0.70
FeO*	7.86	6.49	8.86	8.24	8.72	17.85	21.26	6.85	6.49
MnO	0.20	0.25	0.23	0.11	0.21	0.37	0.48	0.13	0.20
MgO	32.95	33.74	31.09	31.20	32.05	25.60	23.05	33.60	34.26
CaO	1.13	0.83	1.59	1.54	1.19	0.99	1.11	0.93	0.88
Na_2O	0.00	0.00	0.02	0.02	0.04	0.00	0.03	0.00	0.03
K_2O	0.01	0.01	0.00	0.00	0.00	0.00	0.03	0.01	0.00
Cr_2O_3	0.26	0.41	0.71	0.63	0.48	0.25	0.17	0.65	0.56
Total	100.99	100.58	100.20	100.22	100.88	99.96	101.11	100.13	99.64
Cations									
O	6	6	6	6	6	6	6	6	6
Si	1.996	1.998	1.976	1.995	1.989	1.971	1.983	1.979	1.965
Ti	0.002	0.000	0.002	0.002	0.000	0.000	0.002	0.000	0.000
Al	0.020	0.025	0.046	0.043	0.030	0.040	0.035	0.031	0.029
Fe	0.226	0.186	0.259	0.240	0.252	0.545	0.651	0.198	0.189
Mn	0.006	0.007	0.007	0.003	0.006	0.011	0.015	0.004	0.006
Mg	1.690	1.726	1.621	1.617	1.653	1.393	1.259	1.733	1.776
Ca	0.042	0.030	0.060	0.057	0.044	0.039	0.043	0.035	0.033
Na	0.000	0.000	0.001	0.001	0.003	0.000	0.002	0.000	0.002
K	0.001	0.000	0.000	0.000	0.000	0.000	0.001	0.000	0.000
Cr	0.007	0.011	0.020	0.017	0.013	0.007	0.005	0.018	0.015
Total	3.989	3.984	3.990	3.974	3.991	4.006	3.996	3.997	4.014
Mg#†	0.882	0.903	0.862	0.871	0.868	0.719	0.659	0.897	0.904
An	-	-	-	-	-	-	-	-	-

*Total Fe as FeO.

†Mg#=Mg/(Mg+Fe^{2+})

-, no data

Fragmental crystal									
Orthopyroxene									
M3-07G	M3-07G	M3-07G	M3-07G	M3-07H	M3-07H	M3-07H	M3-07H	M3-07H	M3-07I
57.17	54.00	57.50	57.26	55.77	54.05	57.00	57.84	57.53	54.55
0.01	0.00	0.04	0.02	0.03	0.08	0.00	0.00	0.01	0.07
1.03	1.02	0.79	0.65	1.23	1.00	0.54	0.32	0.45	0.91
8.56	18.24	10.60	9.03	13.05	18.60	9.73	8.33	8.28	16.83
0.27	0.37	0.31	0.24	0.36	0.53	0.15	0.14	0.19	0.37
31.46	25.11	30.03	31.37	28.18	25.17	31.85	32.41	32.05	26.17
1.88	1.35	1.36	1.72	2.12	0.80	0.81	1.54	1.67	1.41
0.00	0.02	0.00	0.00	0.01	0.02	0.02	0.00	0.04	0.02
0.00	0.01	0.01	0.00	0.00	0.01	0.00	0.01	0.02	0.00
0.59	0.19	0.31	0.20	0.14	0.31	0.41	0.26	0.26	0.15
100.97	100.32	100.95	100.50	100.88	100.56	100.50	100.85	100.51	100.48
6	6	6	6	6	6	6	6	6	6
1.981	1.969	2.004	1.994	1.975	1.968	1.988	1.999	1.997	1.973
0.000	0.000	0.001	0.001	0.001	0.002	0.000	0.000	0.000	0.002
0.042	0.044	0.032	0.027	0.051	0.043	0.022	0.013	0.018	0.039
0.248	0.556	0.309	0.263	0.386	0.567	0.284	0.241	0.240	0.509
0.008	0.011	0.009	0.007	0.011	0.016	0.004	0.004	0.006	0.011
1.625	1.365	1.560	1.629	1.488	1.366	1.656	1.670	1.658	1.411
0.070	0.053	0.051	0.064	0.080	0.031	0.030	0.057	0.062	0.055
0.000	0.001	0.000	0.000	0.000	0.001	0.001	0.000	0.003	0.001
0.000	0.001	0.000	0.000	0.000	0.001	0.000	0.001	0.001	0.000
0.016	0.006	0.008	0.005	0.004	0.009	0.011	0.007	0.007	0.004
3.990	4.007	3.975	3.989	3.997	4.004	3.996	3.991	3.992	4.005
0.868	0.710	0.835	0.861	0.794	0.707	0.854	0.874	0.873	0.735
-	-	-	-	-	-	-	-	-	-

M3-07I	M3-07I	M3-07I	M3-07I	M3-07I	M3-07I	M2-06D	M2-06D	M2-06D	M2-06D
53.83	56.04	57.39	57.27	55.81	57.55	57.43	57.42	56.98	57.58
0.07	0.03	0.01	0.02	0.00	0.00	0.04	0.00	0.09	0.00
0.52	0.50	0.63	0.70	0.79	0.49	0.97	0.58	1.33	0.85
21.05	11.89	6.42	8.47	10.60	7.31	8.05	9.12	9.23	7.88
0.48	0.24	0.24	0.11	0.29	0.04	0.13	0.27	0.22	0.27
23.59	29.60	33.87	31.90	30.34	33.47	32.86	32.21	31.25	32.58
0.89	1.70	0.94	1.32	1.86	1.17	1.38	1.40	1.88	1.94
0.03	0.00	0.02	0.00	0.02	0.01	0.00	0.00	0.00	0.02
0.01	0.00	0.00	0.01	0.00	0.02	0.00	0.00	0.00	0.02
0.00	0.14	0.52	0.36	0.14	0.42	0.55	0.33	0.47	0.34
100.46	100.13	100.03	100.16	99.84	100.48	101.40	101.33	101.46	101.48
6	6	6	6	6	6	6	6	6	6
1.983	1.986	1.984	1.993	1.975	1.987	1.974	1.984	1.970	1.979
0.002	0.001	0.000	0.001	0.000	0.000	0.001	0.000	0.002	0.000
0.023	0.021	0.025	0.029	0.033	0.020	0.039	0.024	0.054	0.034
0.649	0.353	0.185	0.247	0.314	0.211	0.231	0.264	0.267	0.226
0.015	0.007	0.007	0.003	0.009	0.001	0.004	0.008	0.007	0.008
1.296	1.564	1.745	1.655	1.601	1.722	1.683	1.659	1.611	1.669
0.035	0.065	0.035	0.049	0.071	0.043	0.051	0.052	0.070	0.072
0.002	0.000	0.001	0.000	0.001	0.001	0.000	0.000	0.000	0.001
0.001	0.000	0.000	0.000	0.000	0.001	0.000	0.000	0.000	0.001
0.000	0.004	0.014	0.010	0.004	0.011	0.015	0.009	0.013	0.009
4.005	4.000	3.997	3.987	4.007	3.998	3.998	4.000	3.994	4.000
0.666	0.816	0.904	0.870	0.836	0.891	0.879	0.863	0.858	0.881
-	-	-	-	-	-	-	-	-	-

		Clinopyroxene							Plagioclase
M2-06D	M2-06D	M3-07I	M3-07I	M3-07I	M3-07I	M3-07I	M2-06D	M2-06D	M2-06D
55.82	56.39	53.17	53.36	51.88	52.74	54.42	53.93	53.11	47.14
0.06	0.00	0.06	0.05	0.07	0.08	0.07	0.08	0.03	0.02
0.95	1.00	1.00	1.86	1.56	0.78	0.94	0.92	1.94	33.85
13.94	11.23	9.33	7.23	14.25	9.72	5.60	8.08	6.36	0.47
0.42	0.38	0.23	0.22	0.27	0.22	0.08	0.18	0.27	0.00
28.15	30.06	14.18	16.60	11.81	14.21	18.20	15.12	17.35	0.02
1.90	1.96	21.40	20.90	20.66	21.71	20.46	22.26	20.02	17.35
0.09	0.00	0.33	0.22	0.17	0.22	0.09	0.29	0.13	1.65
0.01	0.00	0.00	0.04	0.00	0.00	0.00	0.00	0.00	0.03
0.12	0.27	0.00	0.25	0.00	0.00	0.46	0.00	0.27	0.07
101.44	101.28	99.71	100.73	100.66	99.66	100.32	100.87	99.48	100.60
6	6	6	6	6	6	6	6	6	8
1.974	1.973	1.987	1.952	1.962	1.979	1.978	1.983	1.955	2.157
0.002	0.000	0.002	0.001	0.002	0.002	0.002	0.002	0.001	0.001
0.039	0.041	0.044	0.080	0.070	0.034	0.040	0.040	0.084	1.825
0.412	0.329	0.292	0.221	0.451	0.305	0.170	0.249	0.196	0.018
0.012	0.011	0.007	0.007	0.009	0.007	0.002	0.006	0.008	0.000
1.484	1.568	0.790	0.906	0.665	0.795	0.986	0.829	0.952	0.001
0.072	0.074	0.857	0.819	0.837	0.873	0.797	0.877	0.789	0.850
0.006	0.000	0.024	0.016	0.012	0.016	0.007	0.021	0.009	0.146
0.000	0.000	0.000	0.002	0.000	0.000	0.000	0.000	0.000	0.002
0.003	0.007	0.000	0.007	0.000	0.000	0.013	0.000	0.008	0.002
4.006	4.003	4.002	4.011	4.007	4.010	3.996	4.006	4.003	5.003
0.783	0.827	0.730	0.804	0.596	0.723	0.853	0.769	0.830	-
-	-	-	-	-	-	-	-	-	85.2

M2-06D	M2-06D	M2-06D	M2-06D
46.23	47.72	47.66	46.67
0.03	0.00	0.00	0.00
34.07	33.27	33.37	33.96
0.52	0.44	0.44	0.39
0.00	0.00	0.03	0.03
0.04	0.05	0.01	0.01
18.01	17.11	16.92	17.74
1.29	1.81	1.81	1.39
0.03	0.00	0.00	0.01
0.02	0.00	0.00	0.02
100.22	100.41	100.24	100.22
8	8	8	8
2.128	2.184	2.184	2.144
0.001	0.000	0.000	0.000
1.848	1.794	1.802	1.839
0.020	0.017	0.017	0.015
0.000	0.000	0.001	0.001
0.003	0.004	0.001	0.001
0.888	0.839	0.831	0.873
0.115	0.161	0.160	0.124
0.001	0.000	0.000	0.001
0.001	0.000	0.000	0.001
5.005	4.999	4.996	4.998
-	-	-	-
88.4	83.9	83.8	87.5

Table S3 Whole rock compositions of volcanic rocks from Mukojima Island Group

Locality	Yon'noiwa	Sasayojima	Mukojima																								
Sample ID	Yon'noiwa	S1-01A	S1-01B	M2-04A	M2-05A	M2-05B	07111601-2	M1-04	M2-01Aα	M4-01	M1-03Cα	M1-02C	M2-03	M2-09B	07111604	M2-06B	M2-06Aβ	M2-06Aα	M2-08	M1-05	M2-02	07111606-1	M2-06C	M2-01C	M1-07D	M1-07Cβ
Rock type	Type1 boninite	Type1 boninite	Bronzite andesite	Type1 boninite	Type1 boninite	Type1 boninite	Type1 boninite	Type1 boninite	Type1 boninite	Type1 boninite	Type1 boninite	Type1 boninite	Type1 boninite	Type2 boninite	Type2 boninite	Type2 boninite	Type2 boninite	Type2 boninite	Type2 boninite	Type3 boninite	Type3 boninite	Type3 boninite	Type3 boninite	Type3 boninite	Type3 boninite	Type3 boninite	Type3 boninite
(wt% oxides on an anhydrous basis)																											
SiO_2	57.56	59.28	59.62	59.05	59.39	59.88	59.83	60.05	59.63	60.13	59.75	58.88	60.06	54.65	55.92	56.74	57.07	56.97	56.75	58.14	57.62	58.01	58.03	59.39	58.43	58.53
TiO_2	0.10	0.09	0.11	0.09	0.09	0.09	0.11	0.10	0.14	0.10	0.10	0.11	0.16	0.16	0.10	0.08	0.08	0.08	0.08	0.10	0.11	0.09	0.09	0.13	0.13	0.14
Al_2O_3	10.35	10.36	13.54	9.39	10.26	10.40	9.67	9.67	9.52	9.56	9.94	10.75	10.58	11.05	11.12	10.66	10.78	11.01	10.99	7.94	8.29	8.66	9.37	9.34	9.82	10.22
FeO*	8.71	8.61	8.60	8.40	8.43	8.50	9.09	9.45	8.63	9.17	9.18	9.01	9.04	8.76	9.00	8.84	8.82	8.87	9.00	8.45	8.52	8.70	8.83	8.47	8.54	8.62
MnO	0.16	0.15	0.13	0.16	0.16	0.15	0.17	0.19	0.17	0.18	0.17	0.17	0.17	0.20	0.16	0.17	0.16	0.16	0.16	0.18	0.17	0.18	0.18	0.17	0.16	0.16
MgO	14.12	9.88	6.01	14.57	12.78	12.08	12.69	11.83	11.11	11.41	11.34	11.01	10.81	14.66	13.70	13.46	13.15	13.02	12.91	15.48	15.32	15.35	13.86	11.72	11.54	11.27
CaO	7.23	9.15	9.25	6.41	6.70	6.37	6.28	6.93	8.96	7.56	7.51	7.37	6.94	9.11	8.77	8.96	8.85	8.76	9.01	8.43	8.65	7.79	8.32	9.05	9.59	9.29
Na_2O	1.41	1.66	2.21	1.45	1.62	1.62	1.33	1.37	1.45	1.35	1.33	1.72	1.58	1.14	0.76	0.87	0.88	0.92	0.91	0.95	0.94	0.97	1.04	1.36	1.25	1.43
K_2O	0.35	0.80	0.50	0.46	0.55	0.88	0.80	0.38	0.37	0.52	0.65	0.96	0.64	0.25	0.46	0.21	0.19	0.19	0.18	0.32	0.35	0.24	0.26	0.33	0.51	0.31
P_2O_5	0.02	0.02	0.03	0.02	0.02	0.03	0.02	0.02	0.02	0.03	0.02	0.02	0.03	0.02	0.01	0.02	0.02	0.01	0.01	0.02	0.02	0.02	0.02	0.02	0.02	0.02
FeO*/MgO	0.62	0.87	1.43	0.58	0.66	0.70	0.72	0.80	0.78	0.80	0.81	0.82	0.84	0.60	0.66	0.66	0.67	0.68	0.70	0.55	0.56	0.57	0.64	0.72	0.74	0.77
CaO/Al_2O_3	0.70	0.88	0.68	0.68	0.65	0.61	0.65	0.72	0.94	0.79	0.76	0.69	0.66	0.82	0.79	0.84	0.82	0.80	0.82	1.06	1.04	0.90	0.89	0.97	0.98	0.91
Na_2O+K_2O	1.75	2.46	2.71	1.91	2.17	2.50	2.14	1.75	1.82	1.87	1.98	2.68	2.22	1.40	1.22	1.08	1.06	1.12	1.09	1.26	1.30	1.20	1.30	1.69	1.76	1.75
(ppm)																											
V	175	209	261	161	169	166	167	178	208	180	173	199	181	181	215	213	223	201	206	164	152	159	187	160	182	173
Cr	1091	652	227	999	1037	823	795	635	592	559	631	748	575	1078	800	992	958	860	840	1092	961	985	926	722	801	700
Rb	8.64	16.42	14.97	11.49	14.25	13.85	13.17	9.61	8.74	10.32	13.02	16.24	12.95	4.62	3.79	4.06	3.82	3.70	3.35	7.67	5.86	7.02	7.41	8.45	9.34	8.25
Sr	57	67	102	68	77	74	99	77	67	88	102	70	119	72	118	47	43	46	43	61	55	51	59	65	70	77
Y	3.5	4.2	5.2	3.4	3.7	4.2	4.0	3.8	5.1	4.2	3.8	4.5	5.3	4.8	3.1	2.4	2.3	2.3	2.4	4.3	3.6	3.2	3.5	4.8	5.3	5.0
Zr	13.4	22.5	28.1	18.2	20.8	21.9	18.8	18.1	19.1	17.9	18.6	19.8	21.2	12.1	6.0	6.2	6.5	6.7	6.2	14.2	11.9	11.3	11.8	18.4	20.9	17.6
Nb	0.42	0.63	0.95	0.46	0.47	0.48	0.31	0.33	0.25	0.27	0.27	0.36	0.28	0.39	0.21	0.24	0.24	0.26	0.23	0.23	0.19	0.39	0.41	0.24	0.27	0.28
Cs	0.40	0.51	0.63	0.50	0.62	0.49	0.44	0.35	0.28	0.33	0.42	0.36	0.46	0.22	0.17	0.25	0.25	0.26	0.23	0.26	0.23	0.37	0.39	0.28	0.25	0.26
Ba	32.0	38.7	62.6	40.7	45.9	39.6	33.0	33.1	28.4	30.5	31.7	28.6	44.6	15.1	6.2	16.8	14.2	12.8	11.7	20.8	14.4	28.9	31.3	26.5	24.5	27.8
La	0.78	1.05	1.32	0.93	1.03	1.08	0.96	0.77	0.74	0.92	0.73	0.83	0.73	0.61	0.35	0.44	0.42	0.45	0.40	0.64	0.48	0.66	0.68	0.67	0.75	0.60
Ce	1.53	2.10	2.66	1.76	2.02	2.11	1.72	1.55	1.67	1.63	1.45	1.73	1.71	1.51	0.77	0.96	0.94	0.99	0.92	1.27	1.12	1.29	1.31	1.62	1.71	1.38
Pr	0.22	0.28	0.33	0.24	0.27	0.29	0.26	0.22	0.24	0.23	0.22	0.24	0.25	0.24	0.13	0.14	0.13	0.14	0.13	0.19	0.16	0.21	0.19	0.23	0.25	0.21
Nd	1.06	1.33	1.67	1.14	1.17	1.31	1.13	1.09	1.23	1.13	0.99	1.20	1.26	1.14	0.64	0.63	0.62	0.68	0.64	0.98	0.83	0.92	0.93	1.18	1.31	1.13
Sm	0.33	0.40	0.49	0.32	0.35	0.37	0.35	0.34	0.45	0.39	0.33	0.40	0.46	0.42	0.26	0.20	0.19	0.21	0.21	0.35	0.30	0.29	0.32	0.40	0.44	0.39
Eu	0.13	0.13	0.17	0.10	0.12	0.12	0.16	0.13	0.15	0.15	0.12	0.14	0.16	0.15	0.09	0.10	0.08	0.08	0.08	0.13	0.10	0.11	0.12	0.15	0.17	0.13
Gd	0.46	0.46	0.60	0.39	0.41	0.53	0.45	0.43	0.58	0.45	0.44	0.52	0.56	0.58	0.39	0.27	0.25	0.29	0.27	0.46	0.39	0.39	0.42	0.56	0.60	0.56
Tb	0.07	0.09	0.11	0.07	0.07	0.08	0.08	0.08	0.10	0.08	0.08	0.09	0.11	0.10	0.07	0.04	0.04	0.05	0.05	0.08	0.08	0.07	0.07	0.10	0.11	0.10
Dy	0.46	0.48	0.67	0.43	0.45	0.51	0.50	0.50	0.69	0.50	0.49	0.58	0.73	0.70	0.43	0.29	0.28	0.31	0.30	0.50	0.46	0.45	0.43	0.64	0.71	0.62
Ho	0.12	0.12	0.16	0.10	0.11	0.12	0.11	0.12	0.16	0.13	0.12	0.13	0.16	0.16	0.10	0.07	0.07	0.07	0.07	0.12	0.11	0.10	0.11	0.15	0.16	0.15
Er	0.37	0.40	0.53	0.34	0.37	0.38	0.38	0.39	0.47	0.39	0.37	0.43	0.53	0.50	0.32	0.26	0.28	0.26	0.25	0.39	0.36	0.33	0.34	0.48	0.50	0.47
Tm	0.08	0.07	0.09	0.06	0.06	0.07	0.08	0.06	0.08	0.09	0.06	0.08	0.08	0.09	0.06	0.06	0.05	0.05	0.05	0.07	0.06	0.06	0.06	0.08	0.09	0.09
Yb	0.46	0.49	0.62	0.39	0.43	0.48	0.42	0.45	0.56	0.44	0.42	0.54	0.57	0.54	0.43	0.36	0.36	0.39	0.36	0.45	0.40	0.38	0.42	0.52	0.56	0.54
Lu	0.09	0.09	0.12	0.07	0.08	0.09	0.08	0.09	0.09	0.08	0.08	0.10	0.10	0.09	0.08	0.07	0.06	0.07	0.07	0.08	0.07	0.07	0.07	0.09	0.10	0.10
Hf	0.37	0.50	0.72	0.46	0.50	0.53	0.48	0.48	0.50	0.47	0.47	0.47	0.54	0.34	0.18	0.17	0.17	0.19	0.18	0.34	0.29	0.31	0.32	0.47	0.49	0.45
Ta	0.033	0.060	0.090	0.039	0.038	0.041	0.027	0.028	0.017	0.009	0.014	0.037	0.021	0.035	0.006	0.009	0.010	0.019	0.008	0.026	0.007	0.032	0.036	0.010	0.030	0.022
Pb	1.94	1.46	2.27	1.43	1.46	1.66	1.51	1.61	1.05	1.33	1.37	1.10	1.19	0.80	2.04	0.76	0.76	0.96	0.82	0.80	0.75	1.53	1.68	0.87	0.87	1.08
Th	0.18	0.14	0.19	0.22	0.24	0.24	0.11	0.11	0.18	0.08	0.09	0.12	0.20	0.14	0.05	0.18	0.18	0.14	0.17	0.08	0.16	0.09	0.20	0.18	0.08	0.13
U	0.13	0.14	0.18	0.12	0.14	0.13	0.11	0.11	0.08	0.09	0.09	0.13	0.09	0.06	0.04	0.07	0.07	0.07	0.06	0.08	0.06	0.10	0.12	0.07	0.08	0.08
Ba/La	41.0	36.8	47.5	44.0	44.7	36.6	34.3	42.8	38.1	33.0	43.5	34.4	61.2	24.6	17.9	37.8	33.8	28.4	28.9	32.6	29.9	43.4	45.9	39.5	32.6	46.2
Ba/Yb	70.0	79.8	101.6	103.9	106.6	83.0	78.6	72.9	50.4	68.6	75.6	52.7	78.1	27.8	14.2	46.8	39.3	32.7	32.9	46.8	36.3	75.8	73.7	50.8	43.6	51.6
Zr/Ti	0.023	0.040	0.041	0.035	0.037	0.039	0.029	0.029	0.023	0.029	0.032	0.030	0.022	0.013	0.010	0.013	0.013	0.014	0.012	0.023	0.018	0.021	0.022	0.023	0.027	0.021

*Total Fe as FeO.

					Harinoiwa				Tatamiiwa	Nakodojiri															
M2-01B	M2-01A	M1-07Cα	M4-04 C	M4-04 A	H1-03A	H1-03B	H1-01Aβ	H1-01 Bα	T1-01	N1-06C	N2-08B	N1-06B	N2-03B	N2-07	N2-02α	N2-01Aα	N3-10B	N1-03C	N3-11	N3-06B	N2-10A	N1-09Aβ	07111706	N1-08C	07111708-2	N2-01BβL
Type3 boninite	Type3 boninite	Type3 boninite	Type3 boninite	Type3 boninite	Bronzite andesite	Bronzite andesite	Bronzite andesite	Bronzite andesite	Bronzite andesite	Type1 boninite	Type1 boninite	Type1 boninite	Type1 boninite	Type1 boninite	Type1 boninite	Type1 boninite	Type1 boninite	Type1 boninite	Type1 boninite	Type1 boninite	Bronzite andesite	Bronzite andesite	Bronzite andesite	Bronzite andesite	Bronzite andesite	Bronzite andesite
60.11	59.63	58.70	59.71	59.90	58.62	59.83	60.89	58.46	59.90	59.30	58.01	58.74	59.52	58.72	58.30	58.80	62.01	60.29	61.70	60.66	60.68	59.85	61.94	60.23	63.57	58.79
0.14	0.14	0.15	0.15	0.16	0.32	0.32	0.41	0.32	0.40	0.12	0.12	0.10	0.09	0.12	0.12	0.12	0.11	0.09	0.12	0.10	0.15	0.13	0.13	0.16	0.16	0.14
9.52	9.52	10.44	10.21	10.12	14.79	14.27	15.10	15.35	15.52	9.77	10.98	9.83	9.79	11.48	11.84	11.82	11.95	10.60	12.07	11.09	13.32	13.52	12.07	13.41	14.24	13.24
8.61	8.63	8.55	8.50	8.55	9.32	9.18	7.78	10.19	8.14	8.43	8.64	9.01	9.24	8.61	8.83	8.72	7.99	9.05	7.65	8.87	7.85	8.37	8.57	8.03	6.71	8.87
0.16	0.17	0.16	0.16	0.17	0.12	0.13	0.12	0.15	0.13	0.16	0.15	0.17	0.16	0.15	0.17	0.15	0.13	0.16	0.13	0.15	0.13	0.13	0.15	0.13	0.08	0.14
11.08	11.11	10.96	9.54	9.41	5.51	5.16	4.09	4.58	4.57	14.34	12.53	12.90	13.23	10.76	10.39	10.20	9.16	10.28	8.66	9.30	6.83	7.23	7.37	6.78	5.60	7.31
8.55	8.96	9.21	9.83	9.83	8.67	8.58	8.46	8.15	8.35	5.99	7.62	7.71	6.34	8.03	8.33	8.24	6.39	7.73	7.22	8.01	8.44	8.40	7.60	8.59	6.59	9.28
1.42	1.45	1.45	1.53	1.51	1.97	2.05	2.65	2.06	2.29	1.40	1.40	1.17	1.18	1.68	1.57	1.52	1.50	1.24	1.92	1.27	2.06	1.85	1.63	2.10	2.06	1.72
0.38	0.37	0.36	0.36	0.34	0.65	0.45	0.46	0.73	0.66	0.48	0.53	0.36	0.42	0.44	0.42	0.40	0.73	0.55	0.49	0.53	0.52	0.51	0.51	0.54	0.96	0.49
0.03	0.02	0.02	0.02	0.02	0.03	0.04	0.05	0.03	0.05	0.03	0.03	0.01	0.02	0.03	0.03	0.02	0.03	0.02	0.03	0.02	0.03	0.02	0.02	0.03	0.03	0.03
0.78	0.78	0.78	0.89	0.91	1.69	1.78	1.90	2.22	1.78	0.59	0.69	0.70	0.70	0.80	0.85	0.85	0.87	0.88	0.88	0.95	1.15	1.16	1.16	1.18	1.20	1.21
0.90	0.94	0.88	0.96	0.97	0.59	0.60	0.56	0.53	0.54	0.61	0.69	0.78	0.65	0.70	0.70	0.70	0.53	0.73	0.60	0.72	0.63	0.62	0.63	0.64	0.46	0.70
1.80	1.82	1.81	1.88	1.85	2.62	2.49	3.10	2.79	2.94	1.88	1.93	1.54	1.61	2.12	1.99	1.92	2.24	1.79	2.41	1.79	2.58	2.36	2.15	2.64	3.02	2.20
159	168	187	191	196		467	286	390	256	164	186	188	160	209	205	216				196	216	256	212	224	212	231
726	743	739	487	499		95	59	4	59	878	794	901	997	595	659	584				486	300	334	295	265	295	247
9.26	8.74	9.52	7.77	8.15		10.69	13.33	10.00	9.65	10.84	13.61	10.96	14.32	11.44	11.08	11.42				13.14	12.75	16.50	13.19	13.11	13.19	12.11
73	67	80	71	72		125	115	114	105	64	100	52	51	70	60	60				72	98	72	81	96	81	75
5.0	5.1	5.2	5.2	5.5		8.1	12.5	6.8	12.7	3.5	3.8	3.4	2.6	4.0	3.9	4.1				3.8	4.9	4.7	4.1	4.9	4.1	4.5
20.0	19.1	21.0	19.9	19.8		28.5	43.3	30.9	39.7	18.5	20.0	19.2	15.9	22.4	19.5	19.2				19.9	27.0	26.2	24.1	27.4	24.1	20.7
0.25	0.25	0.29	0.29	0.32		0.52	0.58	0.55	0.54	0.27	0.38	0.35	0.31	0.42	0.40	0.41				0.47	0.51	0.52	0.52	0.51	0.52	0.44
0.25	0.28	0.28	0.28	0.29		0.37	0.55	0.39	0.45	0.45	0.56	0.45	0.47	0.50	0.51	0.50				0.62	0.56	0.70	0.60	0.54	0.60	0.50
28.3	28.4	28.3	24.9	27.5		28.9	33.0	24.5	22.2	19.2	28.7	24.5	23.5	28.0	28.1	28.7				34.7	34.1	36.9	40.4	33.9	40.4	27.9
0.62	0.74	0.76	0.68	0.76		1.10	1.50	0.85	1.33	0.60	0.65	0.67	0.46	0.81	0.75	0.73				0.75	1.09	0.85	0.91	1.06	0.91	0.76
1.45	1.67	1.70	1.61	1.69		2.71	3.81	1.96	3.59	1.22	1.37	1.33	0.87	1.54	1.42	1.46				1.38	2.17	1.78	1.70	2.12	1.70	1.50
0.22	0.24	0.24	0.23	0.27		0.37	0.54	0.30	0.52	0.17	0.20	0.18	0.12	0.23	0.22	0.21				0.21	0.30	0.23	0.26	0.31	0.26	0.22
1.15	1.23	1.29	1.19	1.25		1.86	2.96	1.53	2.83	0.83	1.01	0.87	0.60	1.04	0.96	1.03				0.97	1.47	1.17	1.14	1.48	1.14	1.14
0.39	0.45	0.44	0.46	0.44		0.63	1.06	0.53	1.09	0.26	0.30	0.27	0.14	0.32	0.32	0.32				0.31	0.46	0.37	0.36	0.44	0.36	0.34
0.13	0.15	0.17	0.16	0.16		0.24	0.39	0.22	0.44	0.08	0.11	0.10	0.06	0.11	0.10	0.11				0.09	0.14	0.13	0.12	0.15	0.12	0.12
0.53	0.58	0.59	0.58	0.61		0.87	1.37	0.71	1.47	0.35	0.39	0.33	0.26	0.42	0.38	0.43				0.38	0.59	0.48	0.47	0.57	0.47	0.49
0.09	0.10	0.11	0.11	0.11		0.15	0.26	0.14	0.29	0.06	0.07	0.06	0.05	0.07	0.07	0.07				0.07	0.10	0.08	0.08	0.10	0.08	0.08
0.63	0.69	0.70	0.66	0.69		1.02	1.75	0.92	1.80	0.41	0.47	0.41	0.32	0.49	0.47	0.48				0.46	0.64	0.54	0.49	0.65	0.49	0.56
0.14	0.16	0.16	0.15	0.17		0.22	0.40	0.23	0.41	0.11	0.12	0.10	0.08	0.13	0.12	0.13				0.12	0.15	0.13	0.12	0.15	0.12	0.15
0.45	0.47	0.52	0.51	0.52		0.75	1.19	0.65	1.26	0.33	0.36	0.33	0.26	0.41	0.38	0.42				0.40	0.51	0.45	0.42	0.52	0.42	0.46
0.08	0.08	0.09	0.09	0.10		0.13	0.20	0.11	0.24	0.06	0.07	0.06	0.05	0.08	0.07	0.08				0.07	0.09	0.09	0.07	0.09	0.07	0.09
0.54	0.56	0.56	0.61	0.61		0.83	1.31	0.78	1.35	0.43	0.47	0.42	0.36	0.52	0.50	0.52				0.51	0.61	0.61	0.50	0.62	0.50	0.61
0.09	0.09	0.10	0.11	0.11		0.14	0.21	0.13	0.22	0.07	0.08	0.08	0.07	0.09	0.10	0.10				0.09	0.11	0.11	0.09	0.11	0.09	0.11
0.47	0.50	0.49	0.53	0.46		0.78	1.08	0.76	0.98	0.43	0.46	0.40	0.36	0.52	0.46	0.49				0.47	0.67	0.57	0.57	0.68	0.57	0.51
0.018	0.017	0.031	0.013	0.015		0.036	0.053	0.041	0.049	0.013	0.025	0.042	0.037	0.030	0.032	0.032				0.037	0.038	0.046	0.042	0.036	0.042	0.035
1.28	1.05	0.98	1.28	1.25		1.49	1.29	1.41	1.22	0.84	1.12	1.02	0.97	1.33	1.38	1.43				1.73	1.56	1.44	1.63	1.57	1.63	1.44
0.13	0.18	0.09	0.08	0.08		0.21	0.16	0.15	0.14	0.10	0.14	0.09	0.08	0.16	0.16	0.16				0.14	0.19	0.11	0.12	0.19	0.12	0.17
0.08	0.08	0.09	0.08	0.08		0.16	0.13	0.11	0.11	0.07	0.08	0.08	0.06	0.09	0.08	0.09				0.10	0.12	0.11	0.13	0.12	0.13	0.09
45.9	38.1	37.2	36.4	36.2		26.2	22.0		16.7	31.7	43.9	36.8	51.4	34.8	37.3	39.1				46.2	31.3	43.2	44.3	31.9	44.3	36.9
52.3	50.4	50.6	40.7	44.7		34.7	25.1		16.4	44.7	60.8	58.1	66.3	53.6	56.1	55.1				67.6	56.2	60.8	81.4	54.8	81.4	45.5
0.024	0.023	0.024	0.021	0.021		0.015	0.018		0.017	0.026	0.028	0.033	0.029	0.031	0.028	0.027				0.032	0.030	0.033	0.031	0.029	0.026	0.025

																										Yomejima
07111704-1	N3-12	N3-08	N1-01Aβ	N1-01Bβ	N2-03C	N1-01Aα	N2-01Bβ	N1-09Bβ	N1-09Aα	N1-09Bα	N2-08C	07111714-1	N2-05B	N2-05A	07111701-1	07111701-2	N1-02Aα	N2-04	N1-09C	07111715-1	N1-03B	N2-06	N1-05A	N1-08B	07111703-1	07111903-2
Bronzite andesite	Bronzite andesite	Bronzite andesite	Bronzite andesite	Bronzite andesite	Bronzite andesite	Bronzite andesite	Bronzite andesite	Bronzite andesite	Bronzite andesite	Bronzite andesite	Bronzite andesite	Bronzite andesite	Bronzite andesite	Bronzite andesite	Dacite	Dacite	Quartz dacite	Quartz dacite	Quartz dacite	Quartz dacite	Quartz dacite	Quartz dacite	Quartz dacite	Quartz dacite	Quartz dacite	Type1 boninite
60.83	59.03	64.30	61.02	60.21	63.30	60.84	60.29	59.37	60.82	60.97	60.16	63.69	57.93	58.53	64.05	65.30	73.19	74.68	75.12	74.44	76.05	75.72	74.88	73.11	77.10	56.67
0.17	0.15	0.15	0.16	0.16	0.16	0.17	0.15	0.17	0.15	0.15	0.16	0.15	0.41	0.41	0.29	0.34	0.18	0.20	0.21	0.17	0.21	0.22	0.23	0.28	0.21	0.08
13.67	14.12	13.53	14.17	14.46	13.65	13.98	14.08	15.50	14.31	14.51	15.19	14.70	15.14	15.05	14.07	16.99	13.28	12.79	12.38	13.11	12.24	12.25	12.71	12.85	12.02	8.21
7.84	8.45	6.46	7.69	7.71	7.51	7.86	8.20	8.15	7.96	7.78	8.44	6.92	10.98	10.81	8.29	5.82	3.70	3.35	3.44	3.14	3.18	3.20	3.41	4.58	2.64	9.07
0.13	0.12	0.11	0.11	0.11	0.11	0.13	0.13	0.11	0.12	0.12	0.10	0.11	0.15	0.16	0.11	0.02	0.06	0.06	0.06	0.05	0.05	0.05	0.06	0.08	0.01	0.17
6.18	6.51	4.82	5.46	5.42	5.26	5.44	5.44	5.11	4.99	4.71	4.89	3.69	4.28	4.10	3.46	1.92	1.18	0.86	0.87	0.77	0.67	0.66	0.68	0.79	0.43	18.96
8.51	8.99	7.44	8.42	9.00	7.04	8.66	8.98	8.32	8.32	8.77	8.41	7.58	8.51	8.27	6.62	6.16	3.98	3.17	3.08	3.84	2.81	2.99	3.15	3.62	2.55	5.78
2.13	1.99	2.49	2.25	2.26	2.30	2.31	2.16	2.46	2.52	2.35	1.88	2.49	1.87	1.91	2.43	3.04	2.90	3.50	3.36	2.81	3.28	3.15	3.43	3.16	3.64	0.81
0.52	0.63	0.66	0.69	0.64	0.64	0.58	0.55	0.79	0.78	0.62	0.73	0.63	0.70	0.71	0.62	0.39	1.47	1.34	1.44	1.63	1.46	1.72	1.40	1.46	1.39	0.23
0.03	0.02	0.05	0.03	0.03	0.04	0.03	0.03	0.02	0.04	0.03	0.03	0.04	0.04	0.04	0.04	0.02	0.05	0.05	0.05	0.05	0.04	0.05	0.06	0.07	0.02	0.02
1.27	1.30	1.34	1.41	1.42	1.43	1.45	1.51	1.60	1.60	1.65	1.73	1.87	2.57	2.64	2.40	3.03	3.14	3.87	3.93	4.07	4.73	4.85	5.06	5.82	6.17	0.48
0.62	0.64	0.55	0.59	0.62	0.52	0.62	0.64	0.54	0.58	0.60	0.55	0.52	0.56	0.55	0.47	0.36	0.30	0.25	0.25	0.29	0.23	0.24	0.25	0.28	0.21	0.70
2.65	2.62	3.15	2.95	2.90	2.93	2.89	2.70	3.25	3.29	2.97	2.61	3.12	2.56	2.63	3.06	3.43	4.38	4.84	4.80	4.45	4.74	4.88	4.82	4.62	5.03	1.04
231	216				233	251	236	243	233	252	204	229	275	500	426		102	27	34	58	39	32	26	34	27	148
262	159				197	172	157	23	107	105	28	54	31	6	9		14	17	33	12	31	16	12	5	14	1441
13.49	15.47				17.75	13.67	15.45	12.55	16.14	16.62	19.63	18.55	10.50	11.40	16.31		26.92	26.16	30.63	28.52	28.79	29.52	23.79	25.01	36.53	5.98
98	88				99	100	82	109	112	107	100	102	107	116	107		89	92	100	92	95	108	110	113	94	46
5.1	8.6				5.7	5.3	5.4	4.9	5.2	5.6	5.8	6.4	7.6	7.9	8.5		9.0	12.5	13.3	8.8	13.0	29.3	13.3	13.5	12.0	4.4
28.6	26.6				34.7	29.4	25.4	34.4	31.6	35.9	29.5	35.7	27.8	29.1	39.3		56.0	58.5	65.4	54.1	66.7	72.9	66.3	61.2	67.1	10.8
0.55	0.47				0.62	0.49	0.52	0.56	0.49	0.58	0.56	0.74	0.45	0.49	0.67		1.10	1.02	1.03	1.01	1.15	1.27	1.16	1.07	1.25	0.25
0.55	0.63				0.83	0.57	0.68	0.63	0.61	0.63	0.59	0.87	0.38	0.38	0.65		1.35	1.06	1.23	1.35	1.22	1.22	1.25	1.08	0.92	0.32
38.0	27.5				55.2	36.9	39.0	31.3	39.8	41.6	29.7	55.5	21.4	24.7	39.1		79.9	72.3	79.8	83.8	77.9	83.7	73.1	68.5	78.5	17.0
1.09	1.53				1.21	1.08	0.98	0.92	1.13	1.30	1.11	1.45	0.83	0.87	1.37		1.99	2.19	2.28	2.13	2.26	2.62	2.39	2.23	1.41	0.67
2.27	1.60				2.37	2.20	1.99	2.01	2.42	2.68	1.73	2.64	1.96	2.06	3.00		3.93	4.70	4.83	4.18	4.76	5.08	4.98	4.76	1.97	0.91
0.31	0.36				0.34	0.31	0.28	0.28	0.32	0.34	0.31	0.42	0.32	0.31	0.46		0.58	0.66	0.69	0.63	0.67	0.87	0.75	0.70	0.39	0.22
1.45	1.69				1.52	1.50	1.34	1.35	1.52	1.61	1.46	1.90	1.56	1.62	2.16		2.57	3.29	3.23	2.76	3.24	4.42	3.53	3.50	1.78	1.03
0.45	0.52				0.47	0.47	0.41	0.41	0.43	0.50	0.43	0.50	0.59	0.61	0.69		0.73	0.98	0.99	0.77	1.01	1.44	1.12	1.09	0.62	0.34
0.16	0.15				0.15	0.16	0.13	0.15	0.15	0.16	0.13	0.18	0.23	0.25	0.24		0.20	0.28	0.31	0.23	0.28	0.37	0.33	0.35	0.33	0.14
0.62	0.74				0.56	0.54	0.54	0.51	0.56	0.61	0.59	0.66	0.82	0.85	0.94		0.87	1.29	1.25	0.92	1.22	2.30	1.45	1.41	0.90	0.46
0.10	0.13				0.10	0.10	0.10	0.09	0.10	0.10	0.10	0.12	0.16	0.15	0.17		0.16	0.23	0.24	0.16	0.22	0.44	0.26	0.26	0.18	0.08
0.66	0.80				0.67	0.68	0.64	0.59	0.65	0.67	0.65	0.76	1.03	1.07	1.19		1.10	1.53	1.59	1.09	1.50	3.14	1.78	1.74	1.40	0.56
0.16	0.20				0.17	0.17	0.16	0.15	0.16	0.16	0.16	0.19	0.25	0.24	0.26		0.25	0.36	0.37	0.27	0.36	0.81	0.40	0.42	0.37	0.13
0.52	0.68				0.54	0.56	0.52	0.49	0.51	0.55	0.56	0.60	0.75	0.75	0.86		0.83	1.16	1.18	0.89	1.15	2.61	1.31	1.28	1.36	0.43
0.09	0.12				0.10	0.09	0.10	0.08	0.09	0.10	0.09	0.11	0.13	0.14	0.14		0.14	0.20	0.21	0.15	0.20	0.45	0.21	0.24	0.24	0.09
0.63	0.77				0.70	0.64	0.67	0.61	0.64	0.66	0.64	0.77	0.90	0.88	0.96		0.99	1.33	1.36	1.03	1.31	3.01	1.47	1.53	1.76	0.54
0.11	0.14				0.12	0.11	0.12	0.11	0.11	0.12	0.11	0.14	0.15	0.14	0.14		0.17	0.23	0.22	0.18	0.22	0.51	0.25	0.25	0.28	0.11
0.70	0.68				0.83	0.70	0.65	0.82	0.72	0.80	0.71	0.85	0.71	0.70	0.96		1.31	1.37	1.48	1.33	1.52	1.66	1.58	1.47	1.64	0.30
0.043	0.034				0.059	0.038	0.040	0.047	0.042	0.053	0.039	0.059	0.034	0.041	0.052		0.071	0.071	0.081	0.076	0.077	0.092	0.077	0.070	0.091	0.021
1.45	1.35				2.63	1.72	1.82	2.04	1.96	1.86	1.66	2.76	1.16	1.37	1.91		4.47	3.79	3.75	4.34	3.61	4.20	3.79	3.47	1.90	0.98
0.16	0.17				0.17	0.20	0.18	0.16	0.17	0.18	0.18	0.17	0.14	0.12	0.22		0.30	0.32	0.29	0.26	0.30	0.31	0.32	0.32	0.32	0.07
0.11	0.08				0.17	0.13	0.11	0.11	0.13	0.15	0.09	0.17	0.08	0.08	0.13		0.28	0.22	0.24	0.26	0.23	0.25	0.24	0.23	0.28	0.06
35.0	18.0				45.8	34.2	39.6	33.9	35.2	32.1	26.8	38.3	25.7	28.3	28.6		40.2	32.9	35.1	39.4	34.4	31.9	30.6	30.8	55.7	25.6
59.9	35.9				79.3	57.5	58.4	51.4	62.0	63.1	46.3	72.5	23.8	28.2	40.7		81.0	54.5	58.9	81.3	59.4	27.8	49.6	44.8	44.5	31.8
0.028	0.030				0.037	0.029	0.028	0.034	0.034	0.039	0.030	0.041	0.011	0.012	0.023		0.052	0.049	0.052	0.054	0.052	0.056	0.048	0.037	0.054	0.021

										Kitanoshima	Nakanoshima				
07111905-1	07111908-8	Y1-04A	07111907	Y3-03C	Y1-02Aα	Y1-06A	Y1-02Bα	07111903-1	07111901-1	K1-03	07032414-3	NAK1-01	NAK1-02	JB2	
Type1 boninite	Type1 boninite	Type1 boninite	Bronzite andesite	Bronzite andesite	Bronzite andesite	Bronzite andesite	Bronzite andesite	Bronzite andesite	Dacite	Tholeiitic andesite	Tholeiitic dacite	Tholeiitic dacite	Tholeiitic dacite	average	σ
57.23	57.12	58.55	59.08	59.55	59.90	61.83	61.72	64.89	68.11	58.29	71.01	68.14	69.60	52.91	
0.08	0.11	0.14	0.21	0.26	0.13	0.24	0.13	0.17	0.18	0.61	0.49	0.43	0.76	1.17	
9.50	10.41	10.96	14.30	15.37	14.27	14.79	14.43	14.04	14.35	16.10	11.22	13.69	13.11	14.70	
8.69	9.25	9.02	8.75	8.59	9.26	8.18	8.63	7.95	6.54	9.24	5.99	6.31	6.63	14.05	
0.16	0.17	0.16	0.14	0.14	0.14	0.12	0.12	0.12	0.02	0.12	0.11	0.10	0.12	0.20	
16.12	13.47	12.17	6.97	5.22	5.17	3.98	4.04	3.38	1.62	6.36	2.94	2.63	1.72	4.63	
6.61	7.96	7.26	8.57	8.28	8.89	8.25	8.56	7.03	5.57	3.34	3.66	2.19	1.47	9.84	
1.26	1.07	1.41	1.54	2.07	1.73	2.08	1.86	1.87	2.20	4.73	4.08	6.32	6.07	2.00	
0.33	0.42	0.31	0.40	0.51	0.49	0.49	0.49	0.52	1.36	1.17	0.46	0.17	0.41	0.42	
0.02	0.02	0.02	0.02	0.02	0.03	0.03	0.02	0.03	0.05	0.05	0.04	0.03	0.10	0.09	
0.54	0.69	0.74	1.26	1.65	1.79	2.05	2.14	2.35	4.03	1.45	2.04	2.40	3.85		
0.70	0.76	0.66	0.60	0.54	0.62	0.56	0.59	0.50	0.39	0.21	0.33	0.16	0.11		
1.59	1.49	1.72	1.94	2.58	2.23	2.56	2.34	2.40	3.56	5.90	4.54	6.49	6.47		
														n=6	
169		229	249	272	279	278	283	222		303	285	306	163	573	12
1280		812	223	52	97	55	49	21		10	5	8	1	24.3	1.7
8.78		9.30	8.25	8.75	14.53	13.11	13.12	13.55		9.11	3.98	1.78	4.85	6.04	0.16
54		54	72	81	83	83	77	75		146	94	115	108	178	4
2.7		4.3	5.8	7.0	4.6	7.6	4.5	5.6		14.6	10.9	10.2	28.4	24.6	0.3
14.7		17.6	23.8	29.9	21.7	28.8	23.0	26.4		38.8	23.0	30.4	66.9	45.3	0.9
0.45		0.43	0.58	0.66	0.62	0.69	0.79	0.91		0.48	0.25	0.36	0.66	0.43	0.02
0.45		0.52	0.45	0.46	0.78	0.72	0.75	0.70		0.11	0.07	0.05	0.04	0.80	0.03
27.7		29.5	28.7	24.9	46.5	40.7	46.6	42.3		98.5	98.2	16.8	34.2	213	6
0.69		0.81	0.92	0.93	1.15	1.23	1.06	1.17		1.59	0.80	0.89	2.19	2.14	0.02
1.30		1.60	2.01	2.14	2.11	2.61	2.08	2.39		4.41	2.93	3.19	6.42	6.41	0.15
0.19		0.22	0.30	0.32	0.28	0.37	0.28	0.33		0.60	0.46	0.38	0.98	1.03	0.04
0.83		1.10	1.37	1.61	1.26	1.77	1.23	1.64		3.59	2.63	2.27	5.72	5.95	0.16
0.24		0.37	0.52	0.60	0.40	0.58	0.35	0.44		1.30	1.05	0.90	2.17	2.16	0.08
0.08		0.12	0.18	0.24	0.13	0.20	0.13	0.15		0.51	0.37	0.35	0.78	0.78	0.06
0.33		0.47	0.70	0.78	0.50	0.77	0.44	0.59		1.86	1.33	1.19	2.96	2.99	0.16
0.05		0.08	0.12	0.15	0.09	0.15	0.08	0.11		0.33	0.27	0.24	0.57	0.57	0.02
0.39		0.56	0.77	0.93	0.59	0.94	0.53	0.72		2.16	1.72	1.55	3.93	3.89	0.07
0.09		0.14	0.18	0.23	0.14	0.23	0.12	0.16		0.49	0.38	0.33	0.91	0.87	0.02
0.30		0.44	0.62	0.70	0.48	0.74	0.45	0.59		1.49	1.10	1.03	2.50	2.53	0.05
0.06		0.08	0.11	0.15	0.09	0.13	0.10	0.10		0.23	0.17	0.16	0.41	0.41	0.02
0.40		0.58	0.73	0.87	0.64	0.87	0.62	0.76		1.40	1.06	1.06	2.68	2.53	0.05
0.07		0.10	0.14	0.15	0.12	0.15	0.12	0.14		0.21	0.18	0.17	0.40	0.39	0.01
0.41		0.44	0.59	0.76	0.57	0.68	0.55	0.68		1.05	0.64	0.76	1.68	1.39	0.04
0.046		0.037	0.052	0.064	0.050	0.055	0.073	0.075		0.044	0.017	0.033	0.057	0.034	0.002
1.28		1.42	1.83	1.82	2.10	1.89	1.95	1.87		0.64	0.54	0.45	0.92	5.07	0.45
0.11		0.16	0.16	0.16	0.22	0.20	0.18	0.19		0.20	0.07	0.09	0.16	0.27	0.05
0.11		0.10	0.14	0.14	0.16	0.17	0.17	0.16		0.10	0.04	0.07	0.12	0.13	0.01
40.4		36.6	31.1	26.9	40.3	33.1	43.7	36.1		61.8	123.4	18.8	15.6		
69.6		51.0	39.3	28.5	72.6	46.8	75.0	55.8		70.6	92.2	15.8	12.7		
0.030		0.021	0.019	0.019	0.028	0.020	0.030	0.025		0.011	0.008	0.012	0.015		